1-1-2010

Characterizing the Interaction of P. falciparum EBA-175 with its Receptor Glycophorin A

Nichole Salinas

WASHINGTON UNIVERSITY

Division of Biology and Biomedical Sciences

Department of Biochemistry

Characterizing the Interaction of *P. falciparum* EBA-175 with its Receptor Glycophorin A

by

Nichole Diane Salinas

A thesis presented to the
Graduate School of Arts and Sciences
of Washington University in fulfillment of the
requirements for the
degree of Master of Arts

August 2010

Saint Louis, Missouri

Abstract: Malaria causes approximately 2 million deaths each year primarily in children. The clinical manifestations of the disease are the result of invasion and lysis of red blood cells by *Plasmodium* parasites, the deadliest of which is *Plasmodium falciparum*. In order to accomplish this cycle of invasion, *Plasmodium falciparum* utilizes a number of proteins including EBA-175 of the Ebl family of proteins. In this thesis, I examine the interactions between EBA-175 and its receptor GpA and self-association of EBA-175 towards understanding the role of this interaction in invasion. I develop protocols for expression and purification of RII-175, F2-175, GpA, and FITC-RII-175, as well as, protocols for pulldowns of RII-175 by GpA that identify the minimal binding domain of GpA. I also develop and optimize a FACS assay to quantify RII-175 binding to GpA on RBCs and utilize the assay to asses the ability of 3'-siallylactose and a peptide backbone to inhibit binding. I further examine the influence of 3'-siallylactose and a peptide backbone on RII-175 self-association. Lastly, I describe the development of monoclonal antibodies against RII-175 that will be used in future studies to further characterize interactions between RII-175 and GpA. These studies define the minimal binding domain of GpA that interacts with RII-175 is the region corresponding to amino acids 30 to 50. It was also shown that 3'-siallylactose, which is important for receptor binding, is a weak inhibitor of binding while a peptide backbone corresponding to the minimal binding domain cannot inhibit binding alone. Thus, a fully glycosylated region of amino acids 30-50 is required. The self-association studies of the K_d of dimerization of RII-175 is ~10uM consistent with dimerization being important for receptor binding. In agreement with the inhibition studies, 3'-siallylactose and peptide backbone failed to

influence dimerization. Further understanding of the RII-175/GpA interactions will help to define their roles in invasion and can lead to the production of better malaria therapeutics.

Acknowledgements:

I would like to take this opportunity to thank those who have been involved in the process of completing this thesis. I would like to thank my advisor Dr. Niraj Tolia for allowing me the opportunity to develop this project and his continued support during the entire process. I would also like to thank him for allowing me to create new assays and optimization of those assays, the opportunity to guide junior members of the lab, and the maintenance of a fun work environment.

I would also like to thank my thesis committee Dr. Daved Fremont, Dr. Daniel Goldberg, and Dr. Tom Brett for their support throughout my thesis and their insightful advice as to the experiments conducted in my thesis. I would also like to thank Dr. Goldberg for the use of his BD FACSCANTO machine, and Dr. Fremont for the use of his MALS machine, and Dr. Brett for the use of his western blot setup and help with developing a western blot protocol. I would also like to thank Dr. Roberto Galletto for help with the AUC and the maintenance of the Biochemistry department's AUC. I would also like to thank Dr. Kathy Sheehan and the Hybridoma Center at Washington University for the help in developing primary assays for antibodies against RII-175.

Members of the Tolia lab, as well as, those in the Fremont lab and Goldberg lab have also been very helpful in the processes of developing this thesis by providing timely advice on projects and help in using lab equipment and developing protocols.

Finally, I would like to thank my mom, Debra Ratliff, for continued support in everything I choose to do.

Table of Contents:

List of Figures:

List of Tables:

List of Abbreviations:

AMA-1	Apical Membrane Antigen 1
AUC	Analytical Ultra-centrifugation
CHO cells	Chinese Hamster Ovary cells
DBL	Duffy-binding like
DBP	Duffy Binding Protein
DMEM	Dulbecco's Minimal Eagle Medium
DMSO	Dimethyl Sulfoxide
DNA	Deoxyribonucelic Acid
DTT	Dithiolthreitol
EBA-140	Erythrocyte Binding Antigen-140, BAEBL
EBA-175	Erythrocyte Binding Antigen-175
EBA-181	Erythrocyte Binding Anitgen-181, JESEBL
Ebl	Erythrocyte-binding-like Gene Family
EBL-1	Erythrocyte Binding Ligand 1
EDTA	Ethylenediaminetetraacetic Acid

ELISA	Enzyme-linked Immunosorbent Assay
F1	DBL domain F1 of EBA-175, amino acids 153-427
F2	DBL domain F2 of EBA-175, amino acids 442-748
FACS	Flow Associated Cell Sorting/Flow Cytometry
FBS	Fetal Bovine Serum
Fc	The Fc portion of an IgG antibody
FITC	Fluorescein
GpA	GlycophorinA
GpA-FL	GlycophorinA Full Length, amino acids 1 to 60
GpB	GlycophorinB
GpC	GlycophorinC
GpD	GlycophorinD
GpE	GlycophorinE
HCl	Hydrochloric Acid
HEK293T	Embryonic Kidney Cells
HEPES	4-(2-hydroxyethyl)peperazine-1-ethanesulfonic acid

HGPRT	Hypoxanthine-guanine phosphoribosyltransferase
IC50	Inhibition Curve 50% Inhibition
K_d	Dissociation Equilibrium Constant
KDa	kilo-Dalton
mAbs	Mono-colonal Antibodies
MALS	Multi-angle Light Scattering
MES	2-(N-morpholino)ehanesulfonic acid
MSP-1	Merozoite Surface Protein 1
NaCl	Sodium Chloride
PAGE	Poly-acrylamide Gel Electrophoresis
PBS	Phosphate Buffered Saline
PEP	a Peptide Corresponding to amino acids 33-52 of GpA
pHLFchis	a Vector for Mammalian Expression to Proteins
pHLSec	a vVctor for Mammalian Expression of Proteins
PMSF	Phenylmethanesulfonyl fluoride
RII	Region II of EBA-175, amino acids 145-761

RBC(s)	Red Blood Cell(s)
RH	Reticulocyte Binding Homology
SDS	Sodium Dodecyl Sulfate
SL	3’-siallylactose
SLP	3’-siallylactose + PEP
TMB	3,3’,5,5’-tetramethylbenzidine
Tris	2-Amino-2-(hydroxymethyl)-1,3-propanediol
W.H.O.	World Health Organization

Chapter 1: Introduction

Malaria kills approximately 2 million individuals a year and causes illness in approximately 200 million annually [1]. The clinical manifestations of malaria are the result of the invasion and lysis of red blood cells (RBCs) by *Plasmodium* parasites [1]. Of the four species of *Plasmodium* that cause malaria, *Plasmodium falciparum* is the deadliest [1]. *P. falciparum* can be found world wide in tropical regions [fig 1]. The region most affected by *P. falciparum* is sub-Saharan Africa [2].

Plasmodium parasites represent a heavy economic burden for countries where malaria is endemic [2]. As such, research has been conducted with the goal of creating vaccines and or drug treatments against *Plasmodium* parasites. This has become more important as strains of parasites become increasingly drug resistant. A large variety of proteins and cellular processes have been identified as potential targets for vaccines and drugs. One such target is Erythrocyte Binding Antigen (EBA-175), which is involved in the erythrocyte stage of the parasite life cycle and is the focus of this thesis.

1.1: Malaria Life Cycle

The *Plasmodium* parasite has a complicated life cycle that involves two different hosts and multiple stages within each host [1-3]. The two hosts for the parasite are humans and the anopheles mosquito. Within the mosquito, the cycle consists of uptake of gametocytes during a blood meal followed by the formation of a macrogametocyte [3]. The gametocyte develops into an ookinete and then a cyst. The cyst then ruptures

releasing sporozoites that travel to the salivary glands of the mosquito and are ultimately injected into the human host during the next blood meal [3].

Once within the human host the parasite undergoes two main stages in its life cycle. These stages are the liver stage followed by the erythrocyte stage [3]. The liver stage consists of invasion, replication within, and lysis of multiple types of liver cells. The liver stage culminates in the production of merozoites that can go on to infect RBCs [1, 3]. The parasite invades, replicates within, and lyses RBCs in the erythrocyte stage. It is the continual invasion and lysis of RBCs which causes the clinical symptoms of malaria that include fatigue and severe anemia, which can lead to death [1, 3]. This stage is targeted by many antimalarials including the chloroquines. Also included in the erythrocyte stage is the formation of gametocytes during replication within RBCs.

1.2: Invasion of Red Blood Cells by Parasite

Invasion of RBCs in of itself is also a complicated process involving two main pathways of invasion and multiple proteins in each pathway. The overall invasion process can be broken down into four main steps [fig 3] [1]. The first step involves low affinity interactions between the merozoite and RBC. Merozoite Surface Protein-1 (MSP-1) and Apical Membrane Antigen-1 (AMA-1) are both membrane proteins expressed on the surface of merozoites during the erythrocytic stage and are involved in this stage of invasion. Although MSP-1 is the most abundant surface protein, the receptor for MSP-1 and how it mediates attachment have yet to be defined. AMA-1 has two roles

in invasion. The first is attachment through an unknown receptor to the RBC surface and initiation of the second stage [1].

The second stage involves the apical reorientation of the merozoite so that the apical end contacts the RBC membrane and high affinity interactions and the formation of the tight junction [1]. The apical reorientation is initiated by AMA-1 through an unknown mechanism. The proteins responsible for the formation of the tight junction are the Erythrocyte Binding Ligand (EBL) and Reticulocyte-binding Homology (RH) families of proteins are involved in this stage of invasion and are essential for invasion. Both the EBL and RH families of proteins are expressed during the erythrocytic stage. The EBA-175, EBA-140 (BAEBL), and EBA-181 (JESEBL) of the EBL family represent the sialic acid dependent pathway and are important for binding erythrocytes [fig 4]. The RH family of proteins represents both the sialic acid dependent and the sialic acid independent pathway of invasion and are important for binding both erythrocytes and reticulocytes [1].

The third step of invasion is the movement of the tight junction over the surface of the merozoite and the shedding of the protein coat [1]. The parasite utilizes an actin/myosin motor complex to achieve the active invasion of the RBC. The forth step of invasion is the complete invasion of the RBC and the formation of the parasitophorous vacuole [1].

1.3: EBL Family of Proteins

The EBL family of proteins is involved in the sialic acid dependent pathway of RBC invasion. The EBL family includes EBA-175, EBA-140 (BAEBL), EBA-181 (JESEBL), and EBL-1 of *P. falciparum* and Duffy Binding Protein (DBP) of *P. vivax* [fig 4] [1, 4, 5]. The receptors for EBA-175, EBA-140, and EBL-1 are GpA, GpC, and GpB respectively, while the receptor for EBA-181 is still unknown. The receptor for DBP is the Duffy Antigen Receptor for Chemokines [1, 4, 5]. The sialic acid dependence of EBA-175, EBA-140, and EBA-181 was discovered by treating RBCs with neuraminidase from *V. cholerea*, which cleaves the α2-3 linked sialic acid from o-linked glycans [4, 6-10]. Treatment of the RBCs caused the loss of binding by EBA-175, EBA-140, and EBA-181 in rosetting assays [4, 6-10]. In these assays, the malarial protein is expressed on the surface of adherent mammalian cells in tissue culture and RBCs are flowed over the adherent cells. The RBCs form rosettes, large clumps of RBCs, over the top of the cells expressing the malaria protein. A positive result in a rosetting assay is the formation of the rosettes overtop of the adherent mammalian cells.

The EBL family proteins share homology in their receptor binding domains. The receptor binding domains contain one to two Duffy Binding like (DBL) domains and are homologous to Duffy binding region of DBP [1, 5]. The DBL domains are primarily alpha-helical and include multiple conserved cysteines [5]. DBP contains one DBL domain and the others family members contain two DBL domains [fig 4]. The two DBL domains of EBA-175 comprise a larger receptor binding domain named Region II (RII) spanning amino acids 145 to 761. The two DBL domains within RII-175 F1 and F2 span amino acids 153 to 427 and 442 to 748 respectively [5].

1.4: EBA-175

EBA-175 was originally discovered by taking merozoite stage parasite supernatant and incubating the supernatant with RBCs [11]. These experiments showed multiple proteins which bound RBCs including one with a molecular weight of 175kDa. This protein was named EBA-175 [11]. It was later determined that EBA-175 was part of the EBL family proteins and expressed by many strains of *P. falciparum*. Many lab and wild strains such as 3D7 and W2mef use EBA-175 as the primary invasion protein [9].

The receptor for EBA-175 was discovered through rosetting assays [fig 5] [6]. In these assays, RBCs were treated with trypsin and chymotrypsin and RII-175 expressing cells were only able to bind chymotrypsin treated cells. GpA and GpB are the main chymotrypsin resistant, trypsin sensitive proteins on the surface of RBCs. To distinguish between these two receptors, GpA and GpB negative RBCs were then used in rosetting assays and RII-175 was able to bind GpB negative cells but not GpA negative cells [6]. These experiments established GpA as the receptor for RII-175.

EBA-175 has also been suggested as a target for malarial vaccines. EBA-175's potential as a target for vaccine development has been supported by the evidence that antibodies against EBA-175 can be found in patient sera of individuals infected with *P. falciparum* [12, 13]. Individuals who have high titers of antibodies against EBA-175 also have marginal protection against infection by *P. falciparum* [12, 13].

The structure of RII of EBA-175 was recently solved [fig 6] [5]. In the crystal structure, RII-175 appears as a dimer. In the dimer, the F1 of one monomer interacts with the F2 of the monomer in a handshake configuration. The dimer creates two channels going through the center of the dimer, and the surface of these channels is highly basic. The F2 domain of each monomer make up roughly two-thirds of two channels with the other third contributed by the F1 domains. Mutations in the dimer interface showed a loss of RBC binding in rosetting assays and this result supports the biological relevance of the dimer model. Cocrystallization with 3'-siallylactose also showed six glycan binding sites in the dimer with 4 sites inside the channels and the other 2 on the receptor facing surface. The glycan binding sites were found by cocrystallizing 3'-saillylactose with RII-175 [5].

1.5: GpA

GpA is the major siallylated protein on the surface of RBCs and with another transmembrane protein, Band3, make up over 50% of the proteins on the surface of RBCs [15-16]. GpA is a single pass transmembrane protein that can exist as both a homodimer and a heterodimer with GpB on the surface of RBCs. GpA has three extracellular exons with a total of 15 O-linked glycans and 1 N-linked glycan on approximately 60 amino acids. The glycans make up approximately 50% of the total molecular weight of 33kDa. The O-linked glycans are important for receptor binding by RII-175 [15-16].

GpA is part of a family of proteins that includes GpB and GpE and shares approximately 95% sequence homology with its family members [fig 5] [15-16]. It is

thought that GpB and GpE were derived from homologous recombination as is the case for the 43+ known variants of GpA that are derived primarily from GpB but also less commonly with GpE. The majority of the variants are located in exon 3 of GpA. Homologous recombination can occur because GpB and GpE both contain an exon 3 in the nucleotide sequence. GpA is the only family member that expresses an exon 3 due to a splice site mutation in exon 3 of both GpB and GpE. Exon 3 contains four O-linked glycans that are unique to GpA [15-16]. It is plausible that RII-175 may directly contact exon 3 of GpA due to the uniqueness of this sequence.

The rosetting assays and the crystal structure with glycan binding sites suggest two possible models of receptor binding by RII-175 [fig 6] [5]. RII-175's receptor is GpA, which exists on the surface of RBCs as both a homodimer and a heterodimer with GpB. One models suggest are that the GpA dimer threads through the channels to form the complex with the glycans in the right orientation. The other model suggests that the GpA dimer wraps around the outside of the RII-175 dimer and places the glycans in the right orientation [5].

1.6: Focus and scope of thesis

While it is known that GpA is the receptor for EBA-175, little is known about how they interact. It is not known how EBA-175 differentiates between GpA and GpB, which differ by only 32 amino acids. It has yet to be shown if these 32 amino acids are important for the specific binding of GpA by EBA-175. While a dimer model of EBA-175 binding to GpA has been proposed, the exact stoichiometry of binding has yet to be

defined. The crystal structure of the EBA-175/GpA complex has also not yet been solved.

My thesis focuses on the identifying the minimal binding domain of GpA for EBA-175 along with the characterization of binding and the characterization of EBA-175 dimerization. In chapter 2, I describe the development and optimization of expression systems and purification of RII-175 and GpA and the mapping of the minimal binding domain of GpA. In chapter 3, I describe the development and optimization of a functional assay for RII-175 that forms the basis for addressing the receptor specificity of RII-175 and inhibition of receptor binding by components of the receptor described in chapter 4. In chapter 5, I characterize the dimerization of RII-175 using biophysical methods. In chapter 6, I describe the development of monoclonal antibodies against RII-175.

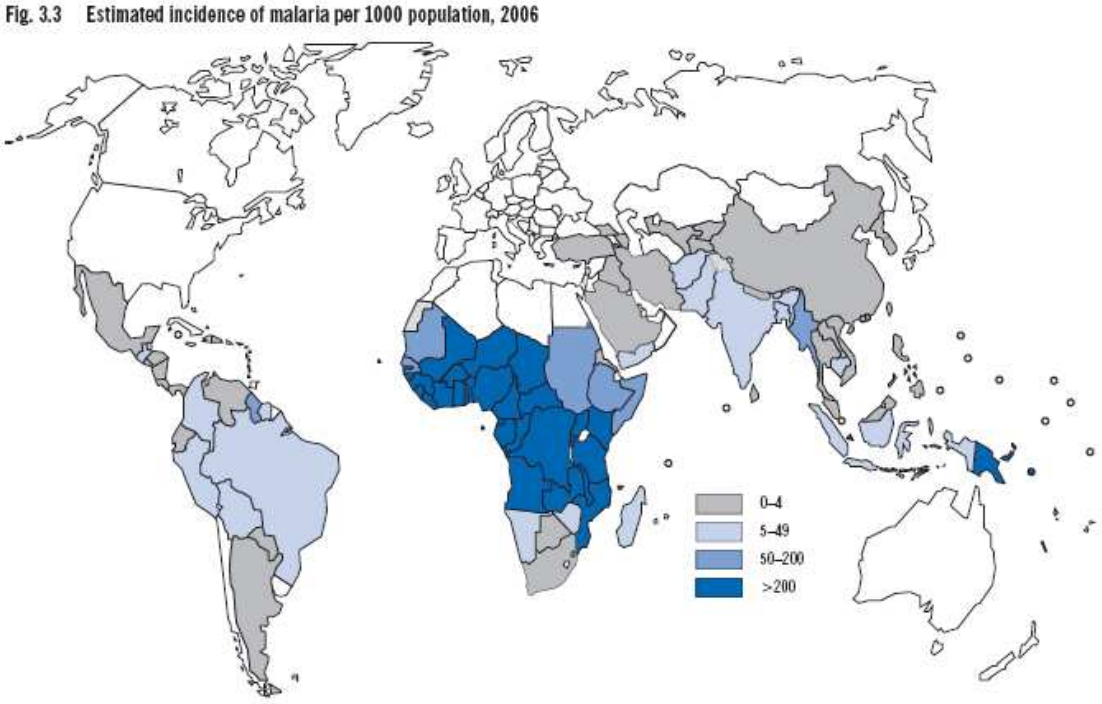

Figure 1: W.H.O. 2006 incidence map of *P. falciparum*[2]

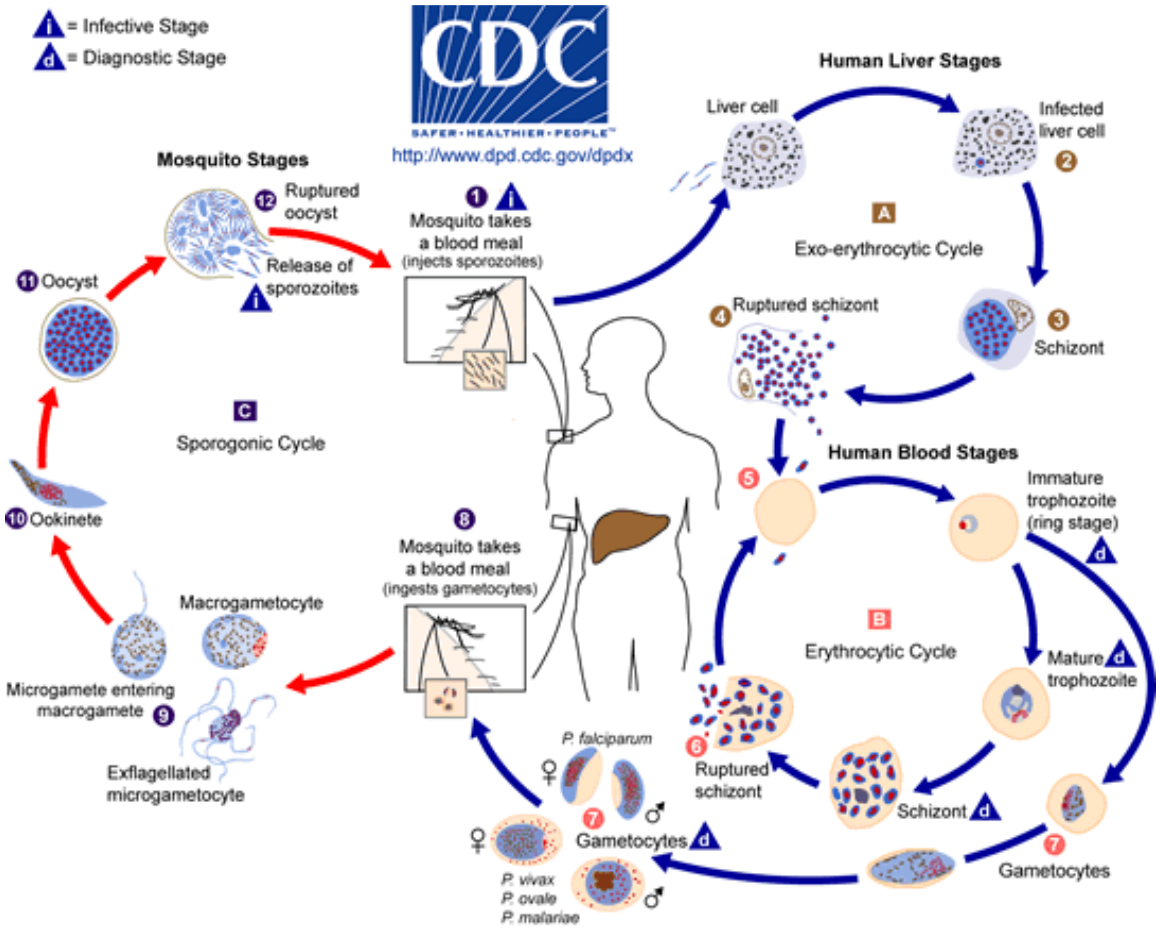

Figure 2: Life cycle diagram for *Plasmodium* parasites [3]

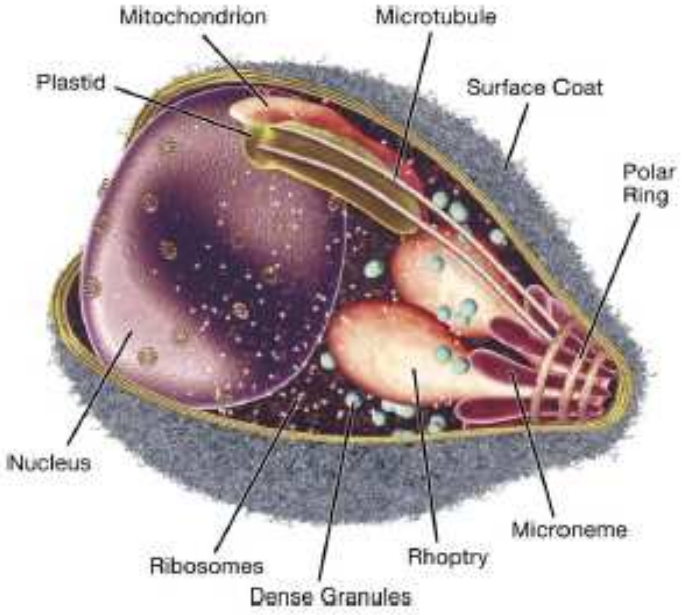

a)

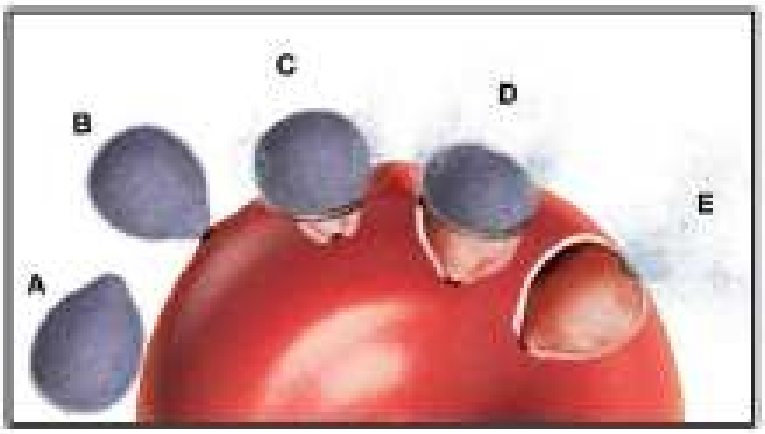

b)

Figure 3: a) Diagram of a merozoite and its organelles, b) Scheme for invasion of RBCs by merozoite [1]

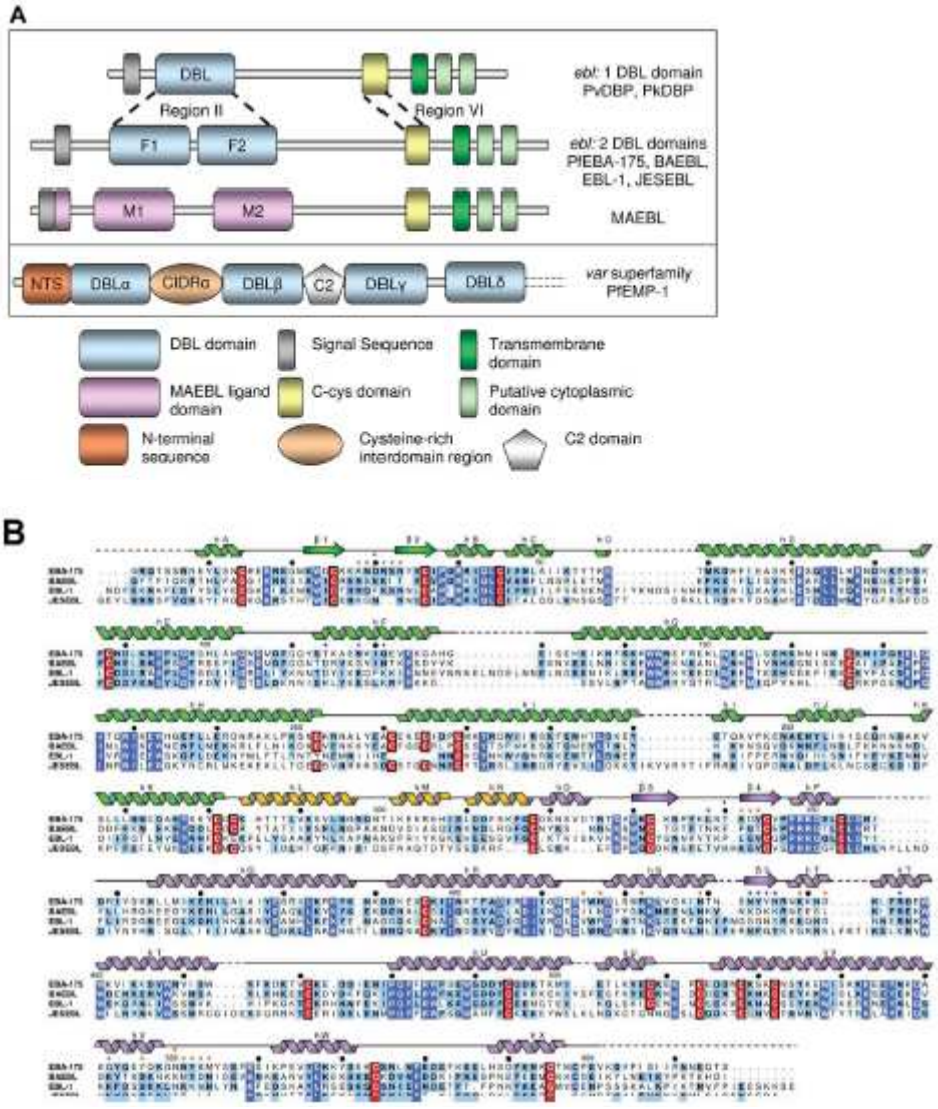

Figure 4: a) Domain structure of EBL family proteins, b) Alignment of EBA-175, EBA-140, EBA-181, and EBL-1 amino acid sequence [5]

a)

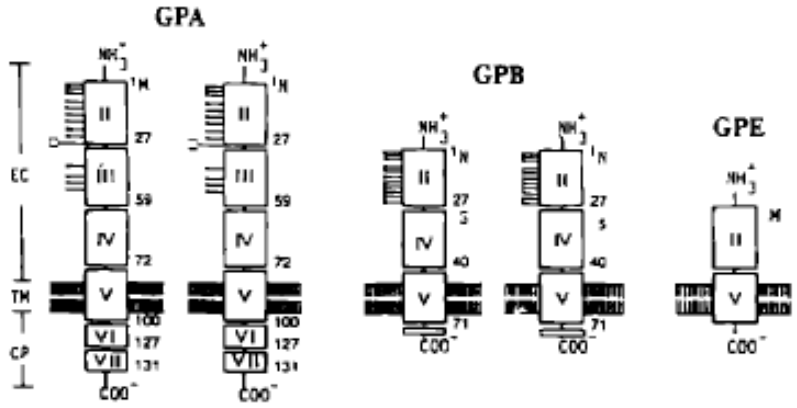

b)

Erythrocyte and treatment*	Binding agent		Region F_2‡
	EBA-175†	Region II‡	
Human (positive for glycophorins A and B)			
No treatment	+	+	+
Neuraminidase	–	–	–
Trypsin	–	–	–
Human glycophorin A–negative [En(a–)]	–	–	ND
Human glycophorin B–negative (S–s–U–)	+	+	ND
Mouse DBA/2			
No treatment	+	+	+
Neuraminidase	–	–	–
Rhesus	+	+	ND
Aotus	–	–	ND
Guinea pig	–	–	ND

*Enzymatic treatments were performed as described (*24*). †A + signifies that EBA-175 binds to erythrocytes; a – indicates no binding. The assay was performed as described (*25*). ‡A + indicates rosetting of erythrocytes on COS cells; a – indicates no rosetting.

Figure 5: a) Exons and glycosylations for GpA, GpB, GpE [15], b) Identification of GpA as the receptor for RII-175 [6]

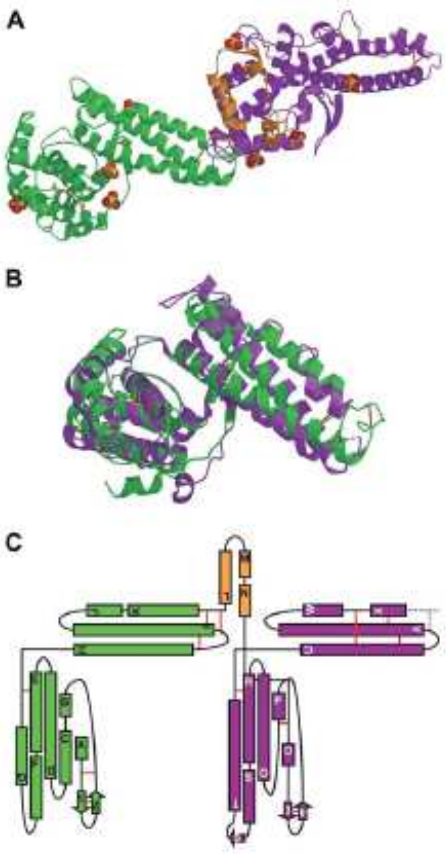

d)

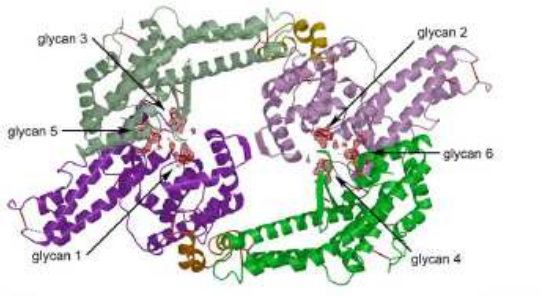

e)

Table 1. Binding Efficiency for RII and Mutants

Mutant Class	Mutation	Binding Ability	No. Glycan Contacts
	Wildtype RII	++++	N/A
Dimer	R446E	–	N/A
Dimer	R446D	–	N/A
Dimer	T114F	+	N/A
Dimer F2	V435D	++	N/A
Glycan 1/2	N417A	++	2
Glycan 1/2	R422E	–	3
Glycan 1/2	K439A	+	2
Glycan 3/4	N33A	+	1
Glycan 3/4	N551A	+++	1
Glycan 3/4	Y552A	+	2
Glycan 3/4	K553A	++	2
Glycan 5/6	K28A	+++	2
Glycan 5/6	R31A	++	1
Glycan 5/6	K341A	+	3
Surface control	E153A	++++	N/A
Surface control	K548A	++++	N/A

Figure 6: a) ribbon structure of RII-175 monomer, b) alingment of F1, green, and F2, purple, c) structure of RII-175 monomer, d) structure of RII-175 dimer with glycan binding sites, e) RII-175 dimer and glycan binding site mutants [5]

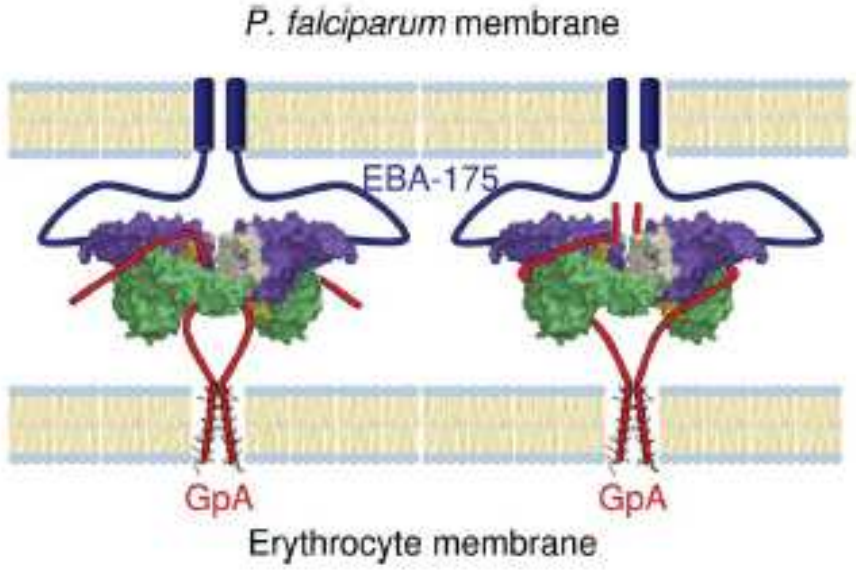

Figure 7: Dimer model of GpA binding [5]

Chapter 2: Expression of RII-175 and GpA and Mapping of the Minimal Binding Domain of GpA

2.1: Introduction

Protein Expression and purification allows for the study of protein/protein interactions outside of the context of cells or organisms and reduces the potential masking properties of other proteins present in cells. RII-175 was previously expressed in *Pichia pastoris* and purified by various chromatography methods [5]. The recombinant RII-175 was a glycosylation mutant where certain residues were mutated to remove potential aberrant glycosylation by *P. pastoris*. The mutations were important for expression because *P. falciparum* lacks complex glycosylation of proteins [5]. Because expression using the *Pichia pastoris* system is labor and time intensive especially for the study of multiple mutations, an *E. coli* system was developed. The *E. coli* system also has the advantage of not requiring the use of glycosylation mutants due to the *E. coli* lacking a glycosylation system and can be readily used to generate multiple mutants when needed.

GpA has also been expressed before using multiple lines of CHO cells [14]. The cell lines used were wild type for glycosylation as well as deficient in various stages of O-linked and N-linked glycosylation. GpA with different types and amounts of glycosylation was produced by using these cell lines. Unfortunately, these GpA

constructs were expressed on the surface of the CHO cells and large quantities could not be produced using this system [14].

Recently a group has developed a protocol for expression of proteins in a mammalian expression system [17]. This system utilizes HEK293T cells and the pHLFchis or pHLSec vectors. These vectors use a β-chicken actin promoter to drive the expression of large amounts of the protein cloned into the various vectors. Both the pHLFchis and pHLSec vector function have signal sequences for the export of the expressed protein outside of the cells. The protein can then be purified from the media [17]. Due to the ability of these vectors to produce large quantities of soluble protein, I optimized this system for GpA in order to express soluble protein, which is an advantage over the CHO cell expression system. This system was also chosen because it allows for the complete glycosylation of GpA, which can not be done in bacterial expression systems.

While the receptor has been identified for RII-175 through rosetting assays, the portion of the receptor directly bound by RII-175 has yet to be identified. Previously, fragments of GpA were tested for their ability to inhibit RBC binding in rosetting assays [6]. These fragments were obtained by enzymatically cleaving GpA obtained from RBCs to produce multiple fragments. No individual fragment was able to inhibit RII-175 binding to RBCs to the same extent as full length GpA [6]. As a result of the enzymatic cleavage of Gpa from RBCs, only a limited number of fragments could be obtained and tested. This method limits the regions that can be used and can cause a binding domain

to be missed due to cleavage within the domain. This may be why none of the fragments produced were able to inhibit RII-175 binding to RBCs. The cleavage sites for trypsin on GpA are found in exon 3, which results in fragments with incomplete exon 3's [6]. This may be important to understanding why the fragments did not inhibit because exon 3 is the only portion of sequence unique to GpA.

In this chapter, I describe protocols that were developed for the production of RII-175 and GpA. These protocols form the basis for the production of recombinant protein for all subsequent studies. In this chapter, I also describe the optimization of a protocol for pulldowns with full length and the truncations of GpA and the binding of GpA truncations by RII-175 to show functionality of the expressed proteins and to identify the minimal binding domain.

2.2: Materials & Methods

2.2.1: Expression of EBA-175. RII-175 (amino acids 145 to 761) and F2-175 (amino acids 442 to 748) were expressed in BL-21 *E. coli* cells using a pet28 vector. The cells were grown shaking at 37^{o}C to an O.D. 600 of 0.6 and induced with IPTG. The cells were then grown for an additional 3 to 5 hours shaking at 37^{o}C. The cells were then pelleted and resuspended in 10mL/L cells of 50mM Tris pH 8, 100mM NaCl, 5mM DTT, 0.25mg/mL Lysozyme, and 1 complete protease tablet per 30mL of buffer and frozen at -80^{o}C. The cells were later lysed using sonication and the inclusion bodies pelleted. The inclusion bodies were washed 3 times in 50mM Tris pH 8, 100mM NaCl, 5mM DTT, 0.5% Triton X-100 and once in 50mM Tris pH 8, 100mM NaCl, 5mM DTT. The protein

was then denatured with 6M guanidine hydrochloride, 50mM Tris pH 8, 100mM NaCl, 5mM DTT overnight at 4^{o}C. 100mg of protein was used per liter of refolding buffer (200mM Tris pH 8, 10mM EDTA, 400mM L-arginine, 0.1mM PMSF, 2mM reduced glutathione, 0.2mM oxidized glutathione). The protein was refolded for 48 to 72 hours at 4^{o}C. The refolded protein was concentrated using Amicon concentrators to a concentration of approximately 15mL per liter of refolding buffer. The concentrated protein was dialyzed overnight at 4^{o}C against 50mM MES pH 6, 200mM NaCl (1L dialysis buffer per 1L refolding buffer). The dialyzed protein was then concentrated to 5mL/1L refolding buffer. Each 5mL of protein was then purified by gel filtration chromatography using a Hiload 16/60 superdex 200 prepgrade column with 10mM MES pH 6, 200mM NaCl and the peak fractions of each run were combined and purified by gel filtration chromatography an additional 2 to 3 times. The peak fractions from the final gel filtration purification were than concentrated to a concentration of 15mg/mL.

2.2.2: Expression of GpA. GpA_FL (aa1-60) and GpA truncations [table 1], cloned into a pHLFchis vector containing the GpA signal sequence, were transiently transfected into 70-90% confluent HEK293T cells using the method described in Aricescu 2006. Media was then harvested four days later. The media was diluted 3 times with His-tag buffer A (50mM Tris pH 8, 100mM NaCl, 10mM Imidazole pH 8). The diluted media was then run over a nickel-agarose column and eluted with His-tag buffer B (50mM Tris pH 8, 100mM NaCl, 500mM Imidazole pH 8). To separate out the various glycosylation states of the GpA produced, the GpA was purified by anion exchange chromatography using a monoQ 5/50 GL column with buffers (A) 25mM Tris pH 8 and (B) 25mM Tris

pH 8, 1M NaCl. A gradient from 0 to 40% of buffer B was used to separate the various glycosylation states which eluted at 130mM NaCl and 230mM NaCl.

2.2.3: GpA Binding in a Pulldown. 40ug of each GpA construct (full length and truncations) was incubated with 1uL 15mg/mL RII-175 and 20uL of ProteinA beads in a total of 100uL in 50mM Tris pH 8, 200mM NaCl, 0.1% Triton X-100 for 30min on ice. The beads were then washed 3 times. The beads were then resuspended in 10uL of SDS-PAGE dye and the samples run on a 10% SDS-PAGE gel.

2.3: Results

2.3.1: RII-175 Expression and Purification

An *E. coli* system was chosen for the expression of RII-175 and F2-175 because it can produce milligram quantities of protein quickly and without the use of glycoslylation mutants. F2-175 was expressed and purified in addition to RII-175 because it has similar binding ability to the full regionII. Both his-tagged and untagged RII-175 and F2-175 were expressed in *E. coli* using the pet28 vector. The denatured protein extracted from the *E. coli* inclusion bodies was refolded in standard refolding buffer as described in Materials and Methods. Multiple methods were tried to purify the refolded protein. The first method of purification was to concentrate 1L of refolded protein which was then purified by gel filtration chromatography with Tris buffer pH 8 and 200mM NaCl. The subsequent peak was purified by cation exchange chromatograpy. Unfortunately, this method resulted in aggregate protein precipitating on the gel filtration column. As a result, other methods of purification were developed.

The next method used was to concentrate the refolded protein and dialyze the protein against 50mM MES pH 6 200mM NaCl. Dialysis at this step prevented precipitation of the protein on the columns. The dialyzed protein was then purified by anion exchange chromatography. The resultant peak was further purified by gel filtration chromatography. Unfortunately, this protein still had aggregate in the purified sample.

The next method of purification was to use the previous method and add two to three additional gel filtration chromatography steps to reduce aggregate contamination. This resulted in protein with minimal aggregate contamination. While this method resulted in pure protein it was time and labor intensive.

The method was modified in an attempt to reduce the time and labor needed to produce the recombinant protein. The method used was to follow the previous method but exclude the cation exchange step because the cation exchange step did not increase the purity of the protein. This method resulted in similar purification to the previous method with one less step.

The final protocol used was to refold the protein in standard refolding buffer and dialyze the refolded protein. The dialyzed protein was then purified by three to four rounds of gel filtration chromatography. A typical GF200 chromatograph and SDS-PAGE gel of the fractions corresponding to the major peak can be found in figure 8. A typical yield for this protocol is 1-5mg per liter of refolding buffer.

2.3.2: GpA Expression and Purification

A mammalian expression system was chosen for GpA because it could be used to produce milligram quantities of completely glycosylated protein quickly. The extracellular portion of GpA (amino acids 1 to 60) was cloned into the pHLFchis construct with the addition of a precision protease site between the GpA sequence and the Fc sequence [fig 9]. The GpA construct was transiently transfected into HEK293 cells. A time course was done to measure the production of GpA over time [fig 9]. The expression of GpA peaked at four days post transfection. All subsequent transfections were harvested four days post transfection.

GpA was purified from the media using a nickel-agarose column. The resulting eluted protein was then used in subsequent experiments. The GpA at this point appears as a smear on an SDS-PAGE gel that is likely the result of various stages of glycosylation in the GpA sample. The different glycosylation states can be further separated by anion exchange chromatography presumably because of the difference in charge represented by the negatively charged sialic acid containing glycans [fig 9].

2.3.3: Expression and Purification of GpA Truncations:

Previously only full length GpA has been expressed and only as a transmembrane protein on the surface of CHO cells. Also, the fragments of GpA used in experiments to inhibit binding were produced through enzyme treatment of GpA from RBCs. This expression system was developed to produce multiple overlapping fragments of GpA and mutants quickly.

Overlapping truncations of the extracellular portion of GpA were cloned into the pHLFchis vector [table 1]. The truncations were transiently transfected into HEK293 cells and the media harvested four days post transfection. All truncations expressed under these conditions [fig 10]. While truncations 3, 5, and 2-4 expressed well, truncation 2 only expressed moderately well and truncations 1 and 4 expressed poorly. Never-the-less, all truncations of GpA can be obtained.

2.3.4: Optimization of Pulldown Conditions

A method to examine protein/protein interactions in the absence of cells has not been developed for Gpa and RII-175, therefore, I developed a pulldown assay to examine the binding of GpA by RII-175 in a cell free assay. The first pulldowns used nickel-agarose beads in conjunction with the his-tag on the GpA [fig 11]. In this pulldown, GpA was purified by cation exchange chromatography, which resulted in three distinct peaks and each peak was incubated with RII-175. Peak 2 and Peak 3 of GpA bound RII-175 in the pulldown. Unfortunately, the RII-175 bound non-specifically to the nickel-agarose beads.

In order to eliminate the non-specific binding of RII-175 to the nickel-agarose beads, the imidazole in the wash buffer was increased from 10mM to 100mM. Peak 2 and Peak 3 of GpA still bound RII-175 in the pulldown. Unfortunately, the RII-175 still bound non-specifically to the nickel-agarose beads.

In order to eliminate any non-specific binding by RII-175, the type of beads used was changed to proteinA-agarose beads [fig 11]. ProteinA-agarose beads can be used

with the GpA constructs because all GpA contructs are conjugated to the Fc portion of an IgG antibody and proteinA binds the Fc portion of antibodies. The three peaks of GpA were again used and peak 2 bound RII-175. All three peaks showed binding, but the higher molecular weight peaks bound RII-175 the most. Unfortunately, while there was less non-specific binding of RII-175 on the proteinA beads, the non-specific binding was not completely eliminated.

In order to eliminate all non-specific binding by RII-175, a detergent was added to the wash buffer [fig 11]. The three peaks of GpA were again used and peak 2 bound RII-175. Only the higher molecular weight peaks bound RII-175. In this pulldown, there was no non-specific binding of the beads by RII-175. The final conditions used in the pulldown were 50mM Tris pH 8, 50mM NaCl, 0.1% Triton X-100 and proteinA-agarose beads.

2.3.5: Pulldown with GpA Truncations

In order to identify the portion of Gpa bound by RII-175, a pulldown was conducted with full length and truncations of GpA. The first pulldown conducted was with the buffer used in the above experiment. At 50mM NaCl, all the truncations bound RII-175.

To eliminate any non-specific binding of RII-175 by a salt gradient was used [fig 12]. The salts used were 50mM NaCl, 100mM NaCl, and 200mM NaCl. All truncations bound RII-175 at 50mM NaCl and 100mM NaCl. At 200mM NaCl, full length GpA and truncation 4 bound RII-175 strongly. Truncation 2 also weakly bound RII-175.

2.4: Discussion

A protocol to purify RII-175 and F2-175 from *E. coli* was developed and optimized. The final yield for this protocol is approximately 1 to 5 mg/ L refolding buffer. A protocol for the production of full length GpA and GpA truncations using HEK293 cells was developed and optimized. The final yield for this protocol is approximately 13mg/L harvested media. The production of purified RII-175 and GpA allows for further investigation into the interactions between RII-175 with itself and its receptor.

To show that RII-175 and GpA (full length and truncations) are functional a pulldown protocol was developed. In the pulldown, RII-175 binds truncation 4 the strongest of all the truncations. Truncation 4 corresponds to amino acids 30 to 50 of GpA and includes all four glycosylations in exon 3. It is likely that amino acids 30 to 50 of GpA are the minimal binding site for RII-175. RII-175 also binds truncation 2 weakly. Truncation 2 contains seven glycosylations and an additional three residues that could potentially be glycosylated. RII-175 may bind truncation 2 weakly because of the large number of glycosylations. The glycosylations are important for binding as evidenced by the loss of binding in rosetting assays upon treatment with neuraminidase. This is also seen in the pulldown with the anion exchange purified GpA. In this pulldown, RII-175 binds only the high molecular weight peaks which may correspond to a higher level of glycosylation. Development of further functional assays for RII-175 are described in the next chapter.

a) b)

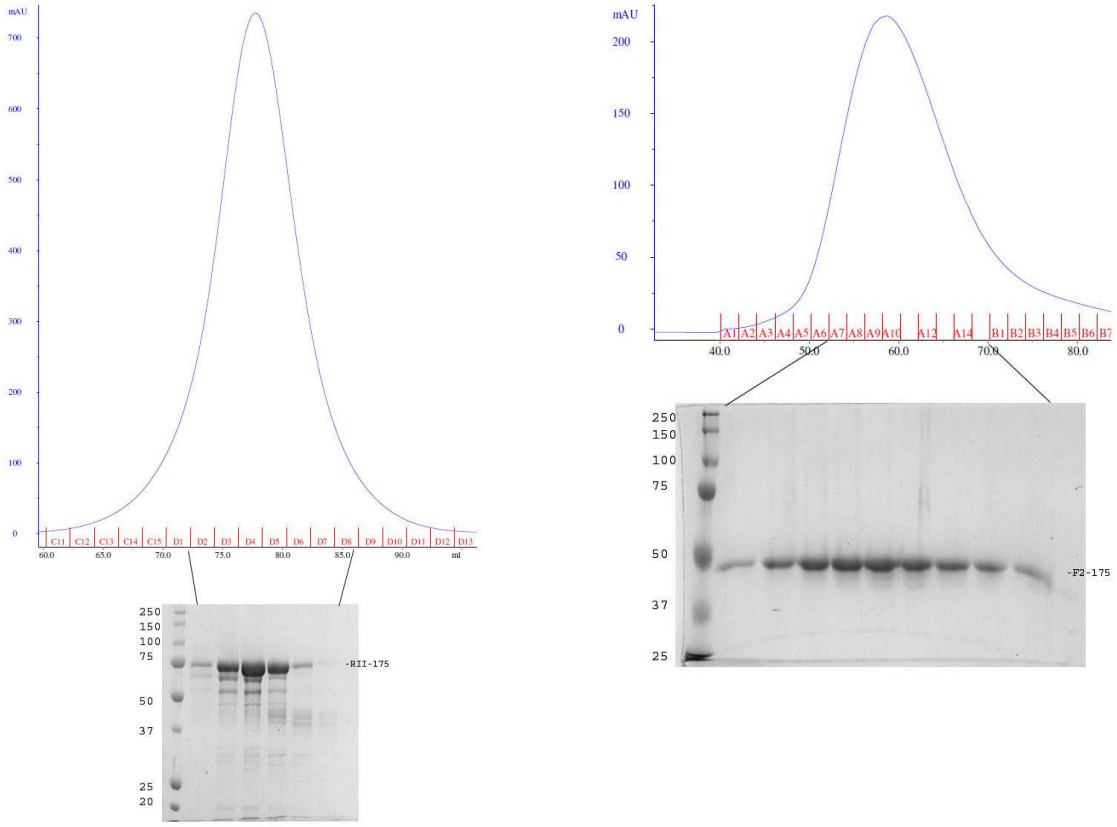

Figure 8: a) GF200 column purification of RII-175, b) GF200 column purification of F2-175

a)

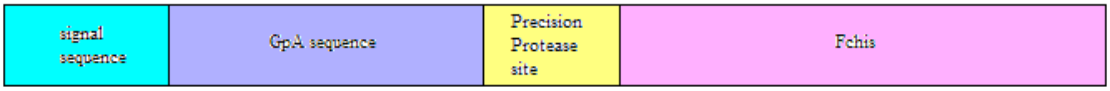

b)

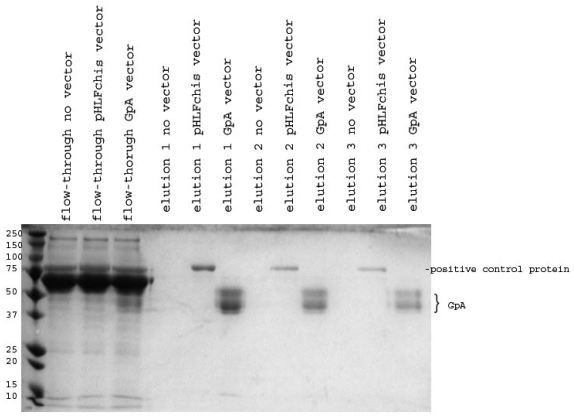

c)

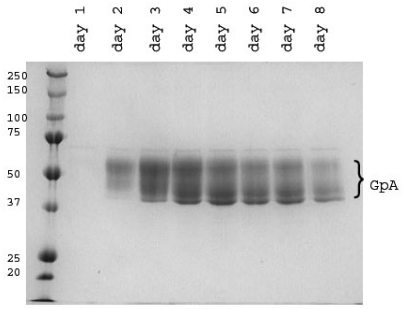

d)

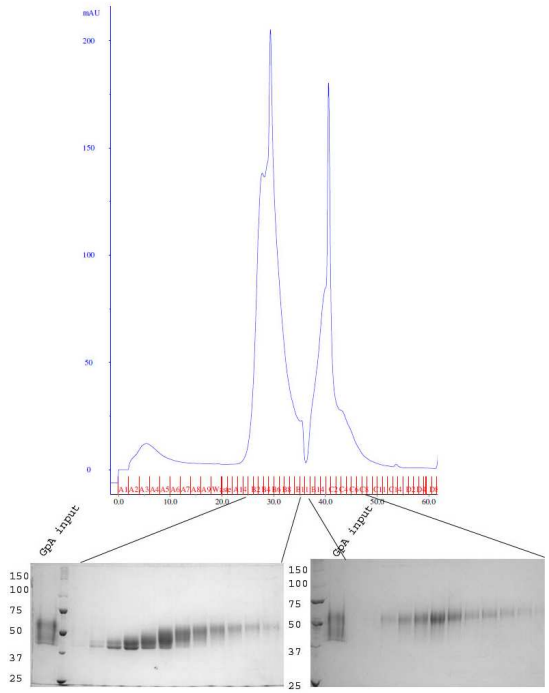

Figure 9: Expression of GpA a) diagram of GpA construct, b) Nickel column purification of HEK293T cells transfected with either no vector, pHLFchis vector, or GpA vector (full length), c) Time course of GpA production by transfected HEK293T cells, d) anion exchange purification of GpA

Truncation:	Sequence:
1	SSTTGVAMHTSTSSSVTKSY
2	TSTSSSVTKSYISSQTNDTHK
3	YISSQTNDTHKRDTYAATPRA
4	KRDTYAATPRAHEVSEISVRT
5	AHEVSEISVRTVYPPEEETGE
2-4	TSTSSSVTKSYISSQTNDTHKRDTYAATPRAHEVSEISVRT

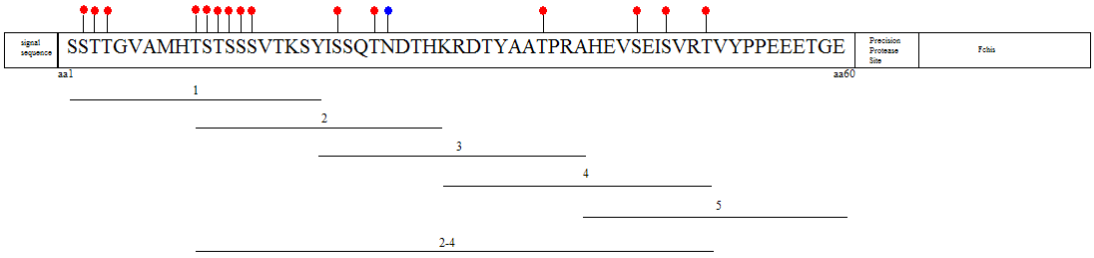

Table 1: Amino acid sequence of the extracellular portion of GpA in each truncation clone and diagram of truncations with glycosylations (red) O-linked, (blue) N-linked

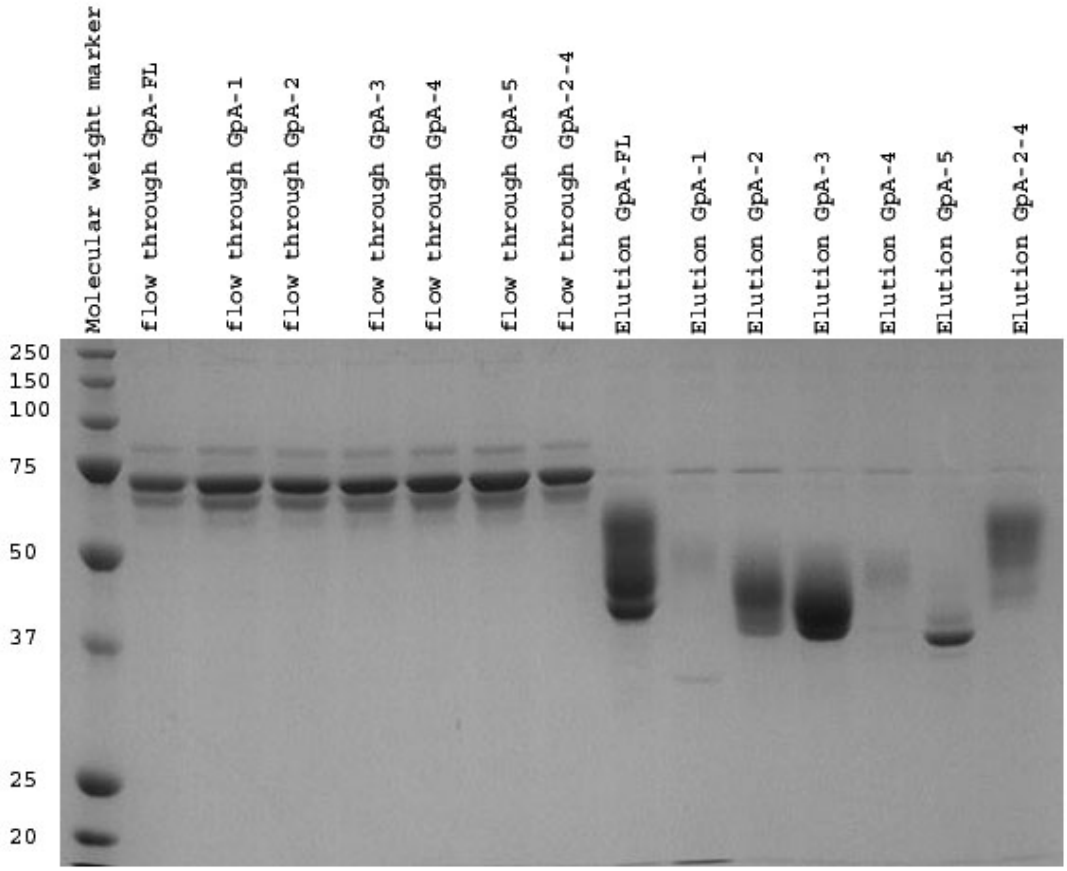

Figure 10: Expression of GpA full length and truncations purified by Nickel-agarose column

a)

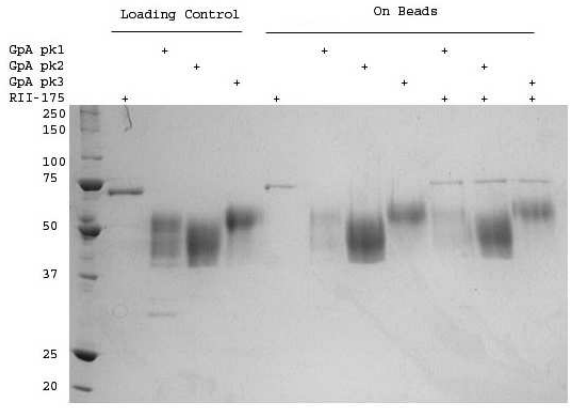

b)

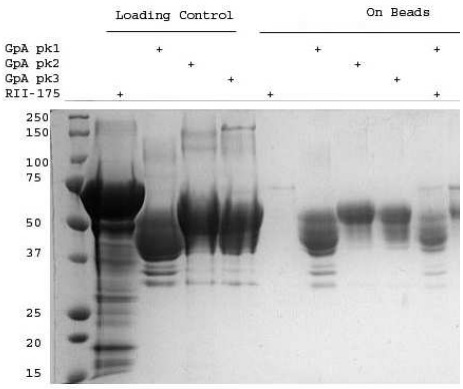

c)

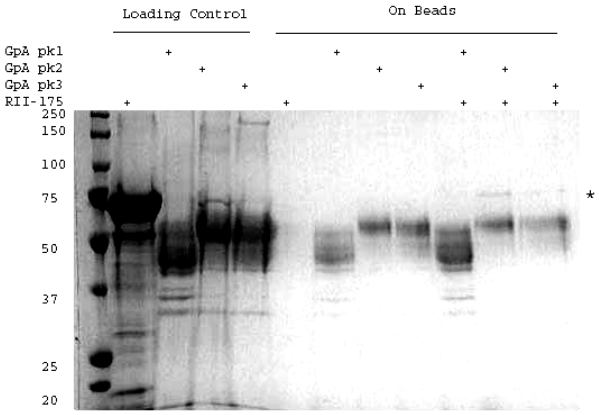

Figure 11: RII-175 Pull down with GpA purified on MonoQ column a) 10mM Imidazole washes on nickel beads, b) proteinA beads, c) proteinA beads with 0.1% trition X-100 washes

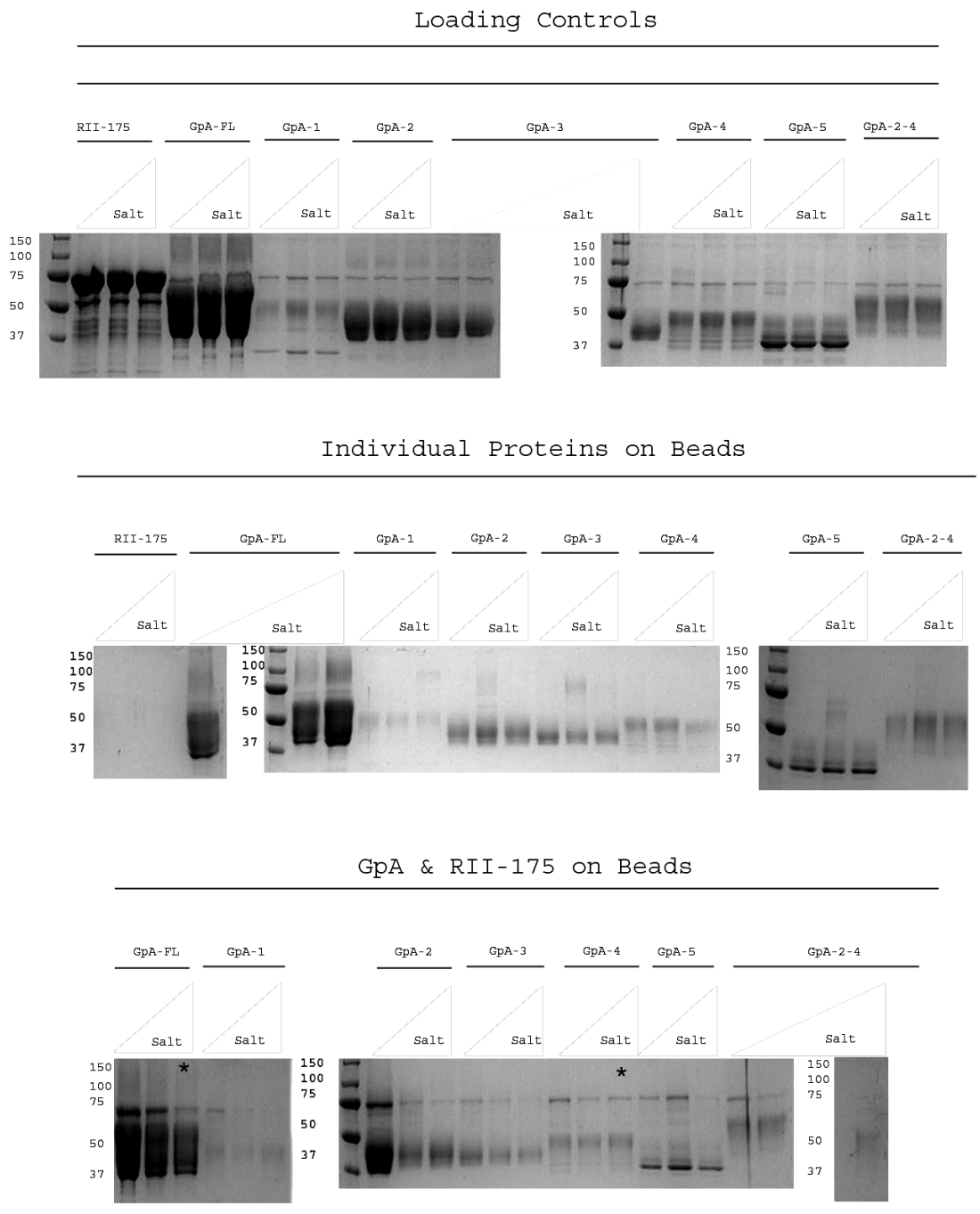

Figure 12: GpA pulldown of RII with full length GpA and GpA truncations

Chapter 3: Validation of Protein Binding in a Functional Assay

3.1: Introduction

Flow Cytometry (FACS) is a method often used to differentiate populations within samples of cells [18]. In FACS, a sample is injected into a flow cell and then flows past a laser at approximately 1 cell at a time. The cell scatters light in both the forward and side directions and is read by a set of detectors [fig 13]. The forward scatter gives the approximate size of the cell that passed by the laser. The side scatter detects organelles like the granules found in neutrophils. Both types of scatter can be used to define different populations in a sample like peripheral blood [18].

FACS can also be used to detect fluorescent stains and dyes by adding additional lasers and detectors. [fig 13] [18]. Fluorescent dyes that bind DNA can be used to detect *P. falciparum* infected RBCs from uninfected RBCs due to only the parasite having DNA. The uninfected RBCs can be separated from infected RBCs based on the detection of fluoresce if the flow cytometer is attached to a cell sorter. Fluorescent dyes conjugated to antibodies can also be used in FACS to detect proteins on the surface of cells or proteins in complex with proteins on the surface of cells [18]. Multiple dyes can be used at once to differentiate between different populations. Both the forward and side scatter and the fluorescence detection can be combined to easily differentiate population of cells in mixed samples [18].

In this chapter, I describe the development of a functional FACS assay for the recombinant RII-175 purified as described in chapter 2. FACS assays can be used to test

a multitude of conditions for binding and can be used to obtain the IC50s for inhibitors and protein/protein interactions on the surface of cells.

3.2: Materials and Methods

3.2.1: Initial Binding of RBCs by RII-175. Red blood cells (RBC) were obtained from the Barnes Jewish Children's Hospital Blood Bank. 500,000 RBCs are diluted in 500uL DMEM with 10% FCS. His tagged 15mg/mL RII-175 was added to a concentration of either 66uM or 9uM and the mixture incubated on ice for one hour. The RBCs were then washed three times with DMEM with 10% FCS. Mouse anti-his antibody from Qiagen was added to the RBCs. Alexafluor 647 conjugated anti-mouse IgG antibody from Invitrogen was diluted 1:500 in DMEM with 10% FCS. 100uL of the diluted antibody was added to the washed RBC and incubated on ice for one hour. The RBCs were then washed three times. The RBCs were then resuspended in 100uL DMEM with 10% FCS. The RBCs were then analyzed using a fluorescent microscope.

3.2.2: Optimization of Enzyme Treatment of RBCs to Prevent Clumping. RBCs were incubated with 1mg/mL chymotrypsin overnight. The cells were then used as described above in RII binding.

3.2.3: Optimization of Anticoagulant treatments to Prevent Clumping. EDTA: RII-175 was incubated with RBCs as described in above in RII binding with the buffer being DMEM 10% FCS 7mM EDTA instead of DMEM 10% FCS. Heparin: RII-175 at 10uM and 1uM was incubated with RBCs in DMEM 10% FCS buffer with heparin at

concentrations of 60units/mL, 30units/mL, or 12 units/mL. The mixture was then incubated with antibodies as described above in RII binding.

3.2.4: Optimization of Salt and Protein Concentration conditions to Prevent Clumping. RII-175-his at 0nM, 40nM, 200nM, 320nM, and 1000nM were each incubated with RBCs in DMEM 10% FCS with 150mM NaCl, 200mM NaCl, 250mM NaCl, 300mM NaCl, 350mM NaCl, and 400mM NaCl for 1 hour on ice. The samples were then washed three times with DMEM 10% FCS that have their corresponding salt concentration. The samples were then incubated with anti-his antibody conjugated to FITC for 1 hour on ice. The samples were then washed three times with DMEM 10% FCS that have their corresponding salt concentration. The RBCs were resuspended in 2mL DMEM 10% FCS that have their corresponding salt concentration and were then analyzed using a BD FACScanto machine available in the Goldberg lab.

3.2.5: FITC labeling of RII-175 and FACS. 1.5mg of 15mg/mL RII-175 was diluted in 1mL PBS pH 6, 50mM EDTA and mixed with 10uL 10mg/mL FITC in DMSO. The mixture was incubated rotating at room temperature for 1hr. The mixture was then diluted in 10mL 25mM MES pH 6, 100mM NaCl. The diluted protein was then run over 2mL monoS sepharose resin and the protein eluted with 5mL 25mM MES pH 6, 500mM NaCl. The protein was then concentrated to 1mL and purified by gel filtration chromatography using a superdex 200 10/300 GL column. Incorporation of the FITC label was verified using a phosphoimager. The resultant labeled peak was then concentrated to 15mg/mL. 1uM RII-FITC was then added to 500,000 RBCs in 500uL of

DMEM 10% FCS 250mM NaCl and incubated for one hour on ice. The cells were washed three times with DMEM 10% FCS 250mM NaCl and resuspended in 2mL DMEM 10% FCS 250mM NaCl. The cells were then imaged using a fluorescent microscope and also analyzed using a BD FACScanto machine available in the Goldberg lab.

3.3: Results

3.3.1: Initial Binding of RBCs by RII-175

To initially asses the ability of the recombinant RII-175 to bind RBCs, 66uM RII-175-his purified as described in chapter 2 was added to RBCs and then incubated with a mouse anti-his antibody followed by a goat anti-mouse IgG antibody conjugated to Alexa 647. The RBCs were then imaged using a fluorescent microscope [fig 14]. Only the RBCs incubated with RII-175 were positive for fluorescence. The RBCs incubated with RII-175 also formed large clumps that do not resuspend and were positive for fluorescence while negative controls lacking RII-175 did not fluoresce or clump. This was also seen when the RII-175 concentration was decreased to 9uM. The clumping only occurs when RBCs are incubated with RII-175 and is therefore RII-175 dependent.

F2-175 has a similar binding ability as RII-175 when used in rosetting assays and was therefore tested for binding RBCs in solution. F2-175-his was also incubated with RBCs at the same concentrations as previously used for RII-175. The F2-175 also clumped the RBCs and these clumps were positive for fluorescence [fig 15]. The F2-175 also clumping indicates that it is a property of the recombinant protein binding to RBCs.

Unfortunately, clumps are not conducive to FACS assays for two main reasons: 1) small clumps that flow through the flow stream will be read as one event instead of multiple events and can under represent the true percentage of the population that is positive for binding, 2) the capillary through which the cells pass is very small and large clumps will clog the system.

3.3.2: Optimization of Enzyme Treatment of RBCs to Prevent Clumping

The only known function for GpA is to prevent clumping of RBCs. To test if the clumping is due to other proteins interacting when GpA is bound by RII-175, enzyme treatment of RBCs was conducted before incubation with RII-175. Specifically chymotrypsin was used because GpA is chymotrypsin resistant and treatment of RBCs with chymotrypsin will cleave other proteins while leaving GpA whole. When these treated RBCs were incubated with the lowest concentration of RII-175 previously used, the RBCs still clumped and the clumps were positive for fluorescence. While this treatment did not inhibit binding, the treatment did not reduce the clumping.

3.3.3: Optimization of Anticoagulant treatments to Prevent Clumping

Anticoagulants are compounds used in solutions containing RBCs to prevent clumping and clotting of RBCs, therefore, I wanted to examine if anticoagulants could prevent the clumping when RII-175 binds RBCs. Two commonly used anticoagulants are EDTA and heparin. RBCs were incubated with the lowest concentration of RII-175 previously used in DMEM with EDTA at concentration of 7mM. The RBCs still

clumped and the clumps were positive for fluorescence. Unfortunately, EDTA did not decrease clumping significantly on its own.

Heparin was also used in an attempt to prevent clumping. RII-175 at 10uM and 1uM was incubated with RBCs and heparin at concentrations of 60units/mL, 30units/mL, or 12 units/mL. RBCs incubated with RII-175 alone clumped cells and were positive for fluorescence [fig 16]. Unfortunately, all concentrations of heparin prevented clumping of RBCs but also prevented RII-175 binding in the 1uM RII-175 samples and greatly reduced binding in the 10uM samples shown by the loss of fluorescence.

3.3.4: Optimization of Salt and Protein Concentration conditions to Prevent Clumping

It is possible that salt and the concentration of protein could affect the clumping of the RBCs. The next treatment used to prevent clumping of the RBCs upon RII-175 binding was a salt gradient combined with a titration of RII-175. RII-175-his at 0nM, 40nM, 200nM, 320nM, and 1000nM were each incubated with RBCs in DMEM with 150mM NaCl, 200mM NaCl, 250mM NaCl, 300mM NaCl, 350mM NaCl, and 400mM NaCl [fig 17]. The concentration of RII-175 with the best overall binding was 1000nM (1uM). The other concentrations did not have high enough signal to justify using. The 1uM sample bound RBCs up to 250mM NaCl, and the clumping decreased as the salt concentration increased [fig 17]. The conditions of 1uM RII-175 and 250mM NaCl were used in all subsequent FACS assays. Thus, it appears that the clumping is due to

electrostatic interactions and these interactions can be limited by increasing the salt concentration in the buffer.

3.3.5: RII-FITC labeling and use in FACS

To make the FACS assay more efficient and reduce the number of washes, RII-175 was labeled with FITC. RII-175 was incubated with either FITC dissolved in DMSO or Carbonate buffer. The lowest concentration of FITC used, 10uL of 10mg/mL DMSO, was able to label the RII-175 [fig 17]. The RII-FITC was run over a cation exchange resin column to purify the RII-FITC from free FITC. The subsequent protein was purified by gel filtration chromatography. The labeled protein ran as one peak and the FITC label was verified by a phosphoimager [fig 18]. The protein was then concentrated to 15mg/mL and used to label RBCs. The FITC labeled RII-175 was able to bind RBCs and was positive for fluorescence [fig 19]. The FITC labeled RII-175 when incubated with RBCs was also able to produce a positive signal in a FACS assay [fig 19].

3.4: Discussion

Recombinant RII-175 that was expressed and purified is functional for RBCs binding, and can now be used to characterize its interactions with GpA and itself. The functional assay developed can be further used to study inhibitors of various kinds, i.e. small molecules, receptor fragments, antibodies, etc. The development of the FITC-RII-175 decreases the amount of time required for the FACS assay and can be used to test inhibitors. One disadvantage to the FITC-RII-175 in a FACS assay is that the label could interfere with the ability of antibodies specific to RII-175 to bind by obscuring the

epitope for the antibody. Receptor specificity of the RII-175 will be described in chapter 4 and utilizes the FACS assay developed in this chapter.

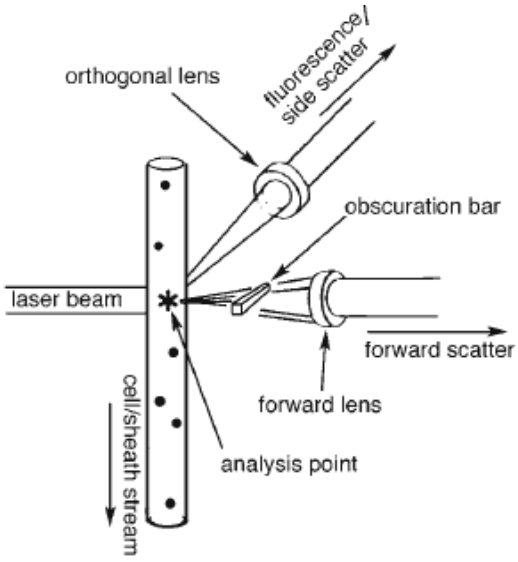

a)

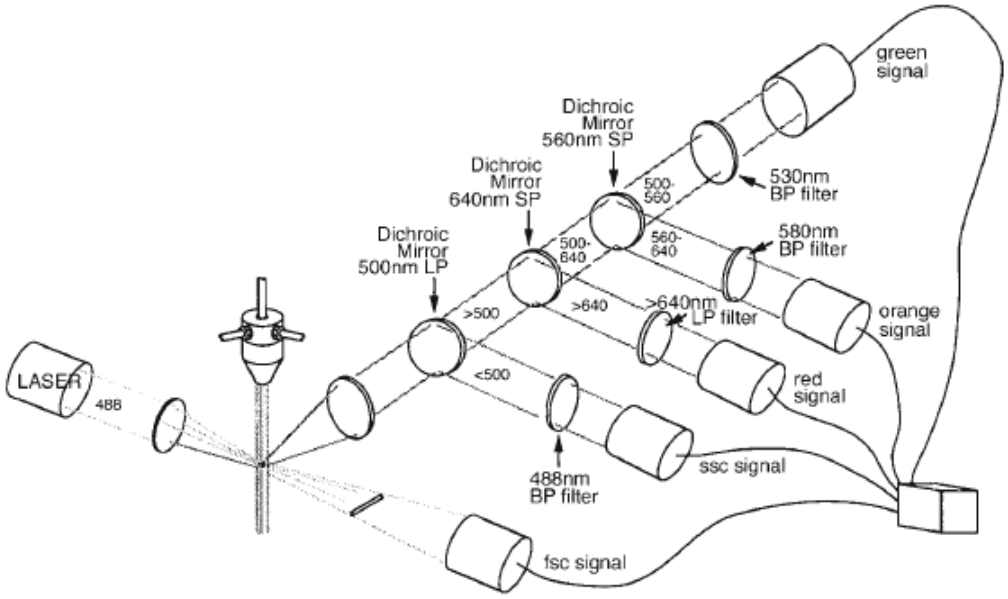

b)

Figure 13: a) diagram of forward and side scatter in FACS, b) diagram of laser, filters, and detectors in FACS [18]

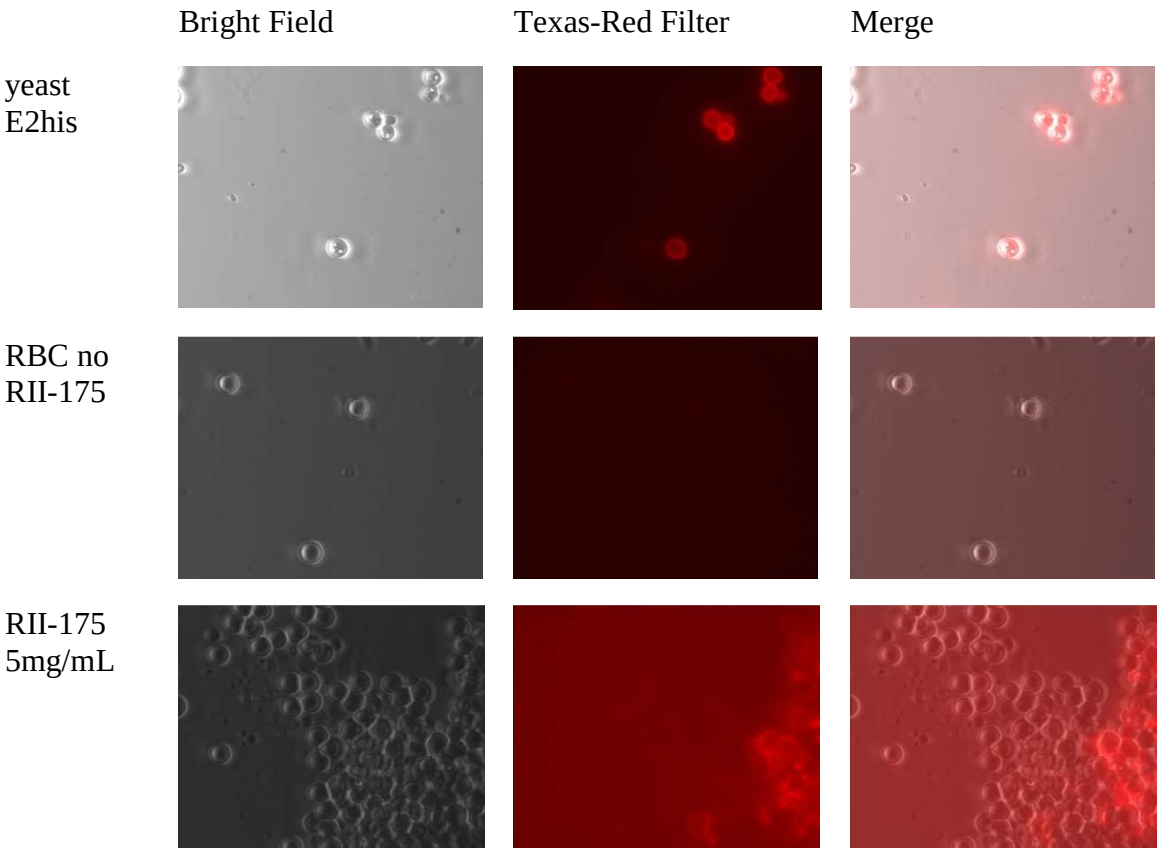

Figure 14: RII-175 binding of RBCs using a secondary antibody conjugated to Alexafluor 647

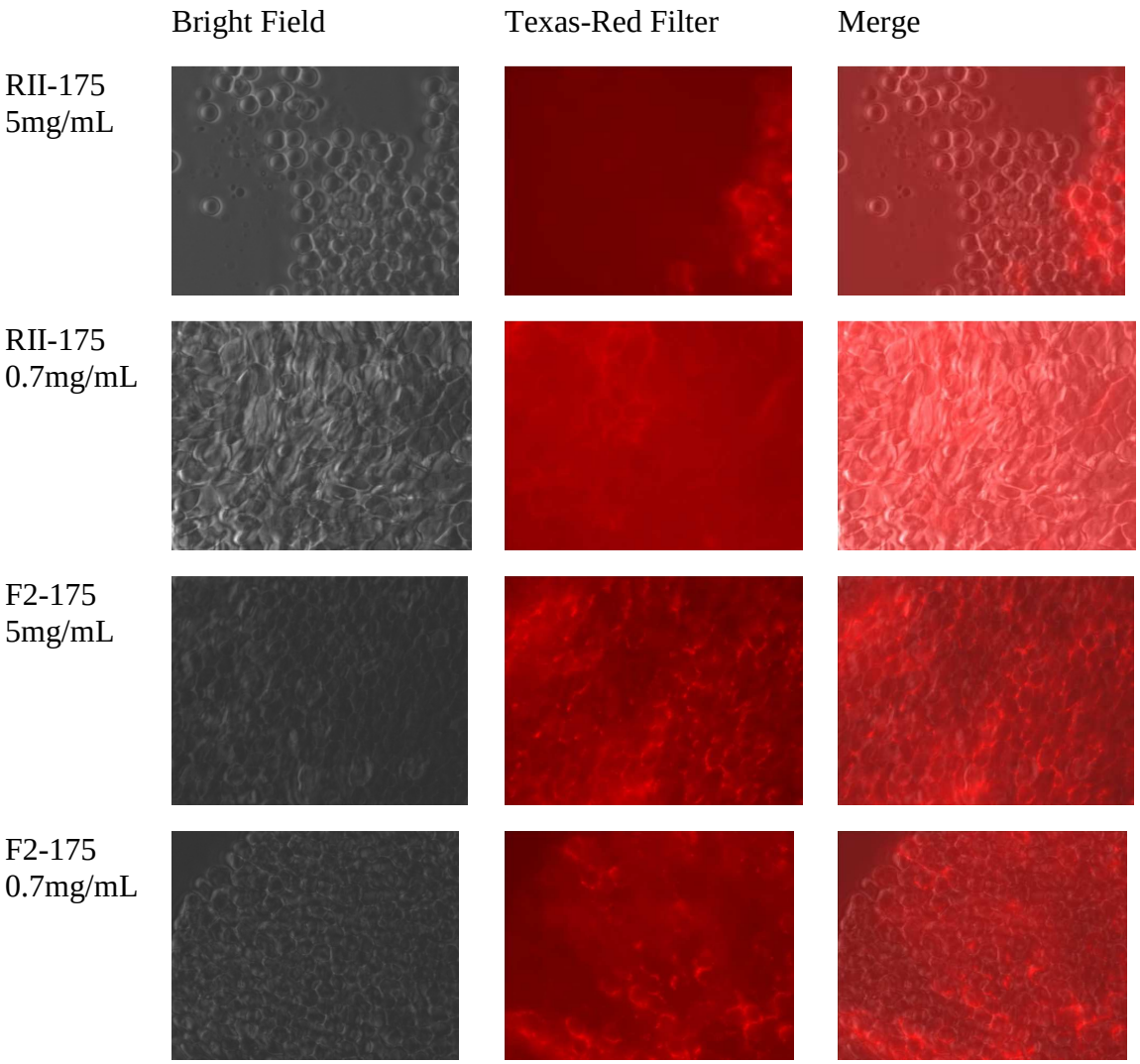

Figure 15: RII-175 and F2-175 binding of RBCs using a secondary antibody conjugated to Alexafluor 647

a)

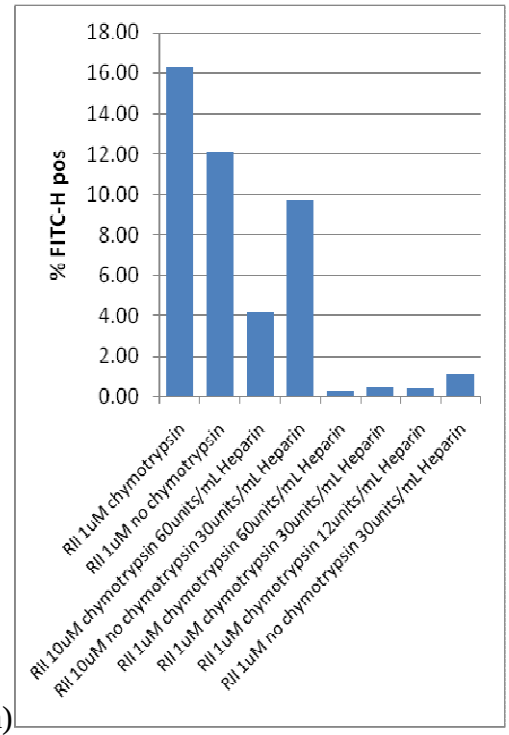

b)

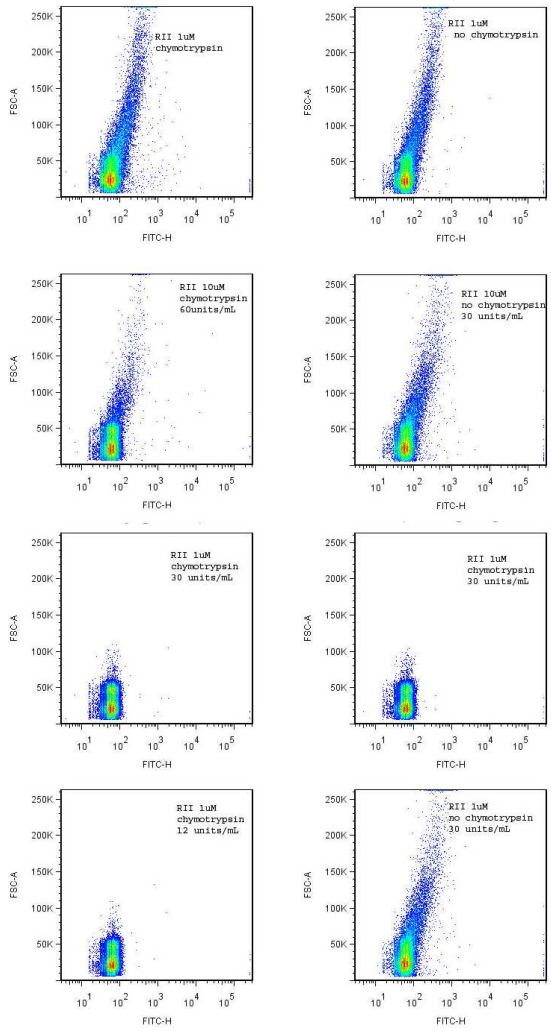

Figure 16: Influence of heparin on RII-175 binding to RBCs, a) percentage of positive cells for heparin samples, b) Dot plots of heparin samples in "a"

a)

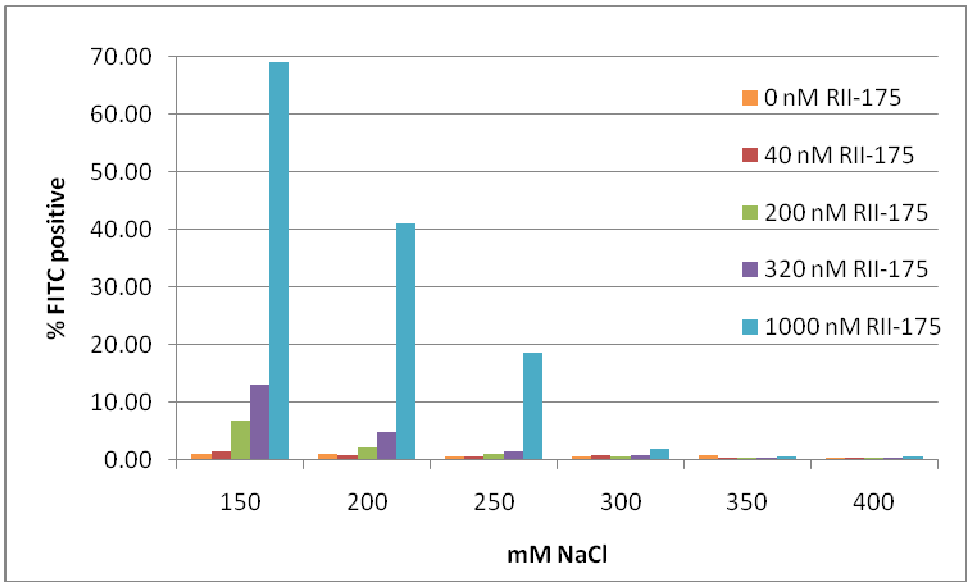

b)

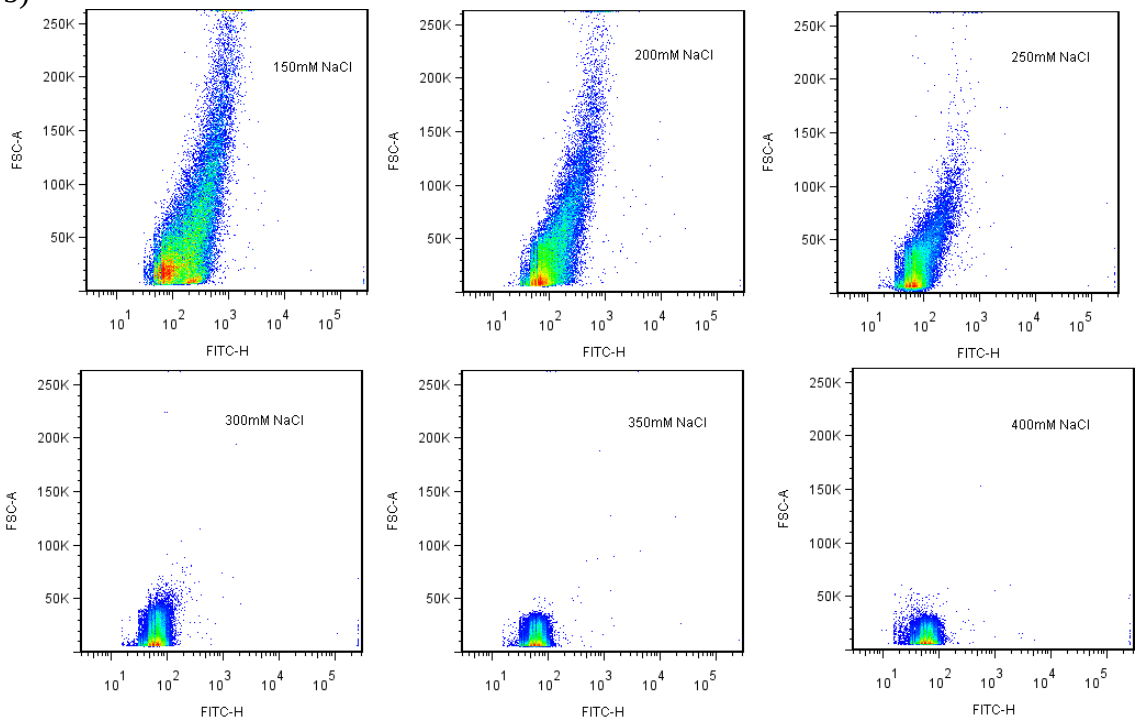

Figure 17: a) Salt gradient and RII-175 titration in FACS, b) Dot Plots for 1000nM RII-175

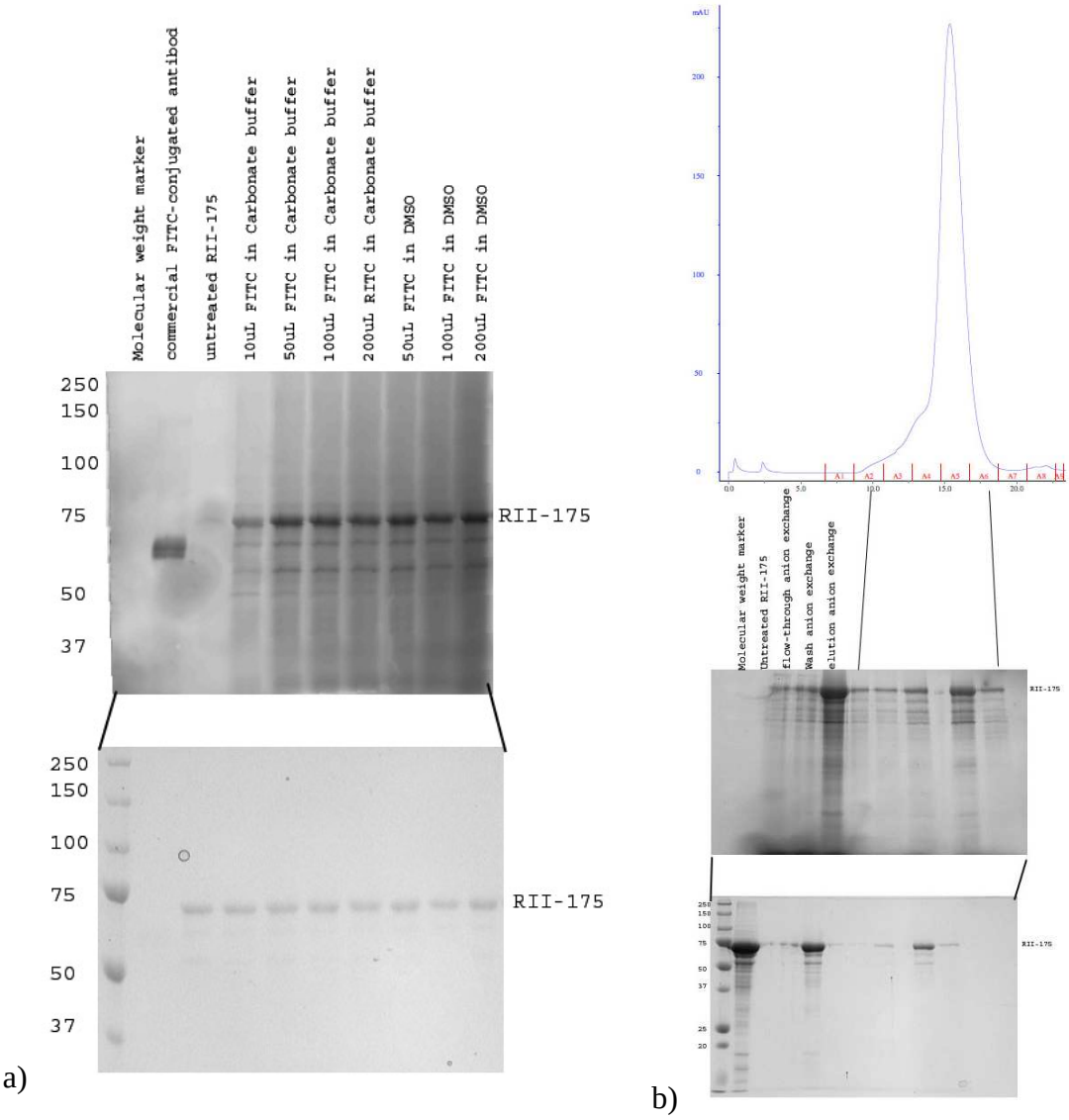

Figure 18: RII-175-FITC, a) FITC titration in Carbonate buffer and DMSO (top) FITC fluorescence detected by phosphoimager (bottom) Commassie Brilliant Blue stain of same gel, b) Gel filtration purification of RII-175-FITC after cation resin purification(on gel) (top) FITC fluorescence detected by phosphoimager (bottom) Commassie Brilliant Blue stain of same gel

a) Bright Field FITC

no RII-FITC

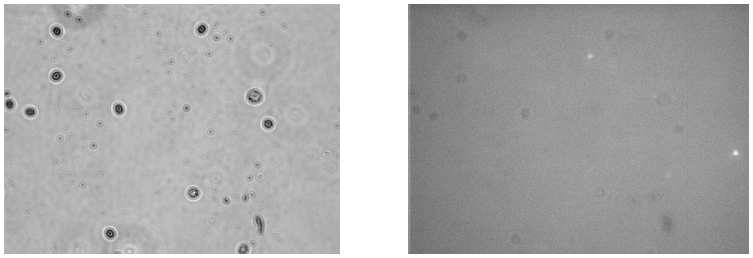

RII-FITC

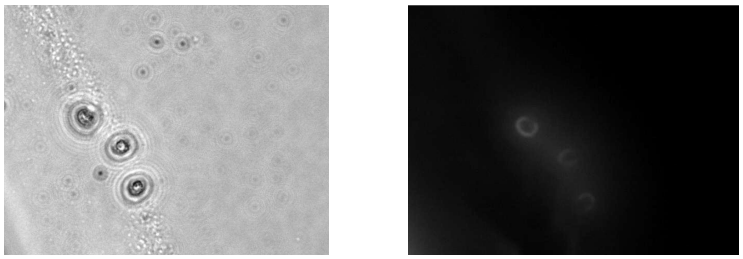

b)

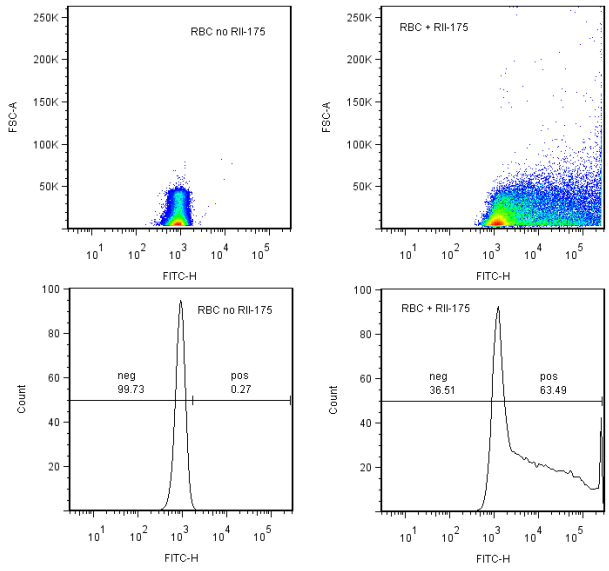

Figure 19: RII-175-FITC binding of RBCs a) RII-175-FITC fluorescence microscopy, b) RII-175-FITC FACS

Chapter 4: Receptor Specificity of RII-175 and Inhibition of Binding by Receptor Components

4.1: Introduction

It has previously been shown that RII-175 binds to GpA on the surface of RBCs. GpA is the main chymotrypsin resistant, trypsin sensitive receptor on the surface of RBCs [6]. Trypsin cleaves GpA at two sites, amino acids 31 and 39, both of which are located in exon 3. Rossetting assays have shown that when RBCs are incubated with either chymotrypsin or trypsin, RII-175 can only bind the chymotrypsin treated cells [6]. This establishes a reproducible pattern for receptor specificity in binding assays.

Binding Assays have also been used to assess the potency of inhibitors. It has previously been shown that SL can inhibit RII-175 binding RBCs in rosetting assays in the low milimolar range [19]. Related compounds have also been analyzed in rosetting assays. Of those tested, SL was the best inhibitor [19]. The major drawbacks to using the rosetting assay are that you cannot readily quantify expression of the malaria protein expressed in tissue culture and its surface expression and it is very hard to accurately quantify the number of RBCs bound to the cells expressing the malaria protein. Along with the inability to quantify the RBCs forming rosettes, it is also difficult to quantify what signifies a rosette (i.e. 5 RBCs or 100 RBCs). Other binding assays like a FACS assay can be used to accurately and quantitatively assess the potency of inhibitors.

In this chapter, I describe the receptor specificity of RII-175 and the use of small molecules in an inhibition study using the quantitative FACS assay developed in chapter 3.

4.2: Materials and Methods

4.2.1: RII-175 binding to RBCs. Red blood cells (RBC) were obtained from the Barnes Jewish Children's Hospital Blood Bank. 500,000 RBCs were diluted in 500uL DMEM with 10% FCS. His tagged 15mg/mL RII-175 was diluted 1:10 in DMEM with 10% FCS. 25uL of the diluted RII-175 was added to the RBCs (1uM RII final concentration) and the mixture incubated on ice for one hour. The RBCs were then washed three times with DMEM with 10% FCS. FITC conjugated anti-his antibody from Invitrogen was diluted 1:500 in DMEM with 10% FCS. 100uL of the diluted antibody was added to the washed RBC and incubated on ice for one hour. The RBCs were then washed three times. The RBCs were then resuspended in 2mL DMEM with 10% FCS. The RBCs were then analyzed using a BD FACScanto machine. All conditions were conducted in triplicate.

4.2.2: Treatment of RBCs. RBCs were incubated with either 2mg/mL Trypsin, 1mg/mL Chymotrysin, or 20uL of anti-GpA antibody from Santa Cruz Biosystems overnight at 4^{o}C. The treated RBCs were then used in binding assays as described above.

4.2.3: IC50 curves. His tagged 15mg/mL was diluted 1:10 in DMEM with 10% FCS. Compound (siallylactose (sl), peptide (pep), or siallylactose & peptide(slp)) was added to 25uL of diluted RII-175 to reach the desired concentration in a total of 50uL and the

mixture incubated at 4^{o}C overnight. The mixture was then added to RBCs prepared as described above in RII binding and the FACS assay conducted as described above in RII binding. All concentrations of inhibitor were conducted in triplicate.

4.3: Results

4.3.1: Receptor Specificity of RII-175

To test receptor specificity, I examined the effects of established enzyme treatments on RII-175 binding in the FACS assay described in chapter 3. RII-175-his was incubated with RBCs that had been treated with chymotrypsin, trypsin, or an antibody against GpA [fig 20]. RII-175 was able to bind the untreated and chymotrypsin treated cells but only minimally bound the trypsin and GpA antibody treated cells. The fluorescence seen in the sample of trypsin treated RBCs with RII-175 is equivalent to that of RBCs not incubated with RII-175. The reduction in binding seen in the GpA antibody sample is significant. The binding pattern for trypsin and chymotrypsin is consistent with previously published data.

4.3.2: IC50 Curves

To look at the influence of the various parts of the receptor, I examined the IC50 of 3'-siallylactose (SL), an unglycosylated peptide of GpA amino acids 27-59 that correspond to exon 3 (Pep), and 3'-siallylactose and the unglycosylated peptide (SLP). SL was tested for inhibition because it has been shown that SL on receptors is important for binding in rosetting assays and can inhibit binding slightly on its own. The

unglycosylated peptide was tested for inhibition to determine the importance of the peptide backbone for binding of receptor by RII-175. RII-175-his was incubated overnight at 4^{o}C in the presence of varying concentrations of SL, Pep, or SLP in the absence of RBCs. The samples were then incubated with RBCs and afterward incubated with anti-his antibody. The compounds SL, Pep, or SLP inhibited binding in the FACS assay to varying degrees [fig 21]. The SL alone was able to inhibit RII-175 binding at an IC50 concentration of 13mM. The Pep alone was unable to inhibit the RII-175 binding as shown by the IC50 concentration of >100mM. The SLP was slightly worse inhibitor of RII-175 binding with an IC50 concentration of 40mM.

4.4: Discussion

The RII-175 expressed and purified is functional and binds to GpA. The receptor specificity is supported by the RII-175 binding to chymotrypsin treated RBCs but not to trypsin treated cells. The receptor specificity is further supported by the reduction in binding upon RBC treatment with anti-GpA antibody, which blocks RII-175 binding by specifically targeting the receptor. It is also interesting that the trypsin cleaves at amino acids 31 and 39, which are in exon 3. This implies that this region may be important for RII-175 binding. The IC50 for SL was in the low milimolar range and implies that SL, while important for binding, is not the only portion of the receptor responsible for interaction with RII-175. The peptide incontrast did not inhibit binding under similar conditions. This may be due to the peptide lacking glycosylation, which is known to be important for binding. Further studies would be to identify the minimal binding domain

of GpA by FACS inhibition assays using GpA truncations and GpA glycosylation mutants.

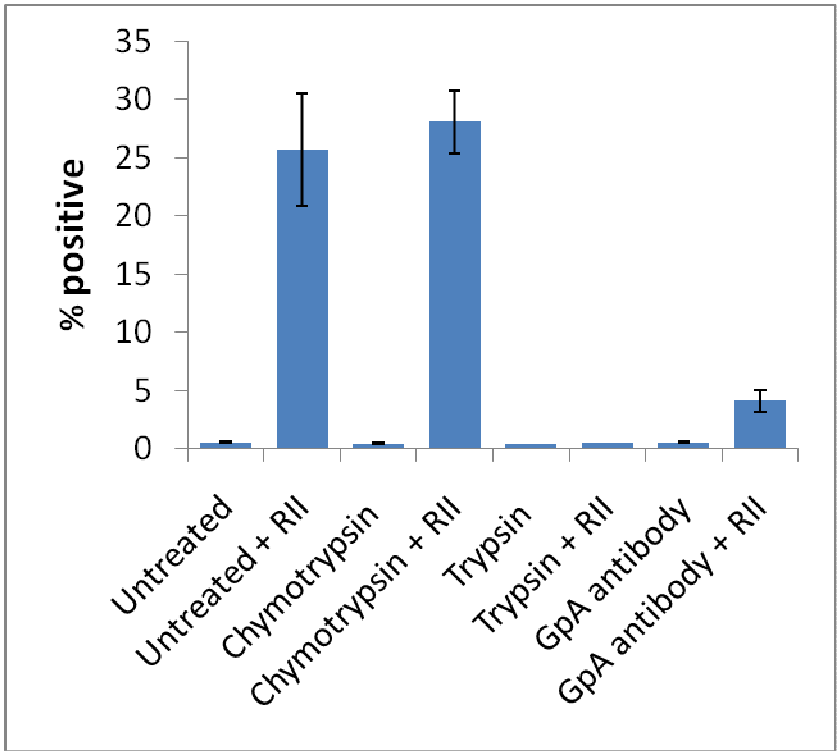

Figure 20: Erythrocyte binding by RII-175 in FACS. Trypsin treatment of erythrocytes or addition of an anti-glycophorin A antibody prevent binding of recombinant RII-175 while chymotrypsin treatment has no effect.

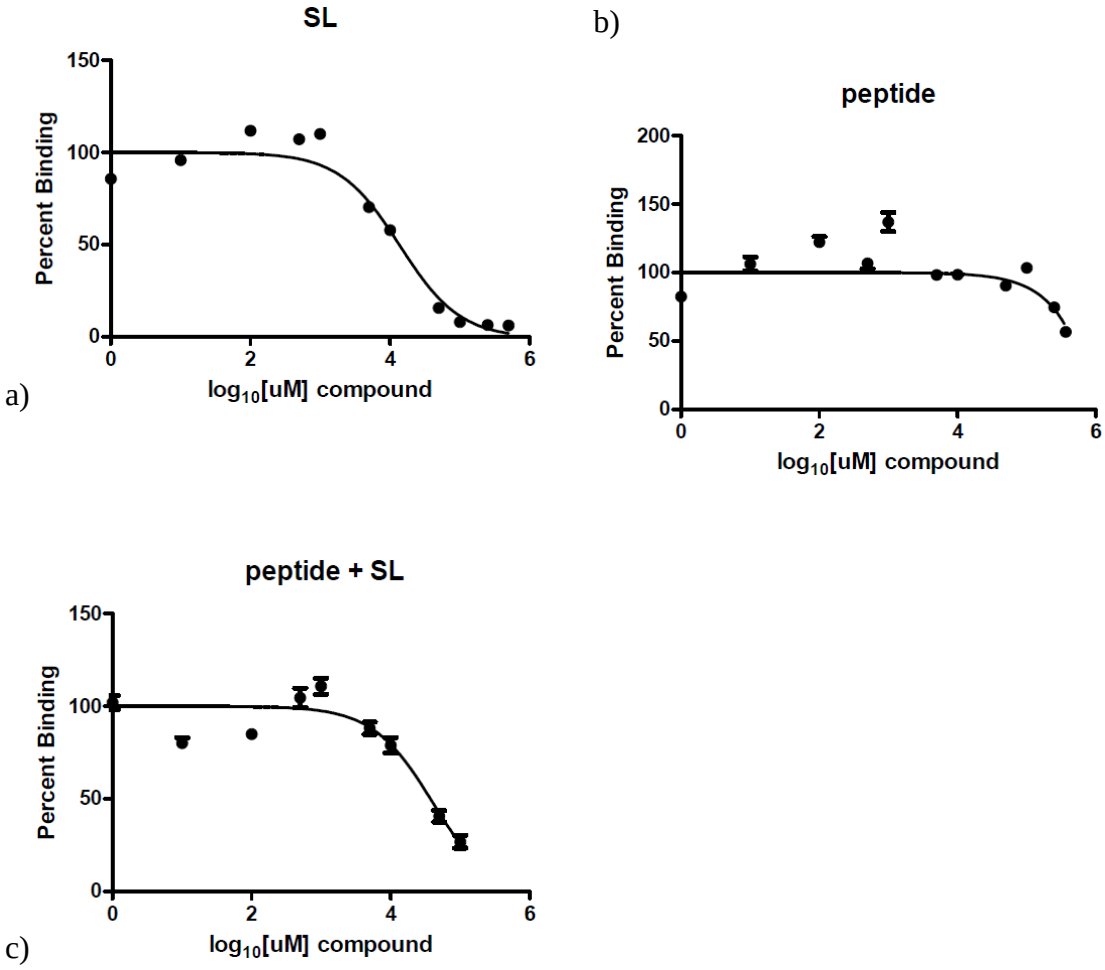

Figure 21: IC50 curves a) 3'-siallylactose (SL), b) peptide corresponding to truncation 4A (peptide), c) SL + peptide

Chapter 5: Protein/Protein Interaction Studies and Dimerization

5.1: Introduction

There are many methods that can be used to characterize protein/protein interactions. These methods include pulldowns, analytical ultracentrifugation (AUC), and multi-angle-light-scattering (MALS). All three methods will be discussed in this chapter. In a pulldown, protein/protein interactions are characterized using a tagged protein of interest as "bait" for other proteins. The tagged protein can be immobilized on agarose beads that are coupled to either a binding partner or antibody for the tag. This allows for controlled experiments with a known amount of the tagged protein of interest. The immobilized protein can then be used to pull other proteins that can bind the "bait" out of solution. The tagged protein of interest and its binding partners can then be determined through electrophoresis. The advantage of this method is that it can help to determine previously unknown binding partners for the "bait" protein and verify known binding partners. The drawback of this method is that it cannot characterize the kinetics or stoichiometry of binding.

AUC has several advantages over pulldowns, one of which is that it can analyze molecular weights of complexes in solution along with affinity constants for complexes. In AUC, the samples can range from hundreds of Daltons to many millions of Daltons and can be used to obtain the average molecular weight of components in solution [20, 21]. In a sedimentation equilibrium AUC experiment, samples are centrifuged at a set speed and the sample allowed to reach equilibrium where the amount of diffusion is equal

to that of the sedimentation. At equilibrium, larger molecules will sediment towards the bottom of the sample channel and smaller molecules will remain towards the top of the channel. Multiple speeds and concentrations can be analyzed together because the molecular weight at any point for a system at equilibrium is dependent on total concentration but is independent of rotor speed or radial position of the sample in the rotor [20, 21].

The molecular weight of the sample can be analyzed using linear regression with set models of association [20, 21]. The first model used is usually a 1-component ideal model, which can give the average molecular weight of the molecules in solution. It is best used with a known molecular weight of the possible species in solution. If the average molecular weight is not that of the monomer and the monomer weight cannot be fit, it indicates that a monomer-n-mer equilibrium may be occurring. If that is the case, a monomer-n-mer model can then be used to obtain the equilibrium constants for the molecule. The n-mer can be varied to achieve the best fit and may be suggested by the average molecular weight from the 1-component ideal model [20, 21]. It is the advantage of being able to determine molecular weight of molecules in solution and the association constants for complexes that make this method ideal for the analysis of RII-175 dimerization and interactions between RII-175 and components of its receptor GpA.

MALS can also determine the molecular weight of proteins and protein complexes in solution [22, 23]. A typical MALS consists of a size-exclusion chromatography column coupled with two to three detectors. The detectors commonly

used are a light-scattering detector and a refractive index detector. An UV absorbance detector can also be used in conjunction with the other detectors. The data from the detectors can be used to determine the size of the protein or complex as it is eluted from the size-exclusion column. The molecular weight can be determined when both the light scattering and refractive index are determined because the amount a protein scatters light is directly proportional to its size. While it is relatively straight forward to determine the molecular weight of a single protein, calculating the stoichiometry of a complex is slightly more complex. To determine a stoichiometry for a complex from MALS data, one must assume a given stoichiometry and verify if that stiochiometry fits the data given [22, 23]. There are a few drawbacks to using MALS to characterize protein-protein interactions and they include that it requires a higher affinity interaction and equilibrium constants cannot be determined.

In this chapter, I will describe experiments designed to characterize the dimerization of RII-175. These experiments include a pulldown with tagged and untagged RII-175, AUC sedimentation equilibrium experiment with and without GpA, and MALS.

5.2: Materials and Methods

5.2.1: RII-175 self association as shown through Pulldowns. 1uL of 1:10 diluted untagged RII-175 and 1:10 diluted his tagged RII-175 were incubated together on Nickel-agarose beads with His-tag buffer A for 30 min on ice. The beads were then washed 3

times. The beads were then resuspended in 10uL of SDS-PAGE dye and the samples run on a 8% SDS-PAGE gel.

5.2.2: AUC.

5.2.2.1: Optimization of Solution Conditions for RII-175 self association: RII-175 was buffer exchanged three times using a spin concentrator with either HEPES pH 7.4 50mM NaCl, HEPES pH 7.4 100mM NaCl, or HEPES pH 7.4 150mM NaCl. The buffer exchanged RII-175 was then diluted to an absorbance at 280nm of 0.8, 0.6, or 0.4. The samples were then run as an equilibrium experiment on a Beckman-Coulter ProteomeLab XL-A analytical ultra-centrifuge. Ultrascan was used to analyze the data produced by the sedimentation experiments.

5.2.2.2.: Determination of the Influence of 3'-siallylactose and GpA Peptide Backbone on RII-175 Self Association. RII-175 was buffer exchanged three times using a spin concentrator with either HEPES pH 7.4 150mM NaCl 4.6uM sl, HEPES pH 7.4 150mM NaCl 3uM sl, HEPES pH 7.4 150mM NaCl 1.5uM sl, HEPES pH 7.4 150mM NaCl 4.6uM pep, HEPES pH 7.4 150mM NaCl 3uM pep, HEPES pH 7.4 150mM NaCl 1.5uM pep, HEPES pH 7.4 150mM NaCl 4.6uM slp, HEPES pH 7.4 150mM NaCl 3uM slp, or HEPES pH 7.4 150mM NaCl 1.5uM slp. The buffer exchanged RII-175 was then diluted to an absorbance at 280nm of 0.6, 0.4, or 0.2 (4.6 uM, 3uM, or 1.5uM) according to the concentration of sl, pep, or slp in the buffer. The samples were then run as an equilibrium experiment on a Beckman-Coulter ProteomeLab XL-A analytical ultra-

centrifuge. Ultrascan was used to analyze the data produced by the sedimentation experiments.

5.2.3: Characterization of RII-175 self association in solution using Multi-angle Light Scattering. RII-175 at a concentration of either 9uM or 30uM in 300uL was buffer exchanged three times using a spin concentrator into MALS running buffer (HEPES pH 7.4 150mM NaCl) and concentrated to 300uL. All 300uL of RII-175 solution was filtered and then injected. The MALS located in the Fremont lab is composed of an Waters 600S HPLC connected to a Wyatt WTC-030S5 gel filtration column (5um coated silica, 300-Å pore), a Waters 996 UV/VIS detector, a Wyatt Optilab-tex refractive index detector, and a Wyatt Dawn-heleos light scattering detector. Astra software is used in conjunction with the MALS to determine the experimental molecular weight of the resultant peaks.

5.3: Results

5.3.1: Optimization of RII-175 Pulldown to Characterize Self Association

RII-175 is a dimer in the crystal structure and the dimer model is supported by mutation studies, but direct interaction between RII-175 monomers has not been characterized. Therefore, a pulldown protocol was developed for RII-175 dimerization to show that RII-175 can interact with itself. RII-175-his was used to pulldown RII-175 on nickel-agarose beads. 5uM RII-175-his and 5uM RII-175 were used in the pulldown. In the pulldown, RII-175-his was able to bind RII-175 [fig 22]. The control of RII-175 on

the nickel-agarose beads had a very small amount of non-specific binding, but the amount seen is not enough to account for that seen in the RII-175/RII-175-his sample.

5.3.2: Optimization of Solution Conditions for RII-175 self association

The optimum conditions for the formation of the dimer in solution have not yet been defined and to determine the conditions a sedimentation equilibrium experiment was conducted with RII-175 in HEPES pH 7.4 buffer with either 50mM NaCl, 100mM NaCl, or 150mM NaCl at speeds of 7.5k, 9k, and 14k. The speeds were chosen according to the Laue equations were the lowest speed is greater than 1.4 for the equation $(M/L)^2$ and the highest speed is greater than 3 for the equation $(H/L)^2$. M is the ideal speed for the molecular weight as chosen from a RPM vs. molecular weight vs. approximate sedimentation coefficient chart originally developed by Chervenka in 1970. Using the chart and a molecular weight of 70kDa for the monomer of RII-175, the speed for M was determined to be 9k. L and H, the high and low speeds, were derived from the previous equations with the chosen M and were determined to be 7.5k and 14k respectively. Unfortunately, the 14k speed was at meniscus depletion for the dimer and no fit was obtained for any of the samples at this speed. Fits could also not be obtained for the highest concentration of RII-175 as based on the variance and residuals and may be due to overloading the cell.

The samples at 4uM and 2uM RII-175 were first analyzed with a 1-component ideal model. In the 1-component ideal model, molecular weight can be fixed, as well as, floated to obtain the average molecular weight of the sample and a fit for each weight

tested [table 2, fig 23-31]. The monomer and dimer weights, 70kDa and 140kDa respectively, were fixed for each sample and the fit obtained for each molecular weight. Neither weight was able to give a reasonable fit as seen by the high variance and the curved residuals. Each sample was then tested with the molecular weight allowed to float. When this was done, the variance and residuals became much more reasonable and the average molecular weight for each sample was obtained. The average molecular weight for the 50mM NaCl, 100mM NaCl, and 150mM NaCl samples were 98.92kDa, 101.6kDa, and 104.02kDa respectively. The average molecular weight being between the ideal for the monomer and dimer molecular weight suggests a monomer/dimer equilibrium.

Based on the results from the 1-component ideal model, a monomer/dimer equilibrium model was then used to analyze all samples at single concentrations at 7k, 9k, 7k and 9k and at all concentrations at 7k and 9k [table 3 and fig 32-43]. The fits and K_ds were obtained for each concentration of salt [table 3]. The K_d for the 50mM, 100mM, and 150mM NaCl sample was 13.19uM, 9.75uM, and 7.90uM respectively. The result that the K_d is in the low micromolar range suggests that the RII-175 is a weak dimer in solution and that the salt concentration in solution has no influence on dimer formation. Based on these results, the salt concentration used in subsequent experiments was 150mM NaCl.

5.3.3: Determination of the Influence of 3'-siallylactose and GpA Peptide Backbone on RII-175 Self Association

A sedimentation equilibrium experiment was conducted with RII-175 in HEPES pH 7.4 150mM NaCl buffer with either SL, Pep, or SLP at a ratio to RII-175 of 1:1. The samples were analyzed with a monomer/dimer equilibrium model and this model was chosen based on the results from the salt gradient experiment [table 4, fig 44-52]. The highest concentration of RII-175 was excluded from the analysis of the SL and SLP samples due to overloading and a small dynamic range of 0.6 to 0.8. The lowest concentration of RII-175 was excluded from the analysis for the SL and SLP samples based on the small dynamic range due to underloading. The K_d for the SL and SLP samples at 7.5k and 9k for the 3uM concentration was 4.19uM and 1.8uM respectively. The K_d for the Pep sample at all speed and concentrations was 2.20uM. The resulting K_d for the SL, Pep, and SLP samples is similar but slightly lower to that obtained in the salt gradient, and this suggests that the presence of 3'-siallylactose and peptide alone and 3'-siallylactose and peptide were unable to greatly influence the K_d of dimerization. The small change in K_d may be due to the SL, PEP, and SLP interacting with the RII-175.

5.3.4: Determination of Oligomerization State in Solution by MALS

To determine if RII-175 is a dimer in solution, MALS was conducted on RII-175 at two concentrations: 9uM and 30uM [fig 53]. 9uM and 30uM are within the range of the K_d seen in AUC in identical buffer. RII-175 ran at a molecular weight of 73 and 70 kDa respectively. This result is different from that seen in AUC experiments and may be due to dissociation of the complex on the column as the protein becomes diluted.

5.4: Discussion

RII-175 is a weak dimer. This is supported by the ability of RII-175-his to bind RII-175 in the pulldown. This is also supported by the AUC data. In the 1-component ideal model, the average molecular weight is around 100kDa, which is between that of the monomer and dimer, 70kDa and 140kDa respectively. The monomer/dimer equilibrium model also supports the weak dimer with the K_d ranging from 7-13uM for the salt gradient sedimentation experiment and 1-14uM for the SL, Pep, and SLP experiments. The dimer is also supported by previous mutation studies. The MALS in contrast did not show any dimer in solution. The protein may have dissociated on the column resulting in only a monomer peak. This result may also be explained by the weak K_d as determined by the AUC.

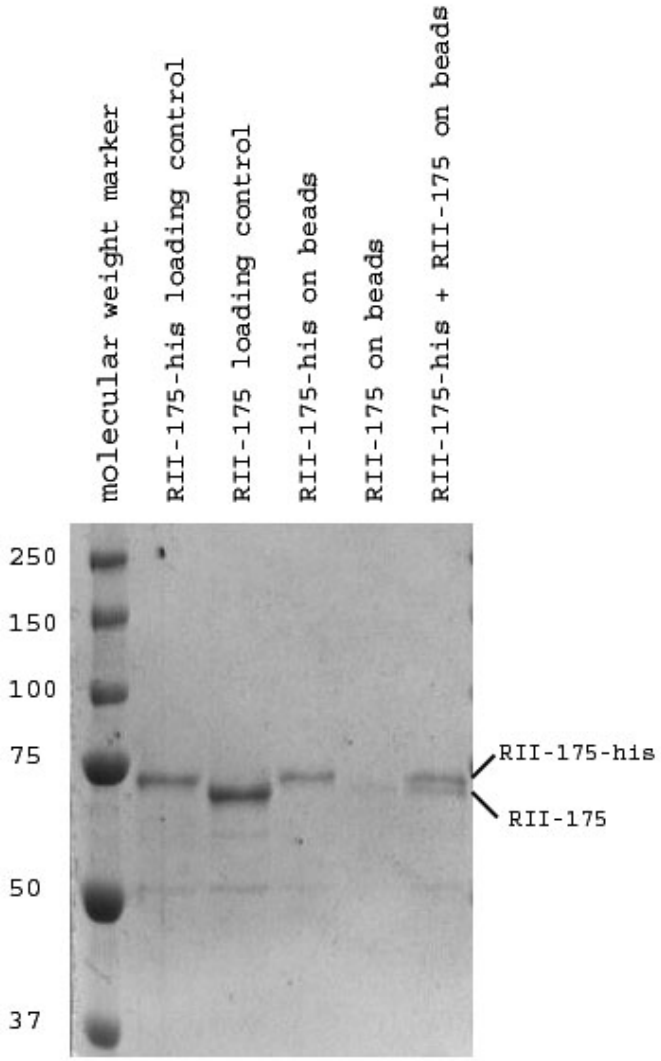

Figure 22: RII-175 dimer pull-down on Nickel-agarose beads

Salt	concentration	MW (kDa)	variance (10^-6)
50mM	4uM, 2uM	98.92	12.2
50mM	4uM, 2uM	70	49
50mM	4uM, 2uM	140	63.4
100mM	4uM, 2uM	101.6	12.2
100mM	4uM, 2uM	70	48.3
100mM	4uM, 2uM	140	66.1
150mM	4uM, 2uM	104.02	19.6
150mM	4uM, 2uM	70	94.5
150mM	4uM, 2uM	140	101

Table 2: 1-Component Ideal Model fits for RII-175 in HEPES pH 7.4 with 50mM, 100mM, or 150mM NaCl

50mM NaCl

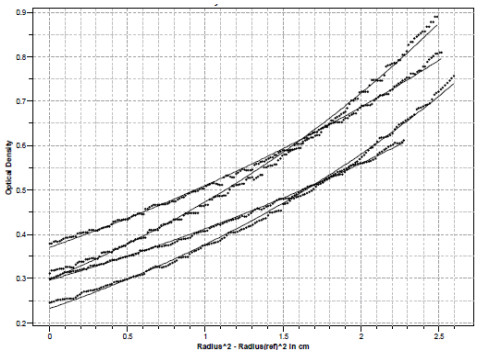

4uM

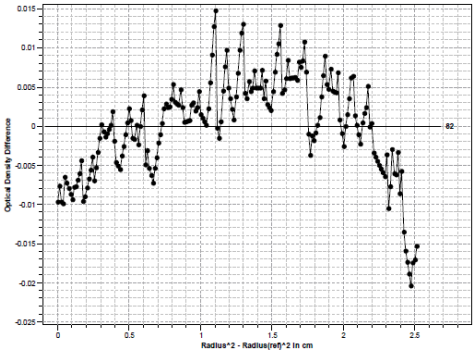

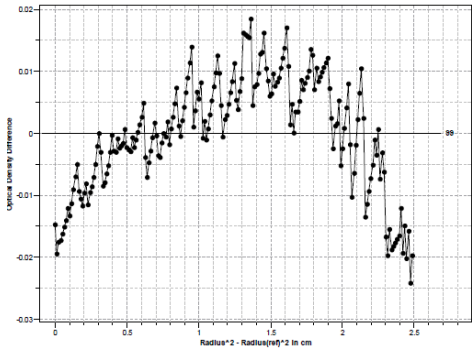

2uM

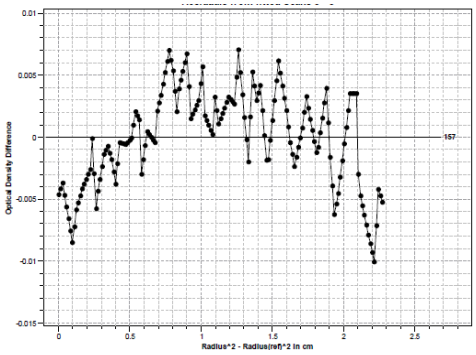

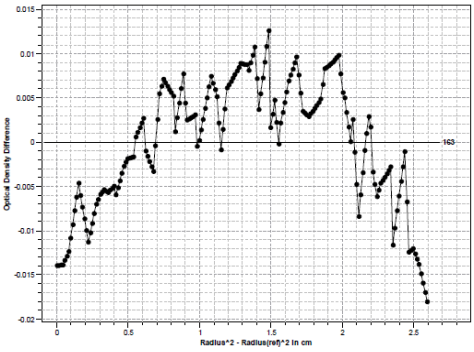

Figure 23: 1-component ideal model using 70kDa molecular weight (left) 7.5k residuals (right) 9k residuals

50mM NaCl

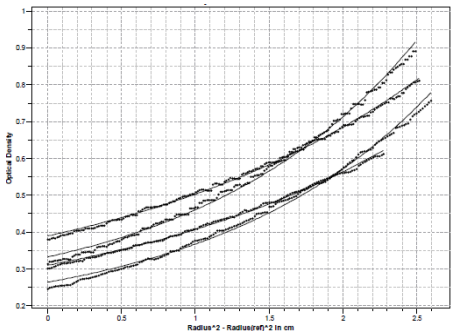

4uM

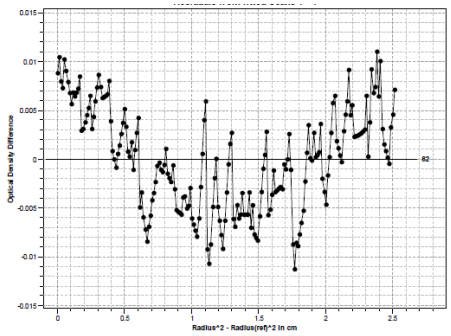

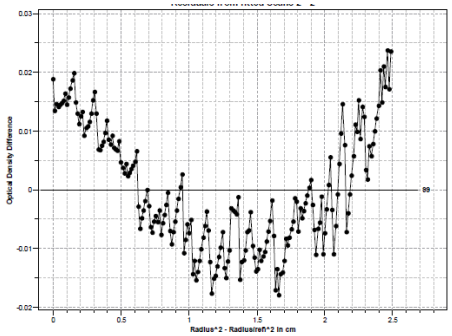

2uM

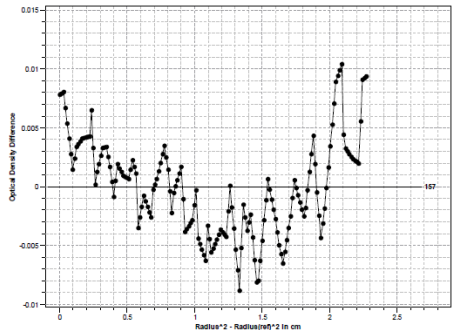

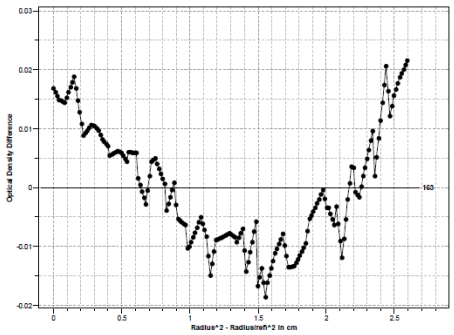

Figure 24: 1-component ideal model using 140kDa molecular weight (left) 7.5k residuals (right) 9k residuals

50mM NaCl

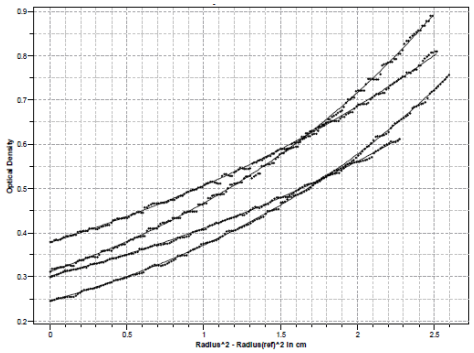

4uM

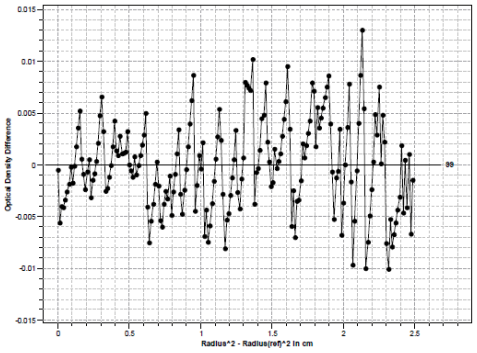

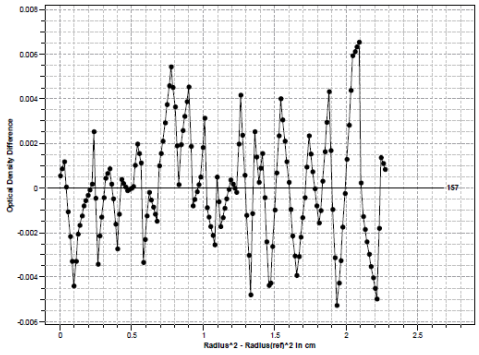

2uM

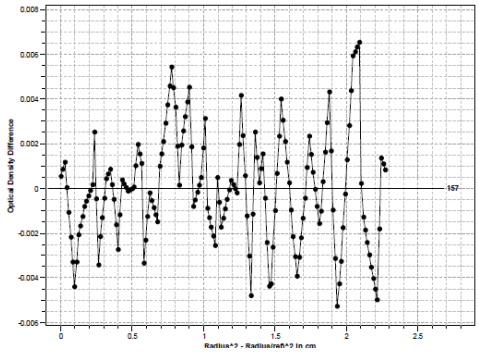

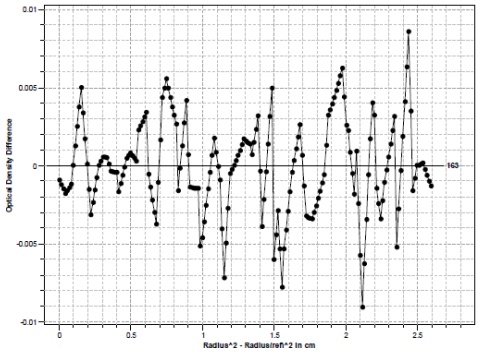

Figure 25: 1-component ideal model using 98.9kDa molecular weight (left) 7.5k residuals (right) 9k residuals

100mM NaCl

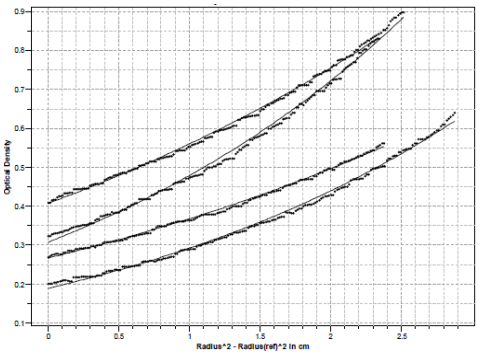

4uM

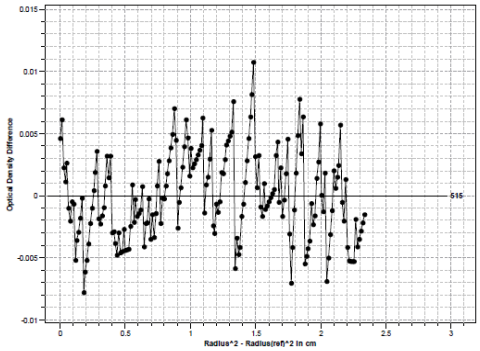

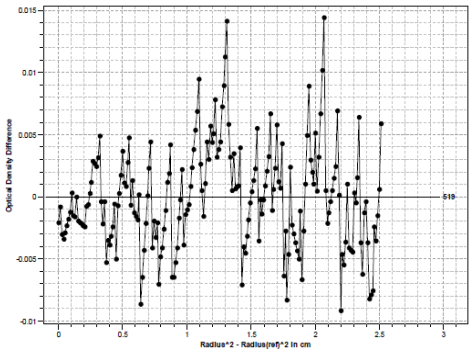

2uM

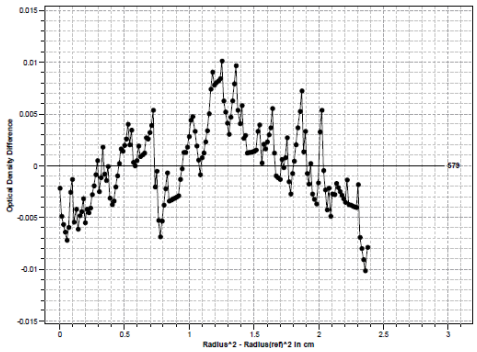

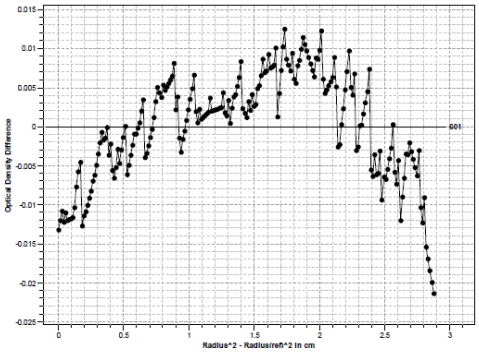

Figure 26: 1-component ideal model using 70kDa molecular weight (left) 7.5k residuals (right) 9k residuals

100mM NaCl

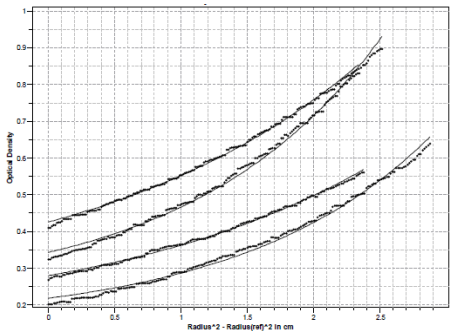

4uM

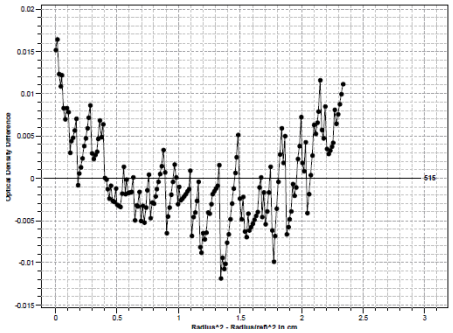

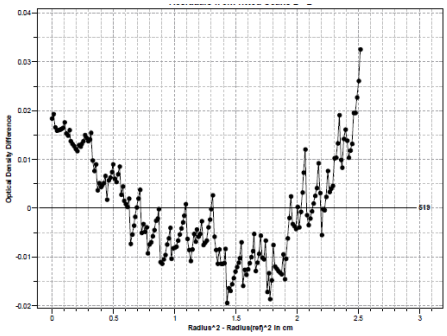

2uM

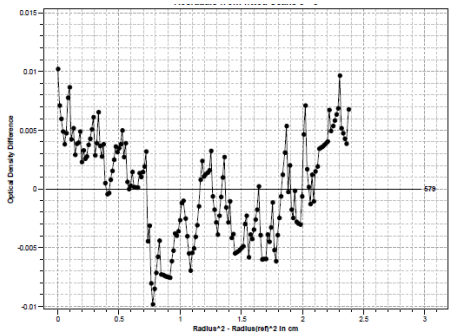

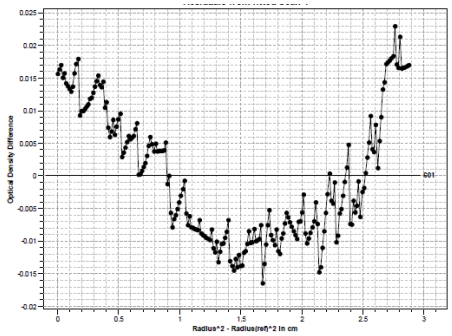

Figure 27: 1-component ideal model using 140kDa molecular weight (left) 7.5k residuals (right) 9k residuals

100mM NaCl

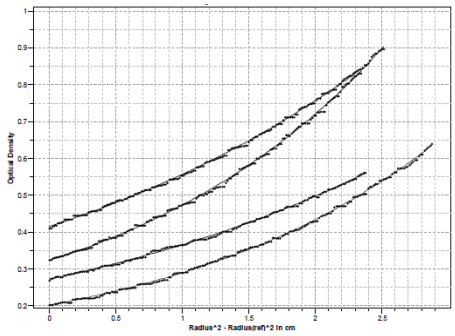

4uM

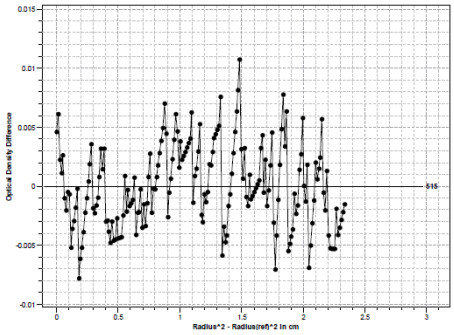

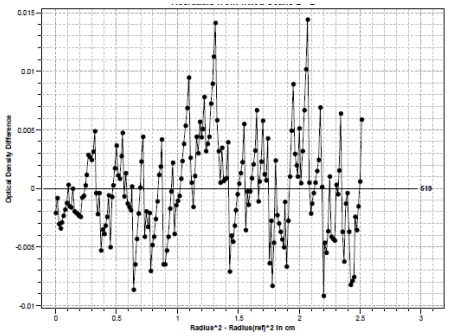

2uM

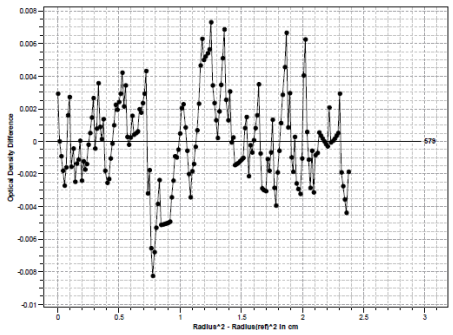

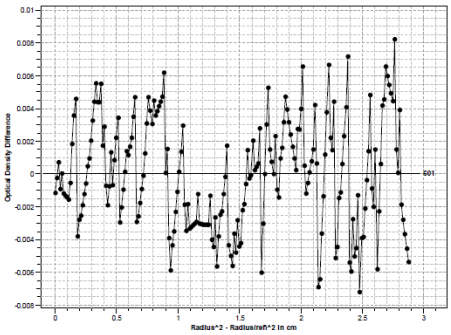

Figure 28: 1-component ideal model using 101kDa molecular weight (left) 7.5k residuals (right) 9k residuals

150mM NaCl

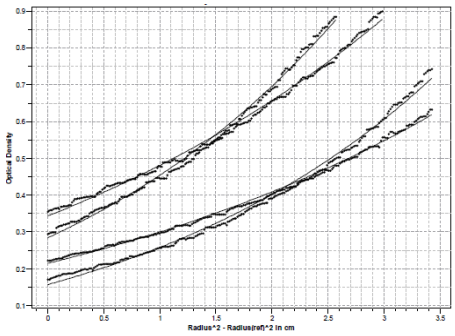

4uM

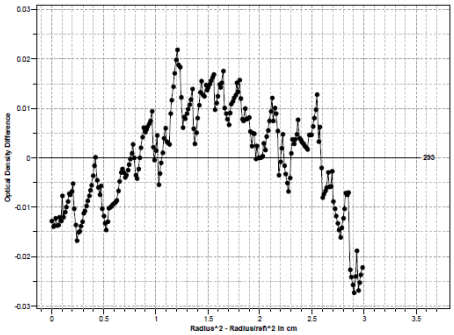

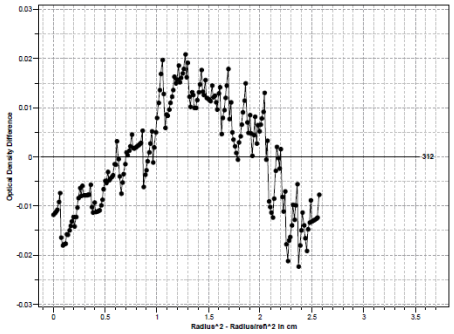

2uM

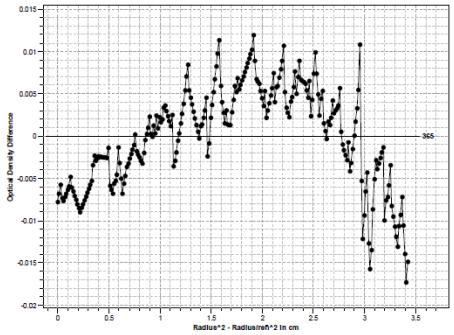

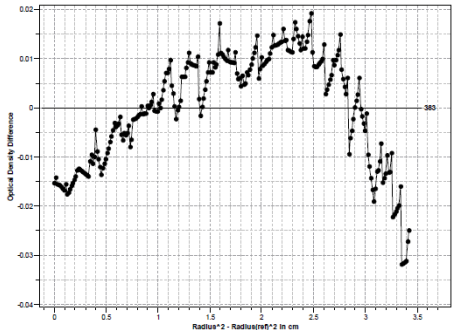

Figure 29: 1-component ideal model using 70kDa molecular weight (left) 7.5k residuals (right) 9k residuals

150mM NaCl

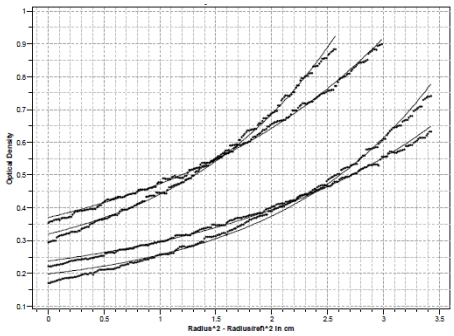

4uM

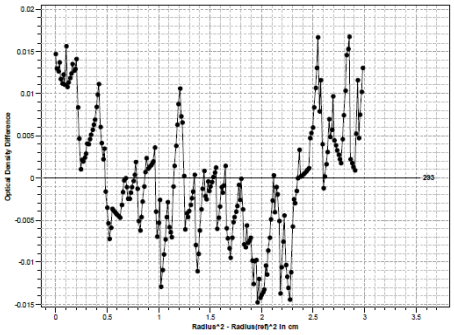

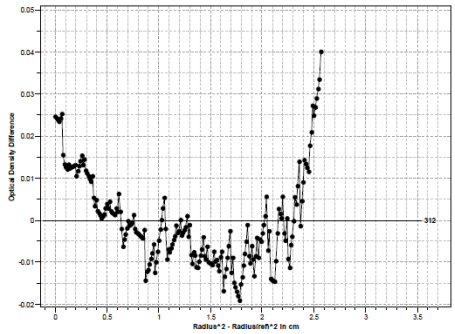

2uM

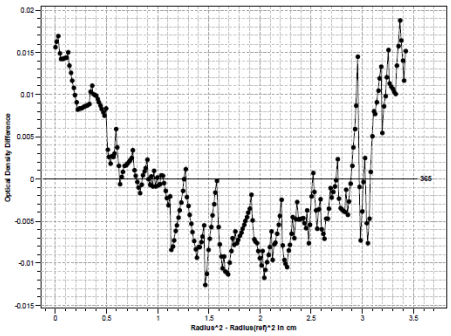

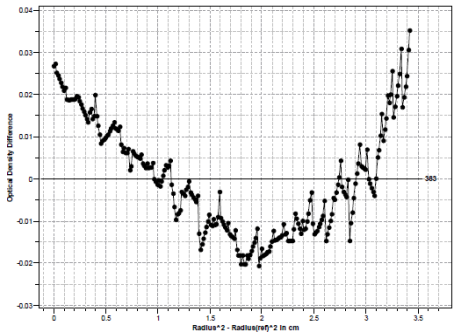

Figure 30: 1-component ideal model using 140kDa molecular weight (left) 7.5k residuals (right) 9k residuals

150mM NaCl

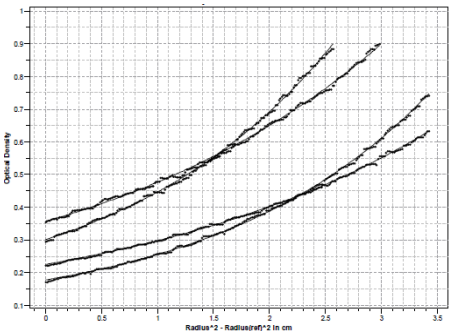

4uM

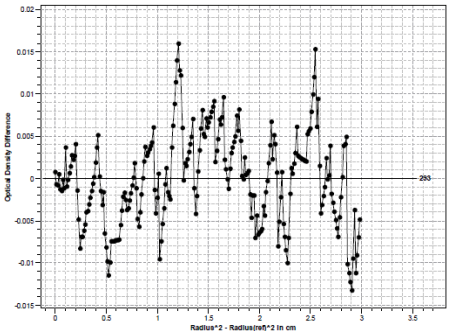

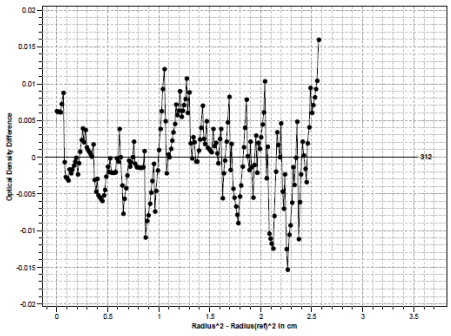

2uM

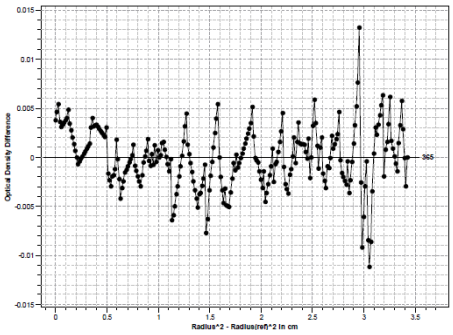

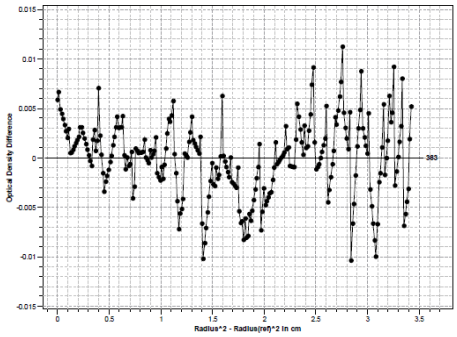

Figure 31: 1-component ideal model ussing 104kDa molecular weight (left) 7.5k residuals (right) 9k residuals

50mM			
concentration	speed	K_d (uM)	variance (10^-6)
4uM	7.5K	5.59	11.50
4uM	9k	13.16	18.10
4uM	7.5k/9k	11.58	15.00
2uM	7.5K	12.46	5.79
2uM	9k	21.13	8.70
2uM	7.5k/9k	15.83	7.30
4uM/2uM	7.5k/9k	13.19	11.50

100mM			
concentration	speed	K_d (uM)	variance (10^-6)
4uM	7.5K	6.57	10.70
4uM	9k	10.02	16.10
4uM	7.5k/9k	8.44	13.60
2uM	7.5K	7.68	7.80
2uM	9k	11.92	10.80
2uM	7.5k/9k	9.94	9.50
4uM/2uM	7.5k/9k	9.75	11.40

150mM			
concentration	speed	K_d (uM)	variance (10^-6)
4uM	7.5K	3.89	25.30
4uM	9k	7.61	23.90
4uM	7.5k/9k	7.09	27.20
2uM	7.5K	8.59	9.36
2uM	9k	8.56	12.80
2uM	7.5k/9k	7.21	12.10
4uM/2uM	7.5k/9k	7.90	18.60

Table 3: K_d and variance for monomer/dimer equilibrium model for 50mM, 100mM, 150mM NaCl samples

50mM NaCl 4uM/7k 4uM/9k

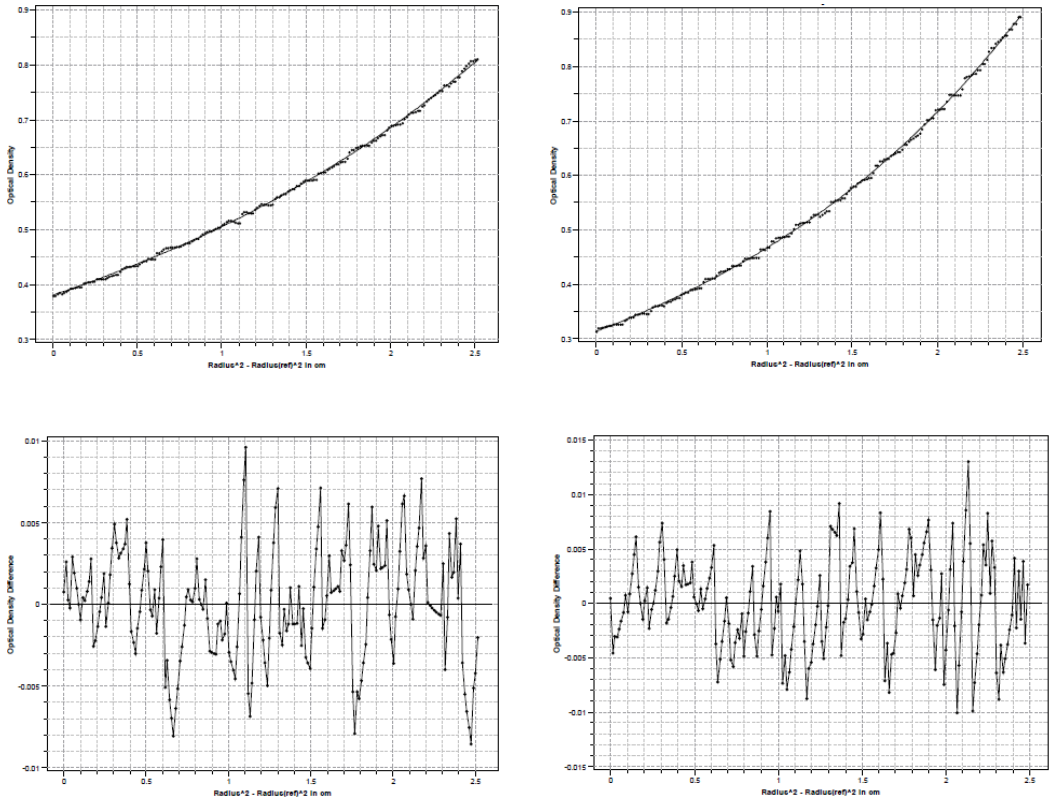

Figure 32: monomer/dimer model overlays and residuals for 50mM NaCl, 4uM RII-175

50mM NaCl 2uM/7k 2uM/9k

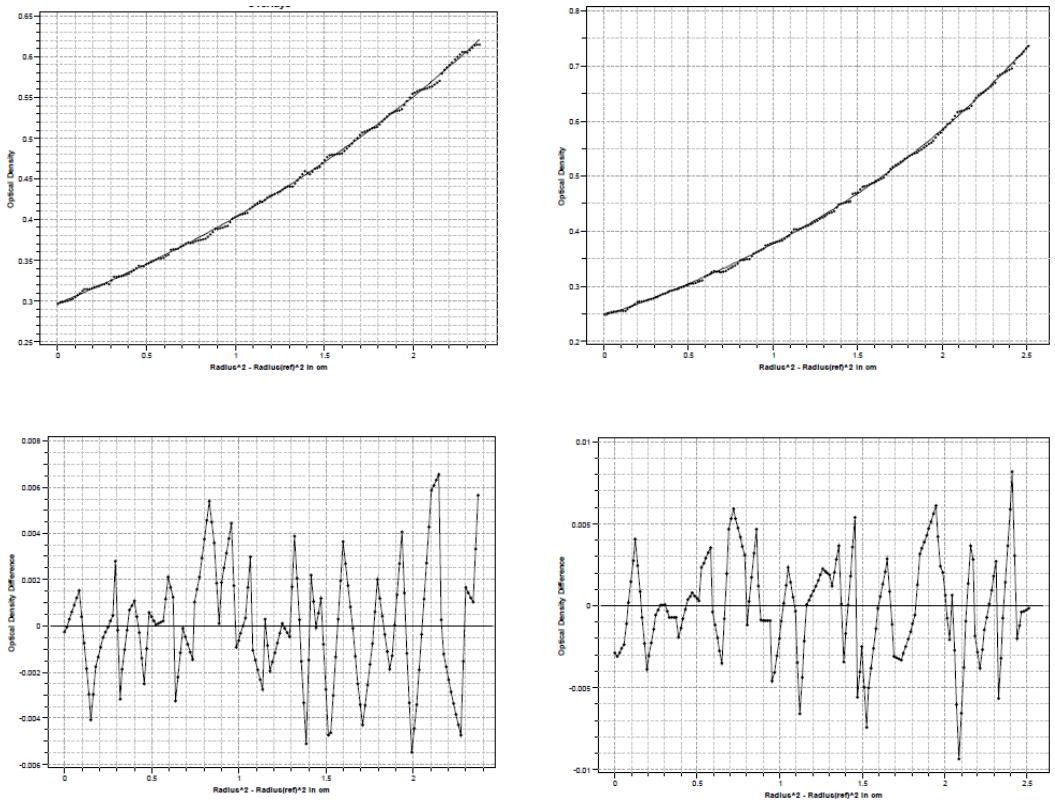

Figure 33: monomer/dimer model overlays and residuals for 50mM NaCl, 2uM RII-175

50mM 4uM/7k, 9k 2uM/7k, 9k

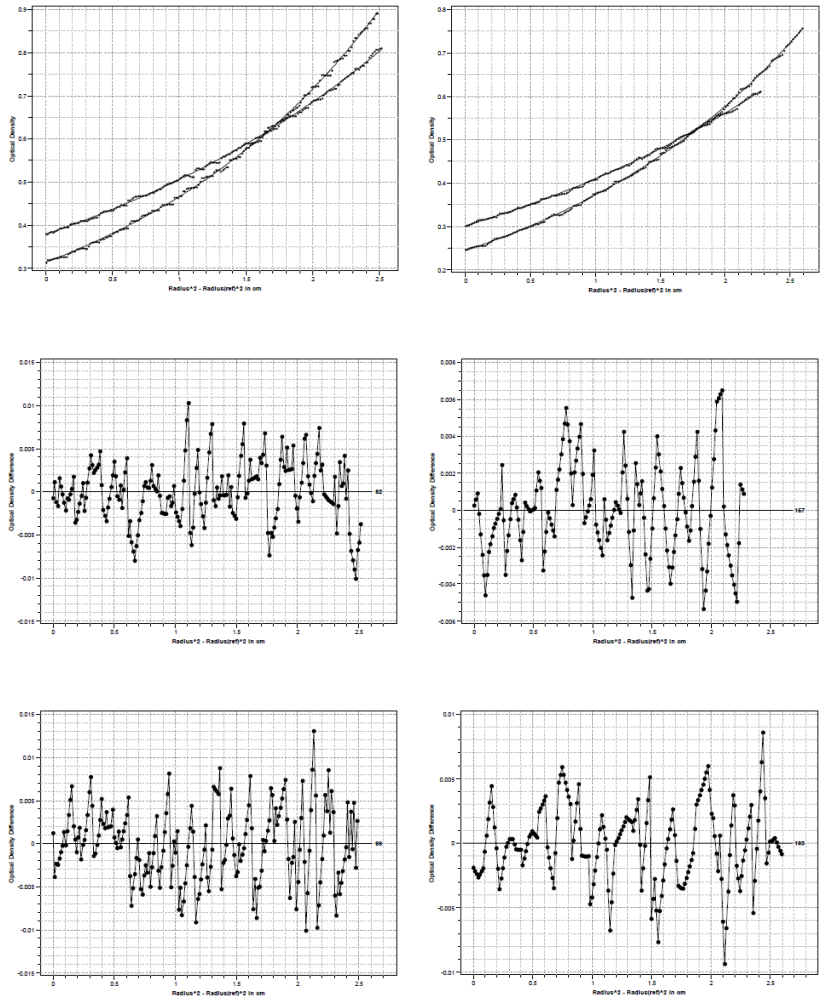

Figure 34: monomer/dimer model overlays and residuals for 50mM NaCl, 7k combined with 9k

50mM

NaCl

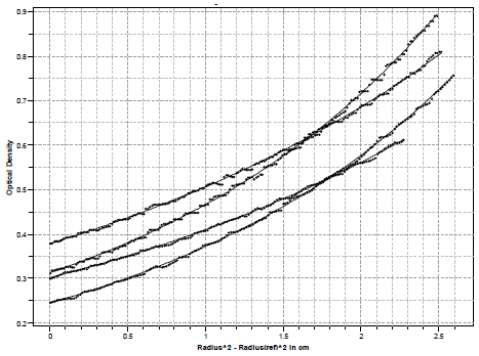

4uM

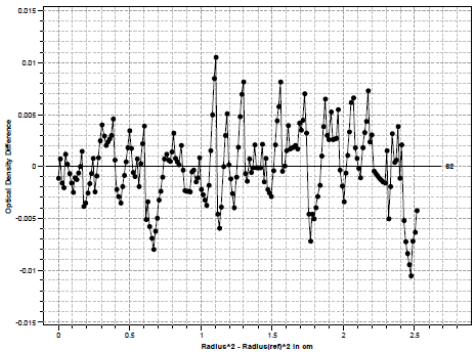

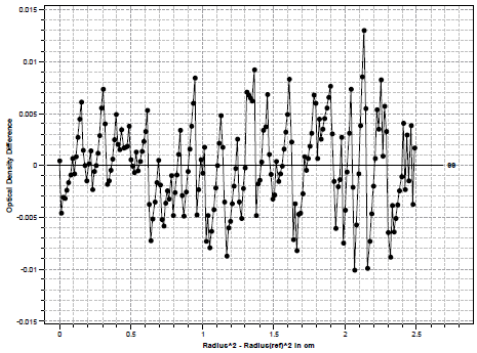

2uM

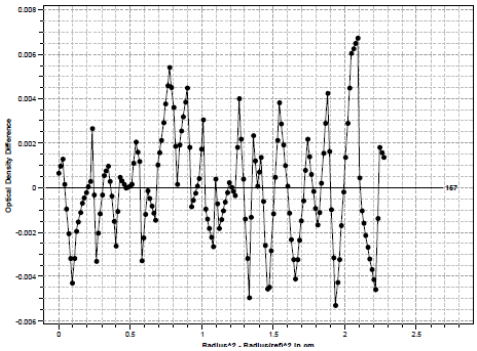

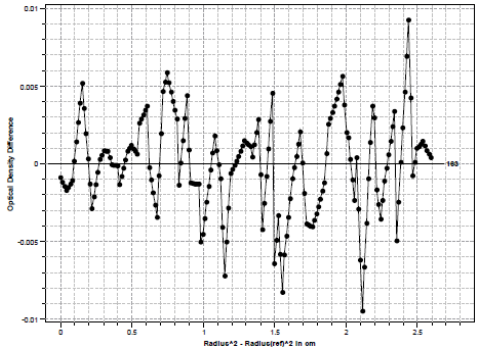

Figure 35: monomer/dimer model (left) 7.5k residuals, (right) 9k residuals for 50mM with 4uM and 2 uM RII-175

100mM NaCl 4uM/7k 4uM/9k

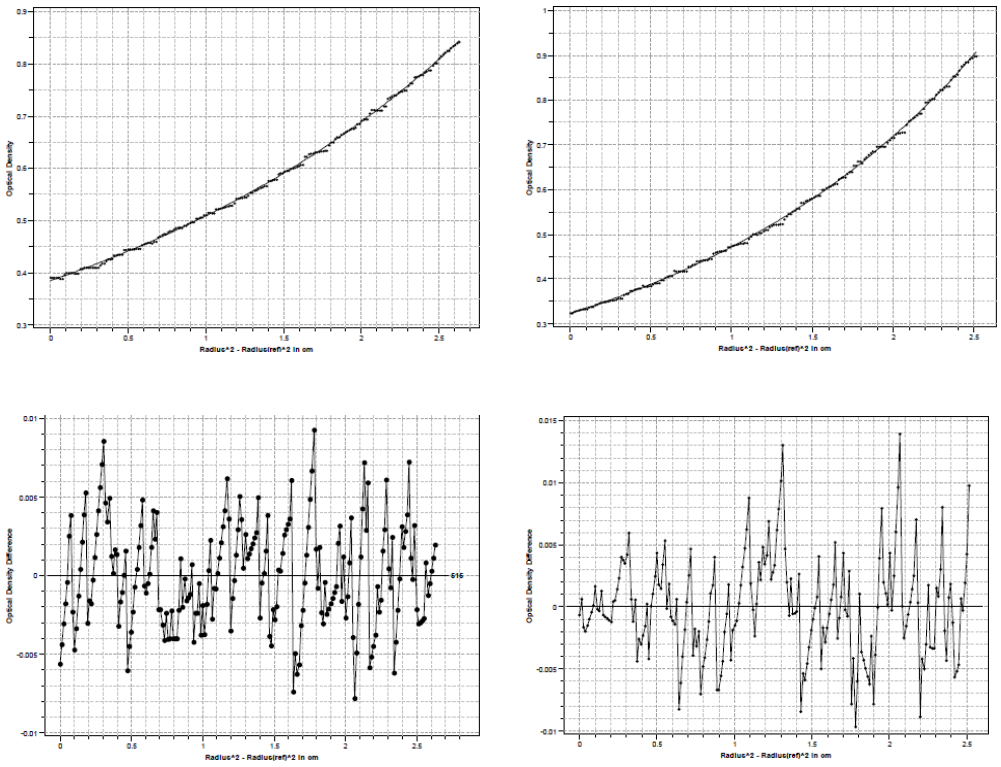

figure 36: monomer/dimer model overlays and residuals for 100mM NaCl, 4uM RII-175

100mM NaCl 2uM/7k 2uM/9k

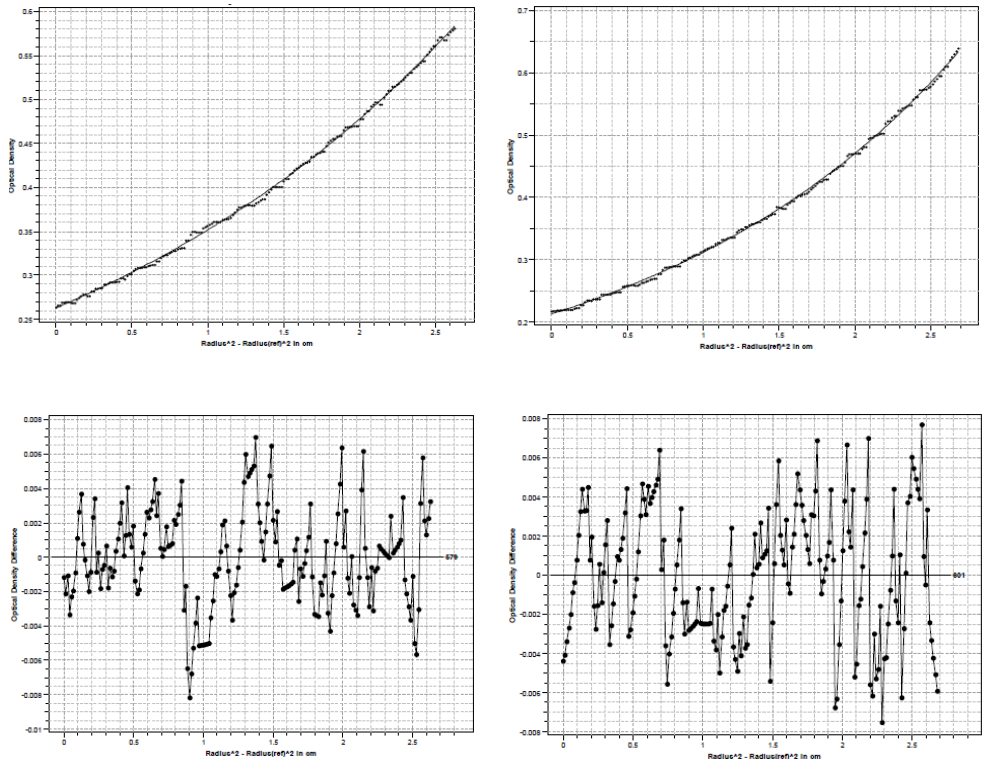

Figure 37: monomer/dimer model overlays and residuals for 100mM NaCl, 2uM RII-175

100mM 4uM/7k, 9k 2uM/7k, 9k

7k

9k

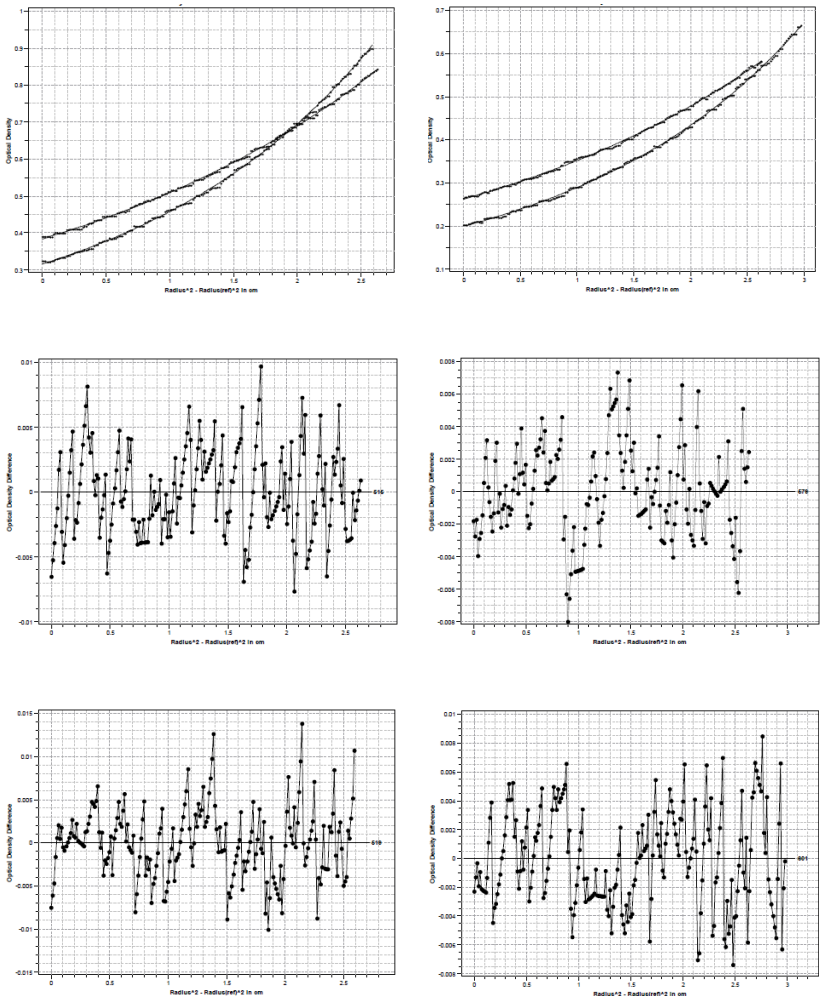

Figure 38: monomer/dimer model overlays and residuals for 100mM NaCl, 7k combined with 9k

100mM NaCl

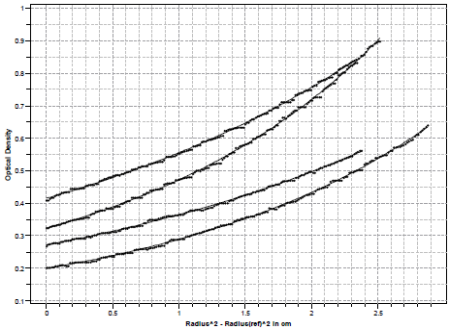

4uM

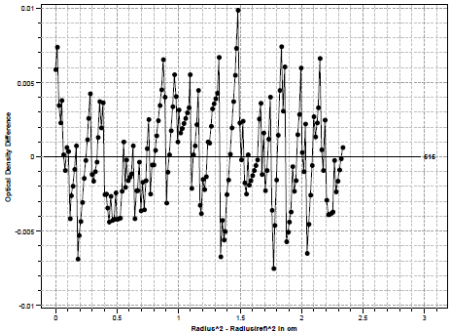

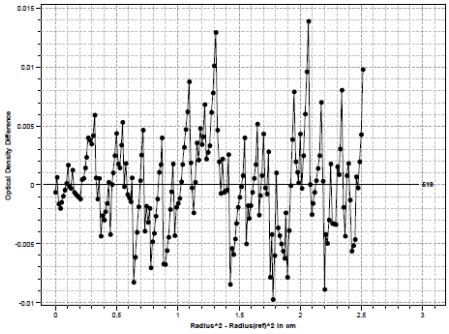

2uM

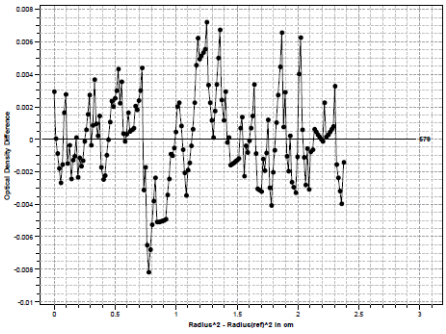

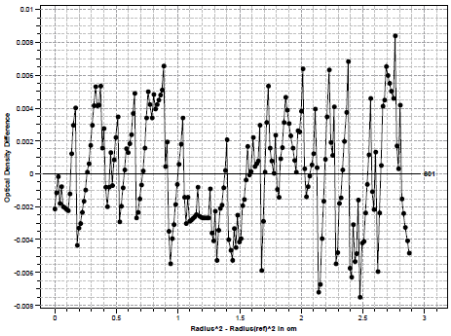

figure 39: monomer/dimer model (left) 7.5k residuals, (right) 9k residuals for 100mM NaCl with 4uM and 2uM RII-175

150mM NaCl 4uM/7k 4uM/9k

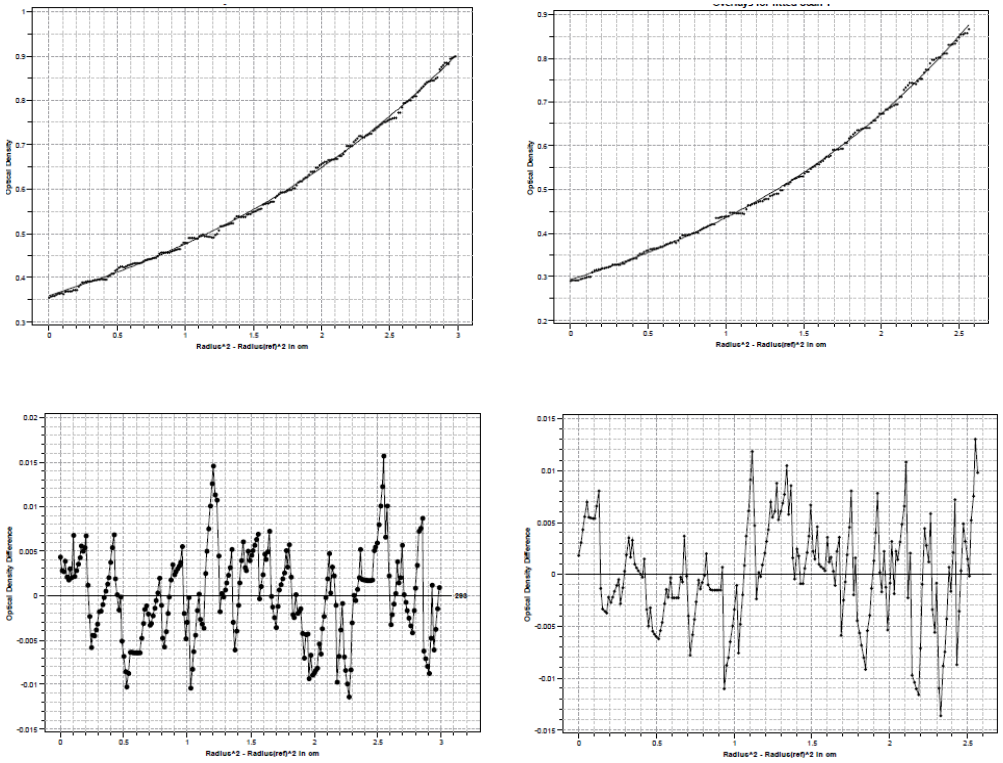

figure 40: monomer/dimer model overlays and residuals for 150mM NaCl, 4uM RII-175

150mM NaCl 2uM/7k 2uM/9k

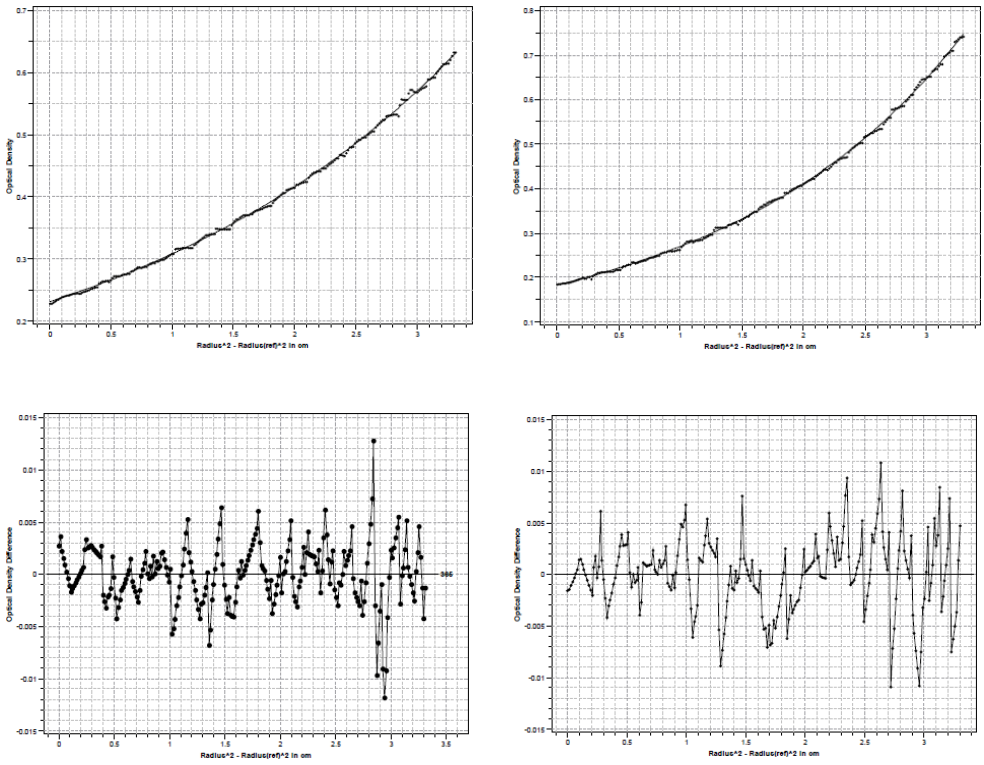

figure 41: monomer/dimer model overlays and residuals for 150mM NaCl, 2uM RII-175

150mM 4uM/7k, 9k 2uM/7k, 9k

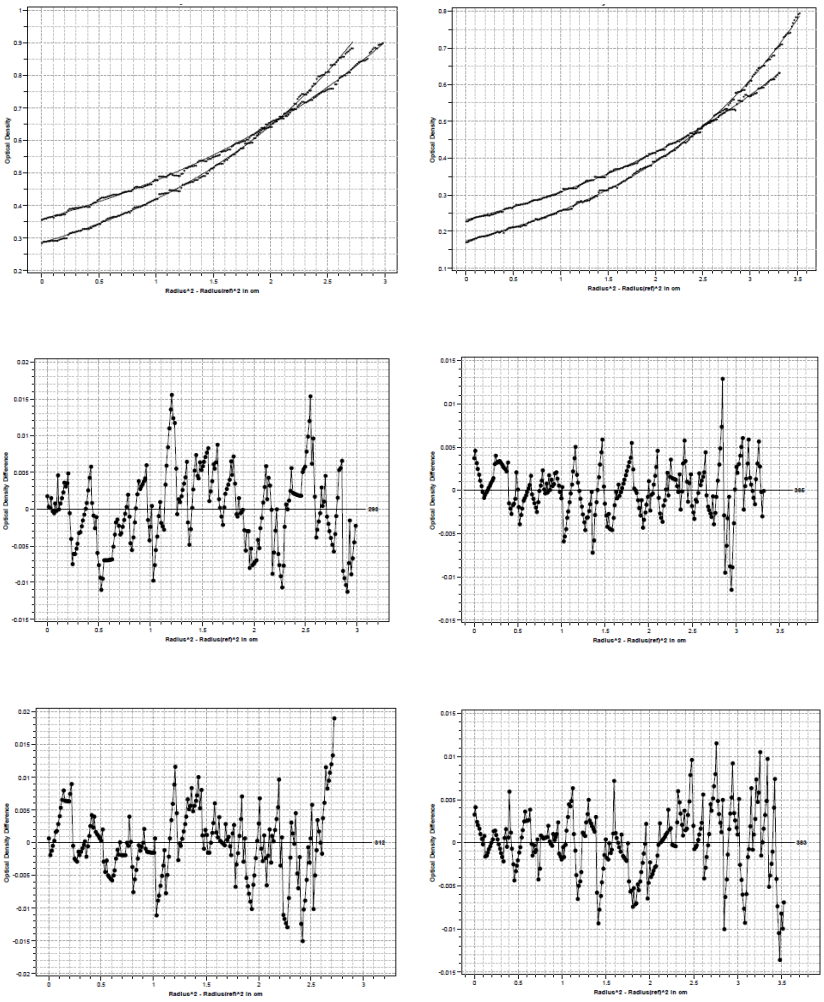

Figure 42: monomer/dimer model overlays and residuals for 150mM NaCl, 7k combined with 9k

150mM NaCl

4uM

2uM

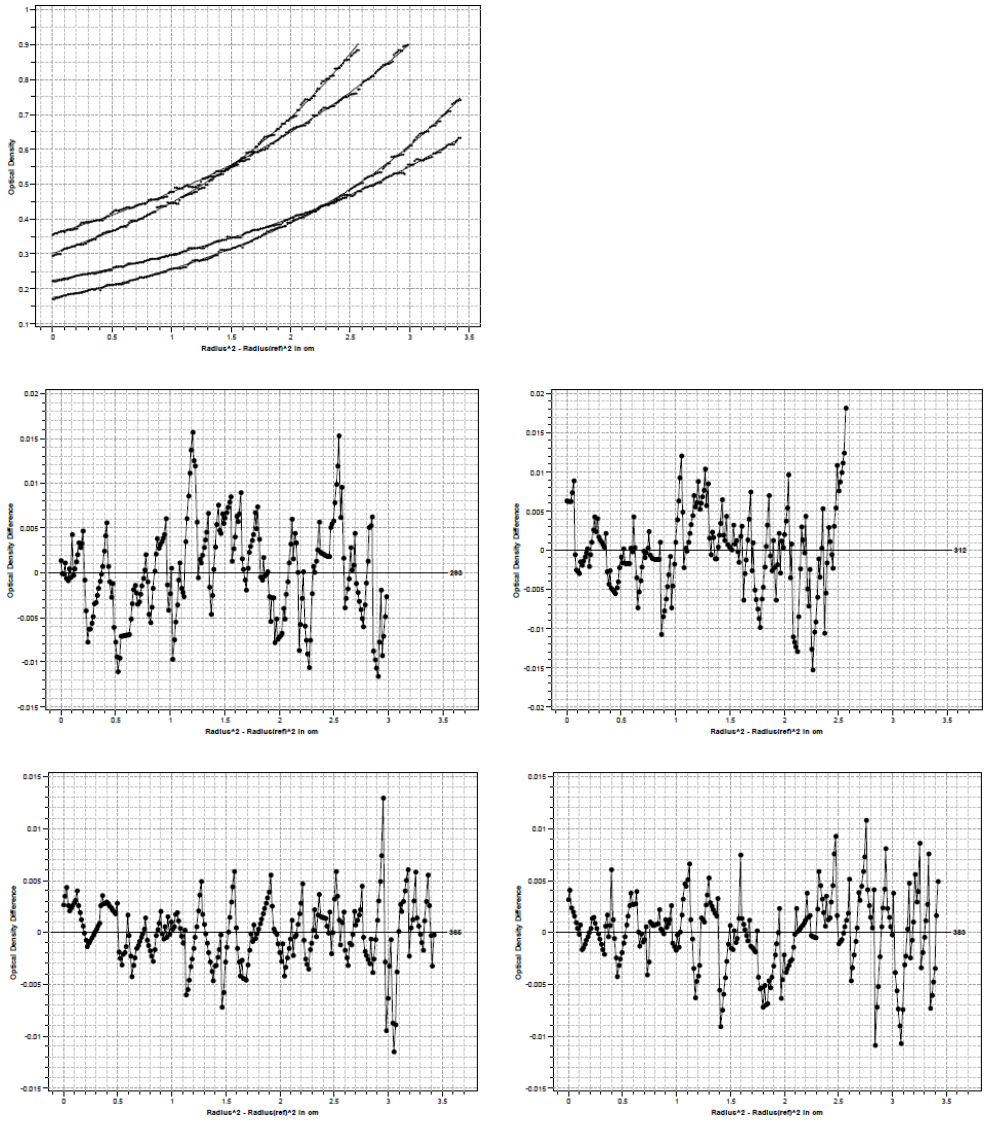

Figure 43: monomer/dimer model (left) 7.5k residuals, (right) 9k residuals for 150mM NaCl and 4uM and 2uM RII-175

SL			
concentration	speed	K_d (uM)	variance (10^-6)
3uM	7.5K	9.52	3.36
3uM	9k	15.82	4.61
3uM	7.5k/9k	4.19	4.24

Pep			
concentration	speed	K_d (uM)	variance (10^-6)
4.6uM	7.5K	10.80	8.61
4.6uM	9k	12.50	14.60
4.6uM	7.5k/9k	2.55	12.00
3uM	7.5K	1.54	8.87
3uM	9k	5.41	8.33
3uM	7.5k/9k	0.89	8.30
1.5uM	7.5K	0.89	7.11
1.5uM	9k	1.44	8.11
1.5uM	7.5k/9k	0.79	7.69
4.6uM/3uM/1.5uM	7.5k/9k	1.55	9.50

SLP			
concentration	speed	K_d (uM)	variance (10^-6)
3uM	7.5K	3.39	3.80
3uM	9k	8.69	3.80
3uM	7.5k/9k	1.80	4.59

Table 4: monomer/dimer model Kd and variance for SL, pep, and SLP

SL 3uM/7k 3uM/9k

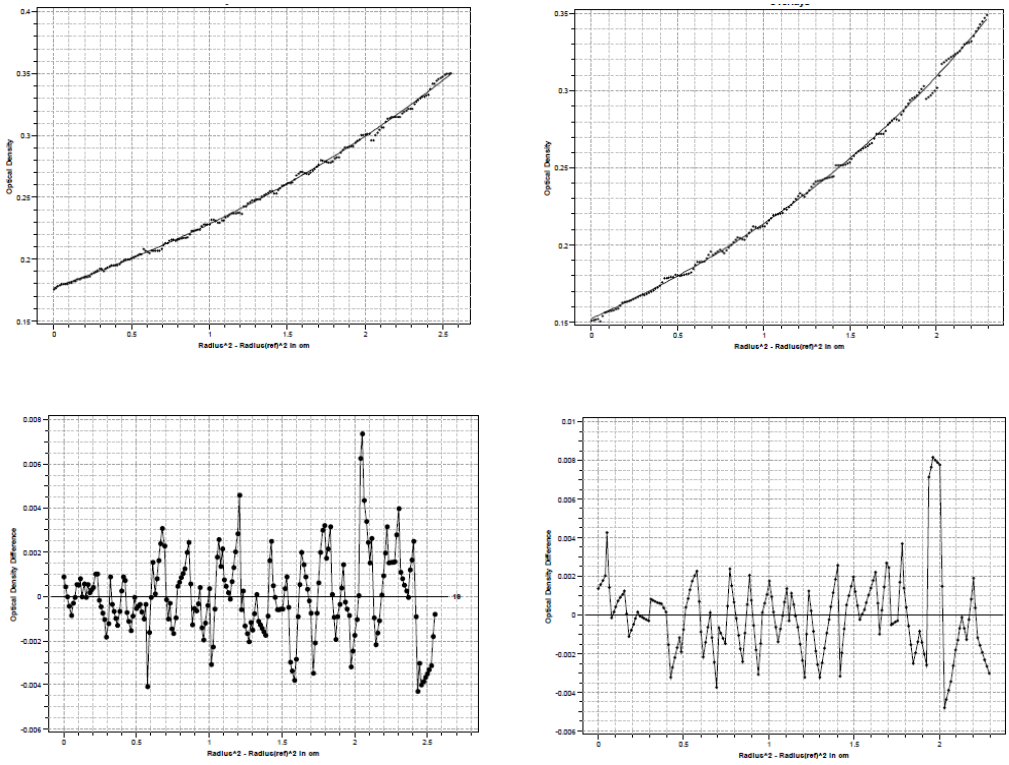

figure 44: monomer/dimer model overlays and residuals for SL, 3uM RII-175

SL 3uM/7k, 9k

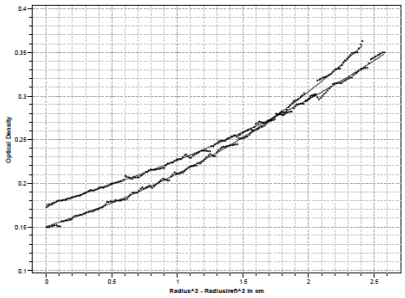

7k

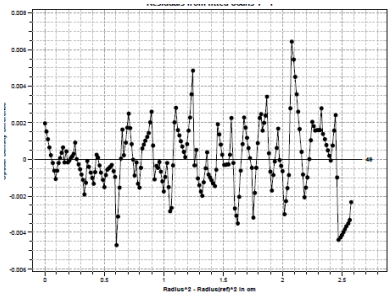

9k

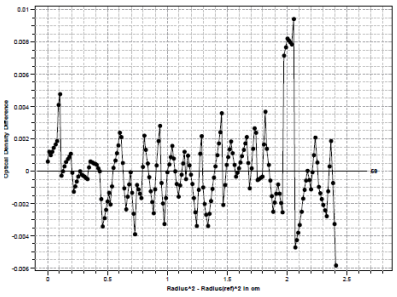

figure 45: monomer/dimer model overlays and residuals for SL, 7k combined with 9k

PEP 4.6uM/7k 4.6uM/9k

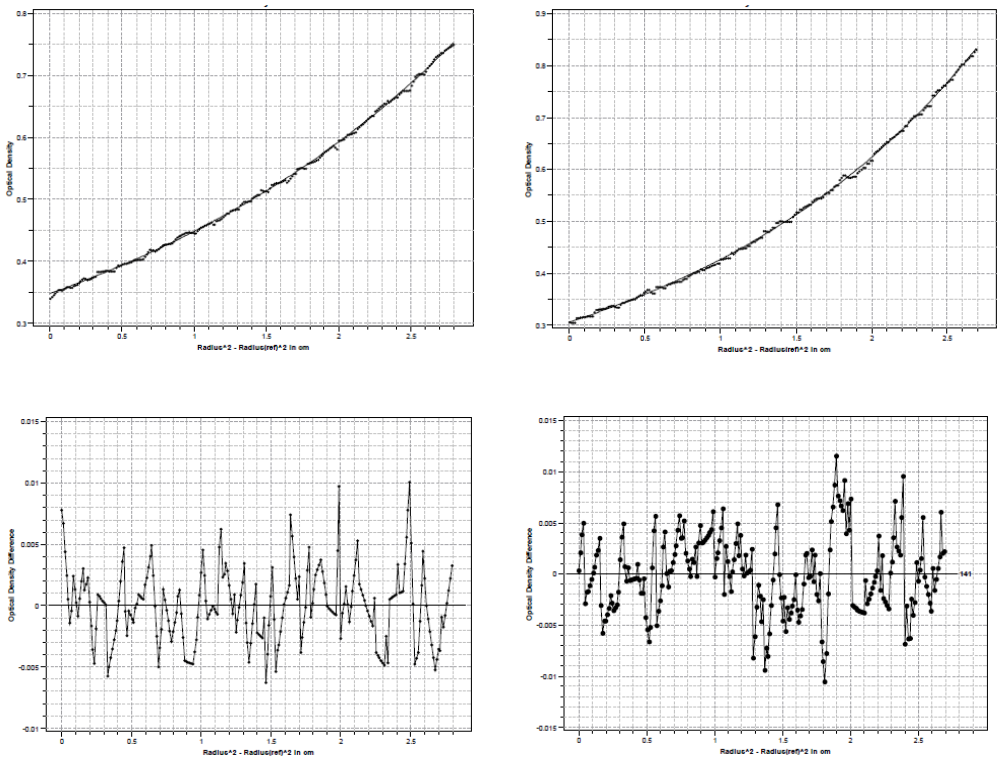

figure 46: monomer/dimer model overlays and residuals for PEP, 4.6uM RII-175

PEP 3uM/7k 3uM/9k

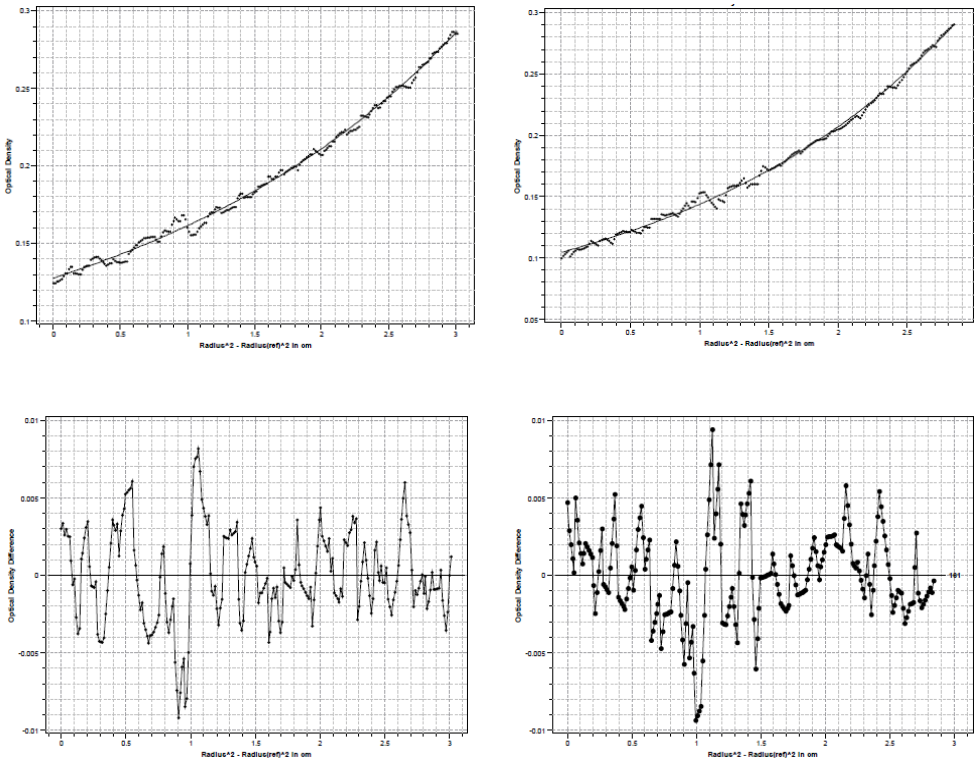

figure 47: monomer/dimer model overlays and residuals for PEP, 3uM RII-175

PEP 1.5uM/7k 1.5uM/9k

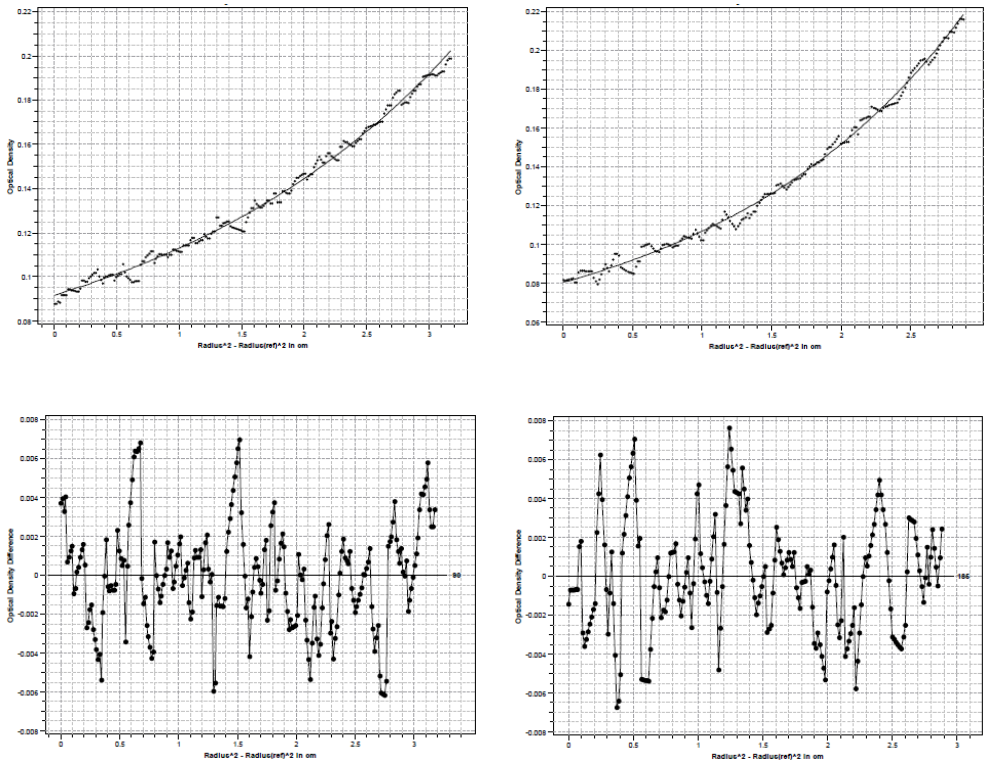

figure 48: monomer/dimer model overlays and residuals for PEP, 1.5uM RII-175

PEP 4.6uM/7k, 9k 3uM/7k, 9k 1.5uM/7k, 9k

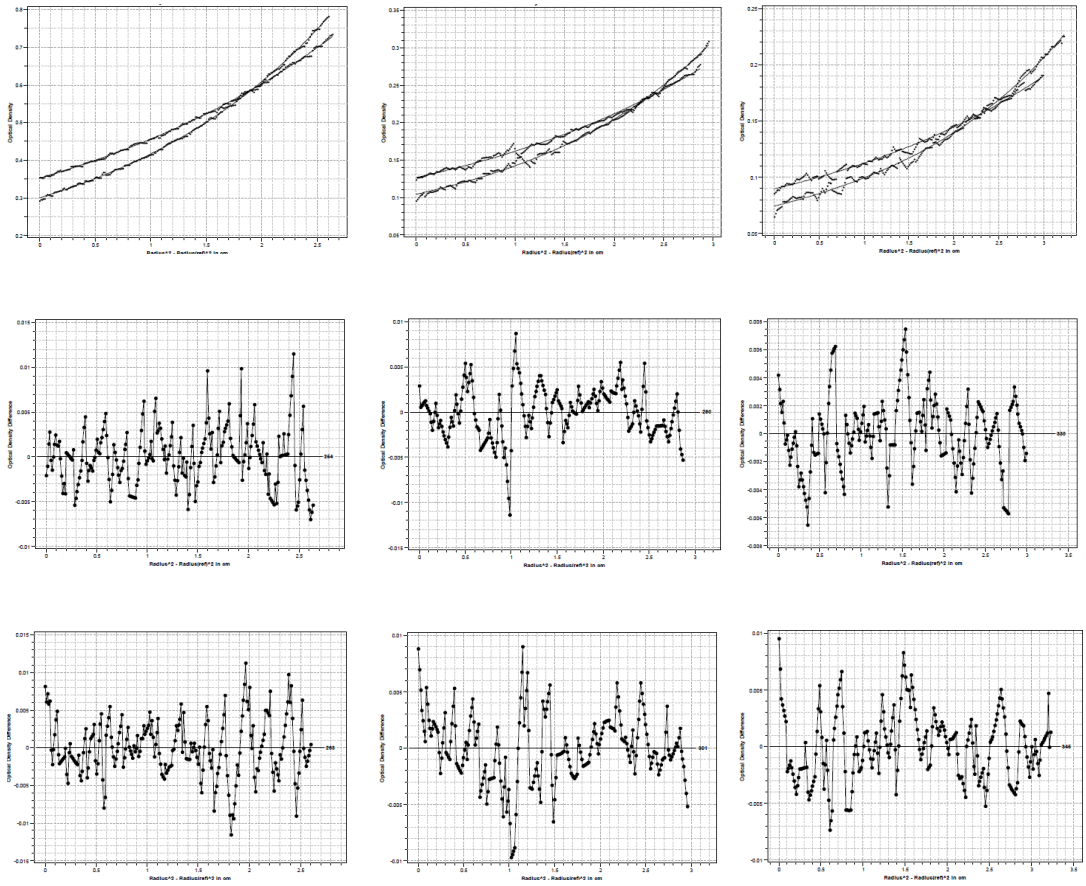

figure 49: monomer/dimer model overlays and residuals for PEP, 7k combined with 9k

PEP

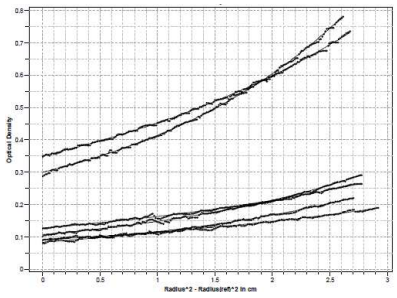

4.6uM

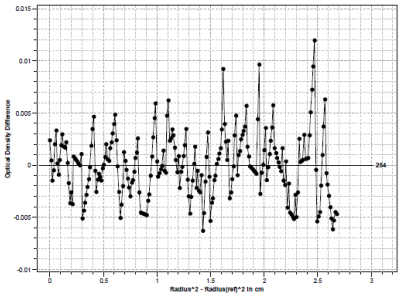

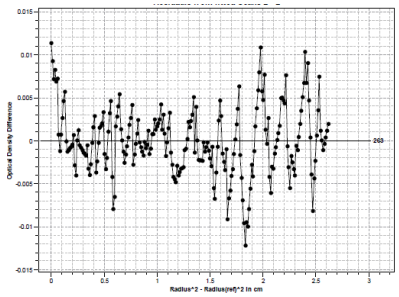

3uM

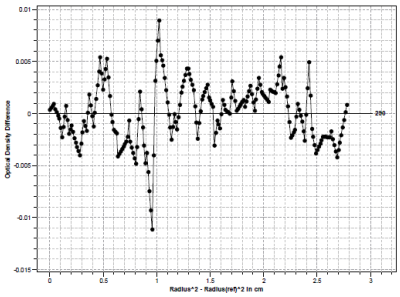

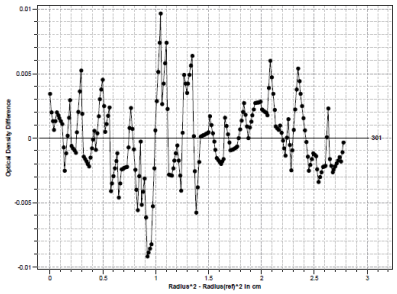

1.5uM

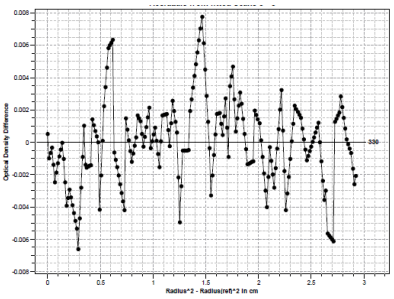

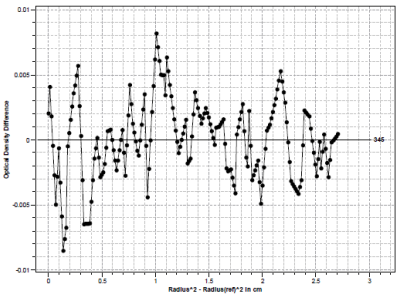

figure 50: monomer/dimer model (left) 7.5k residuals, (right) 9k residuals for PEP, all speeds and concentrations

SLP 3uM/7k 3uM/9k

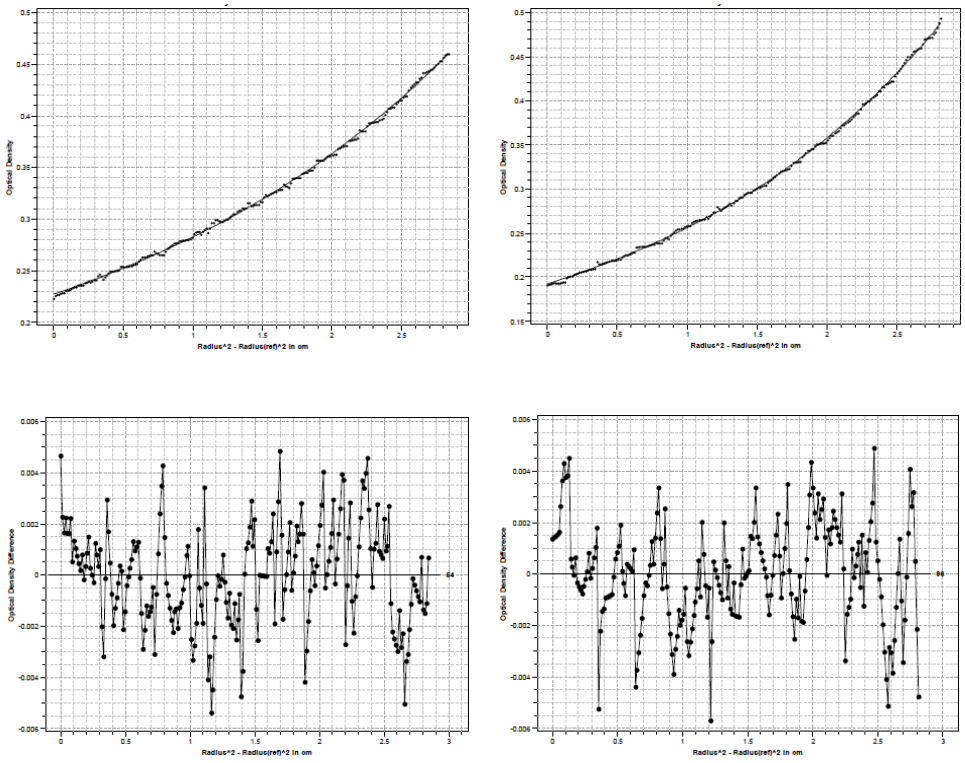

figure 51: monomer/dimer model overlays and residuals for SLP, 3uM RII-175

SLP 3uM/7k, 9k

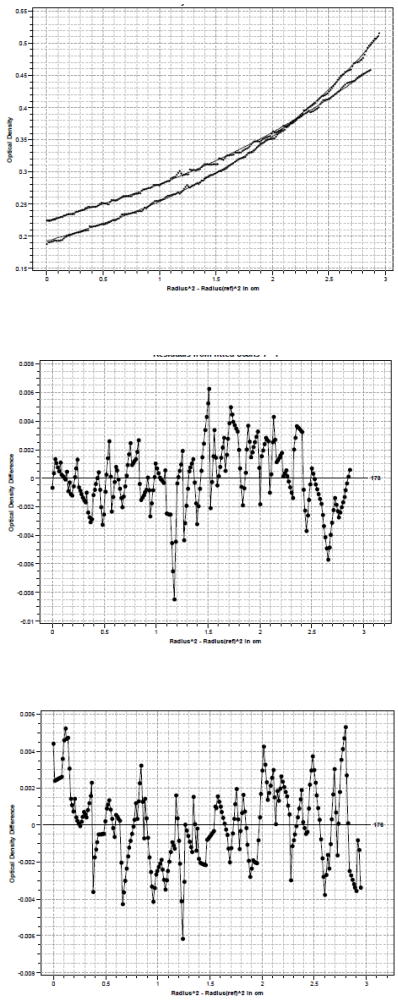

figure 52: monomer/dimer model overlays and residuals for SLP, 7k combined with 9k

a)

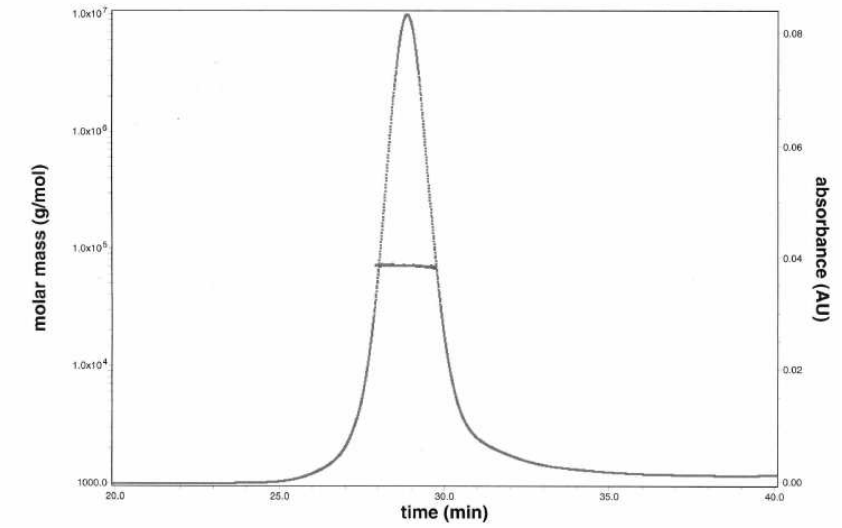

b)

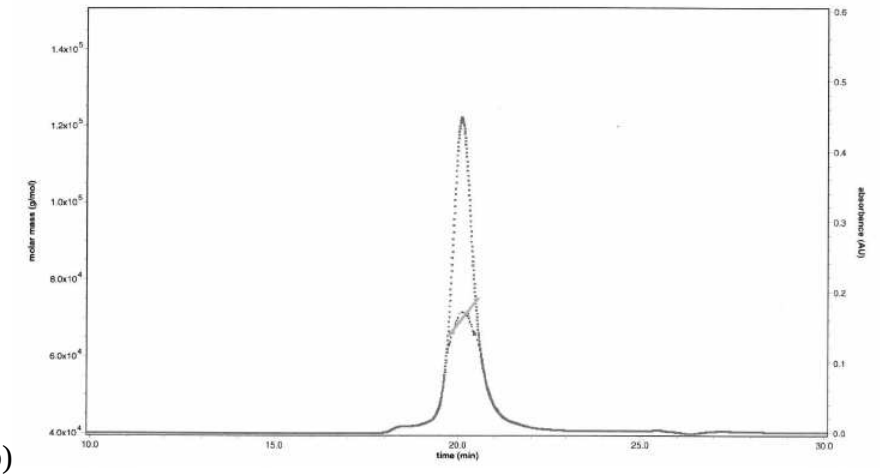

Figure 53: MALS data a) 9uM RII-175 b) 30uM RII-175

Chapter 6: Monoclonal Antibody Generation

6.1: Introduction

Production of antibodies is an important part of the immune response to pathogens. It has been previously shown antibodies against EBA-175 offer marginal protection against *P. falciparum* [12, 13]. To further understand how antibodies interact with RII-175 and how they affect receptor binding, mAbs are being generated against RII-175.

To produce mAbs, mice are injected with antigen and given boosts of the antigen at prescribed times [fig 54] [24]. The polysera of the mice is then tested for reactivity against the antigen used. The spleen cells of a positive mouse are then harvested and fused with a myeloma cells that have a mutation in HGPRT and are grown in media that contains hypoxanthine and thymidine and aminopterin [fig 54]. Aminopterin blocks denovo purine and pyrimidine synthesis. The spleen cells are fused with the myeloma cells and grown in media lacking hypoxanthine. The fused cells will be able to survive but unfused myeloma cells and B cells will not. The B cells do not survive because they are primary cells and the myeloma cells that do not fuse will not survive because they do not have a functional HGRPT enzyme. The fused cells get a functional HGPRT from the B cells and the ability to grow and divide from the myeloma cells. These hybridoma cells will then produce antibodies. The hybridoma cells will then be subcloned to produce mAbs. The mAbs can then be analyzed to for function and epitope [24].

In this chapter, I describe how mAbs were generated against recombinant RII-175 purified as described in chapter 2. In this chapter I also address the development of an ELISA protocol for the detection of antibodies reactive to RII-175.

6.2: Materials and Methods

6.2.1: Antibody Generation. Three mice were immunized with RII-175 by Kathy Sheehan and the Hybridoma Center at Washington University. The mice were given an additional boost of RII-175 before polysera was collected. Polysera was tested by ELISA as described below and the most reactive mouse (588) chosen for sacrifice. The spleen cells of the chosen mouse were fused with myeloma cells by the Hybridoma Center. The hybridomas were expanded and tested for reactivity against RII-175 by ELISA. The resulting top 20 highest positive OD450 hybridomas were subcloned by the Hybridoma Center. The resulting subclones will be analyzed by ELISA and positive subclones will be further subcloned by the Hybridoma Center and tested by ELISA. The positive hybridomas will then be tested for function by FACS and epitope determined. A terminal bleed was also taken from the mouse at the time of sacrifice.

6.2.2: Direct ELISA. RII-175, RII-175-his and DBP were each diluted in Carbonate buffer pH 9.6 to a concentration of 100ug/100uL. 100uL of diluted protein was added to each well of three ELISA 96 well plates such that rows A to D were coated with RII-175 (RII-175-his was added to column 1 instead of untagged RII-175) and rows E to H were coated with DBP. The plates were then left at 4^{o}C overnight to couple the protein to the plate. The plates were then washed three times with PBS 0.5% tween20. 100uL of 2%

BSA in PBS 0.5% tween20 was added to each well to block and incubated at room temperature for one hour. The plates were then washed three times with PBS 0.5% tween20. Polysera was then diluted in a serial dilution starting at 1:100 and going to 1:1,000,000 in PBS 0.5% tween20. The polysera was then added to columns 2 through 6 and incubated at room temperature for one hour. At the same time a mouse anti-6Xhis antibody from Invitrogen was diluted to 1:500 and added to column 1 and incubated at room temperature for one hour. The plates were then washed three times with PBS 0.5% tween20. 100uL of goat anti-mouse IgG antibody conjugated to HRP diluted 1:5000 was then added to all wells in columns 1 to 6 and incubated for one hour at room temperature. The plates were then washed three times with PBS 0.5% tween20. 100uL of TMB substrate was added to all wells in columns 1 to 6 and immediately quenched with 100uL 2M Sulfuric acid. Pictures of each plate were then taken and then the plates were read at a wavelength of 450nm.

6.2.3: Inhibition of RII-175. His tagged 15mg/mL was diluted 1:10 in DMEM with 10% FCS. Polysera from mouse 588 immunized with RII-175 and mouse 592 immunized with DBP were added to 25uL of diluted RII-175 to reach the desired concentration in a total of 50uL and the mixture incubated at 4^{o}C overnight. The mixture was then added to RBCs prepared as described in RII binding in chapter 4 and the FACS assay conducted as described in chapter 4. All concentrations of polysera were conducted in triplicate.

6.3: Results

6.3.1: Reactivity of Mouse Polysera

Three mice were immunized with RII-175 to produce antibodies against RII-175. To determine if the mice produced antibodies against RII-175, polysera was obtained from each mouse. The polysera from the three mice (588, 589, 590) was diluted in a serial dilution (titer) and tested in triplicate for reactivity against RII-175 by ELISA [fig 55]. Mouse 588 had positive titers up to 1:100,000. Mice 589 and 590 had positive titers up to 1:10,000. Mouse 588 was chosen to be sacrificed to produce hybridomas because it had the highest titer of antibodies reactive to RII-175.

6.3.2: Reactivity of Fusions

To produce immortal cell lines that can produce antibodies against RII-175, mouse 588's spleen cells were fused with myeloma cells to produce hybridomas (fusions). The fusions were tested twice for reactivity against RII-175 using ELISAs. The fusions were tested at two time points because a false positive can be seen at the first time point due to B-cells that have not fused with the myeloma cells and continue to produce antibodies until they die. The second time point will not have production of antibodies from unfused B-cells. The ELISAs resulted in 138 wells that had a positive reading of >0.2 at 450nm [fig 56-59]. The fusions with the 20 highest readings were chosen to be subcloned. The fusions with the next 20 highest readings were chosen to be expanded and individually frozen for future studies [fig 60]. The other fusions were pooled and frozen for future studies.

6.3.3: Reactivity of First Round of Subcloned Cell lines

To ensure that the cell lines are clonal, the top 20 highest OD450 for the fusions were subcloned using a serial dilution in 96 well plates were row A was seeded with 100cells/well, row B was seeded with 10cells/well, and rows C to H were seeded with 1cell/well. The subclones were tested for reactivity against RII-175 using ELISAs as described above. The three highest OD450s in each cell line for wells with a dilution of 1 cell/well were determined and the highest of these three wells was chosen to further subclone, while the other wells were expanded and frozen [table 5]. If a cell line did not have any positive readings in rows C to H, the top three highest OD450s in row B or row A were chosen and the highest of these three wells was chosen to further subclone, while the other wells were expanded and frozen [table 5]. These cell lines will need to undergo an extra round of subcloning to insure the culture is clonal. Three cell lines (2F2, 2F7, and 2D7) failed to produce positive subclones at any dilution on multiple plates. The other cell lines all produced positive subclones.

6.3.4: Inhibition of RII-175 RBC binding by Mouse Polysera

It is currently unknown how the antibodies produced by the mouse will interact with RII-175. In order to begin to understand this, the mouse polysera was tested for its ability to inhibit RII-175 binding to RBCs. Mouse polysera was incubated overnight with RII-175. The mixture was then incubated with RBCs. FACS was then done on the RBC mixtures. All dilutions of polysera were able to inhibit binding of RII-175 to RBCs [fig 61]. The dilution 1:5 had the greatest inhibition of binding followed by the 1:10 dilution. The 1:50 dilution showed minimal inhibition of binding. The inhibition suggests that at

least some of the antibodies in the polysera can inhibit binding of RBCs by RII-175. Any mouse RBCs that may be present in the polysera should not inhibit binding because the terminal sialic acids on the O-glycans on GpA are acetylated. This modification has been shown to block binding by RII-175 to the mouse RBCs. Although the mouse RBCs should not inhibit binding, the result could also be explained by the presence of proteases or other components found in the polysera. The purified monoclonal antibodies will eventually provide better evidence for inhibition of RII-175 binding to RBCs.

6.4: Discussion

Mice have been immunized with RII-175 and the titers of the mice tested. All three mice had positive titers to 1:10,000 and mouse 588 was chosen to be sacrificed for formation of hybridomas. The hybridomas were created and 20 chosen to be subcloned based on ELISA results. Of the subcloned cell lines, 3 failed to produce positive subclones in the first round while the other 17 produced positive subclones. The subclones still need to undergo a second round of subcloning before the antibodies can be deemed monoclonal. The polysera was also tested for inhibition of RII-175 binding to RBCs. The polysera was able to inhibit binding, but further characterization remains. The antibodies produced by the hybridomas will also be characterized individually for binding of RII-175, neutralization of binding in FACS assys, and epitope.

a)

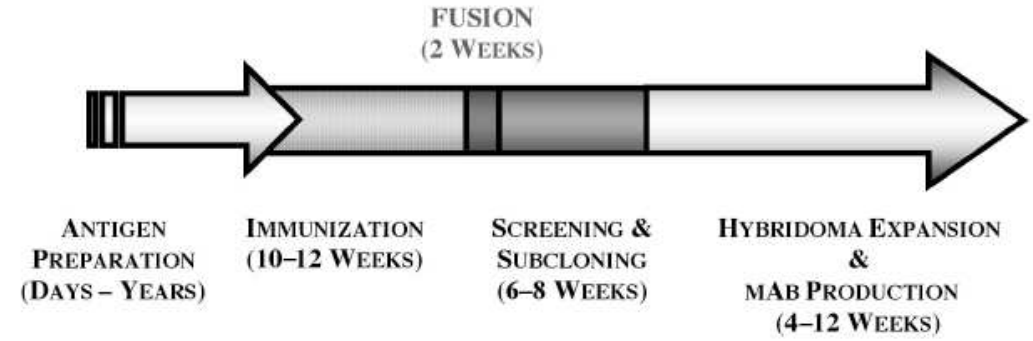

b)

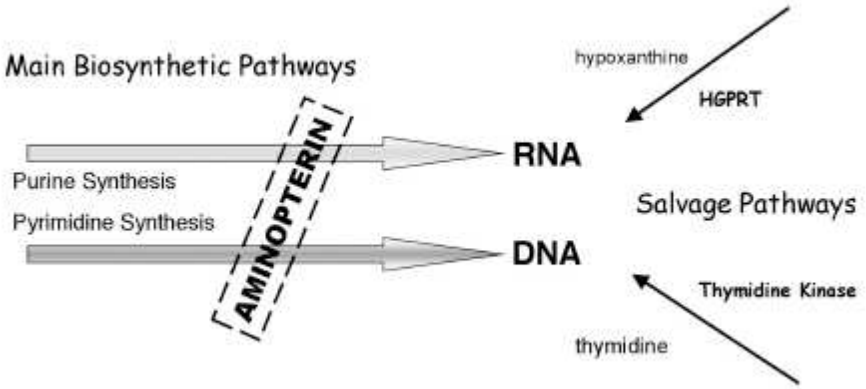

figure 54: a) diagram of the production of mAbs, b) diagram of requirements for fusion media [24]

a)

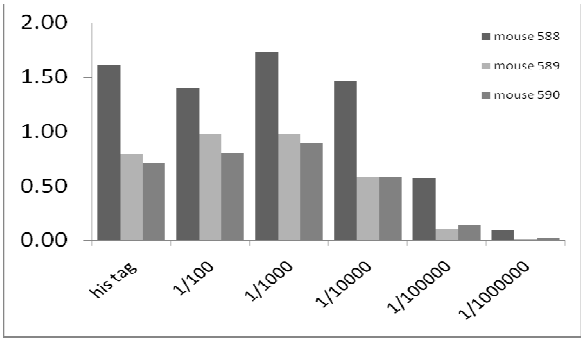

b)

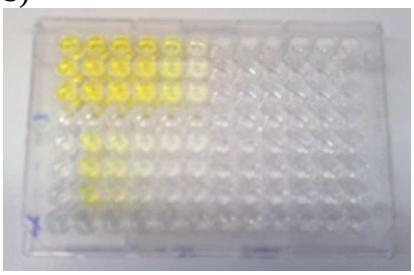

mouse1_588_polysera					
his tag	1/100	1/1000	1/10000	1/100000	1/1000000
1.667	1.456	1.782	1.524	0.531	0.087
1.707	1.33	1.693	1.394	0.561	0.076
1.465	1.4	1.7	1.476	0.629	0.108

c)

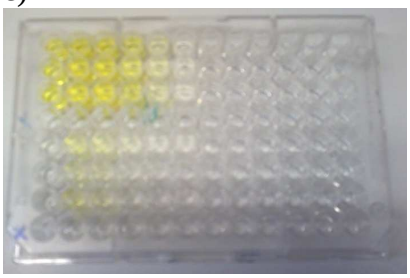

mouse2_589_polysera					
his	1/100	1/1000	1/10000	1/100000	1/1000000
0.75	0.928	0.893	0.545	0.122	0.008
0.794	1.058	1.009	0.611	0.116	0.002
0.851	0.966	1.031	0.594	0.1	0.018

d)

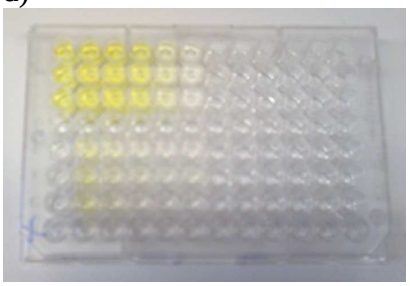

mouse3_590_polysera					
his	1/100	1/1000	1/10000	1/100000	1/1000000
0.779	0.806	0.87	0.596	0.142	0.021
0.702	0.815	0.922	0.577	0.139	0.005
0.654	0.78	0.887	0.571	0.145	0.019

figure 55: a) graph of titers for mouse 588, b) ELISA plate and readings for mouse 588, c) ELISA plate and readings for mouse 589, d) ELISA plate and readings for mouse 590

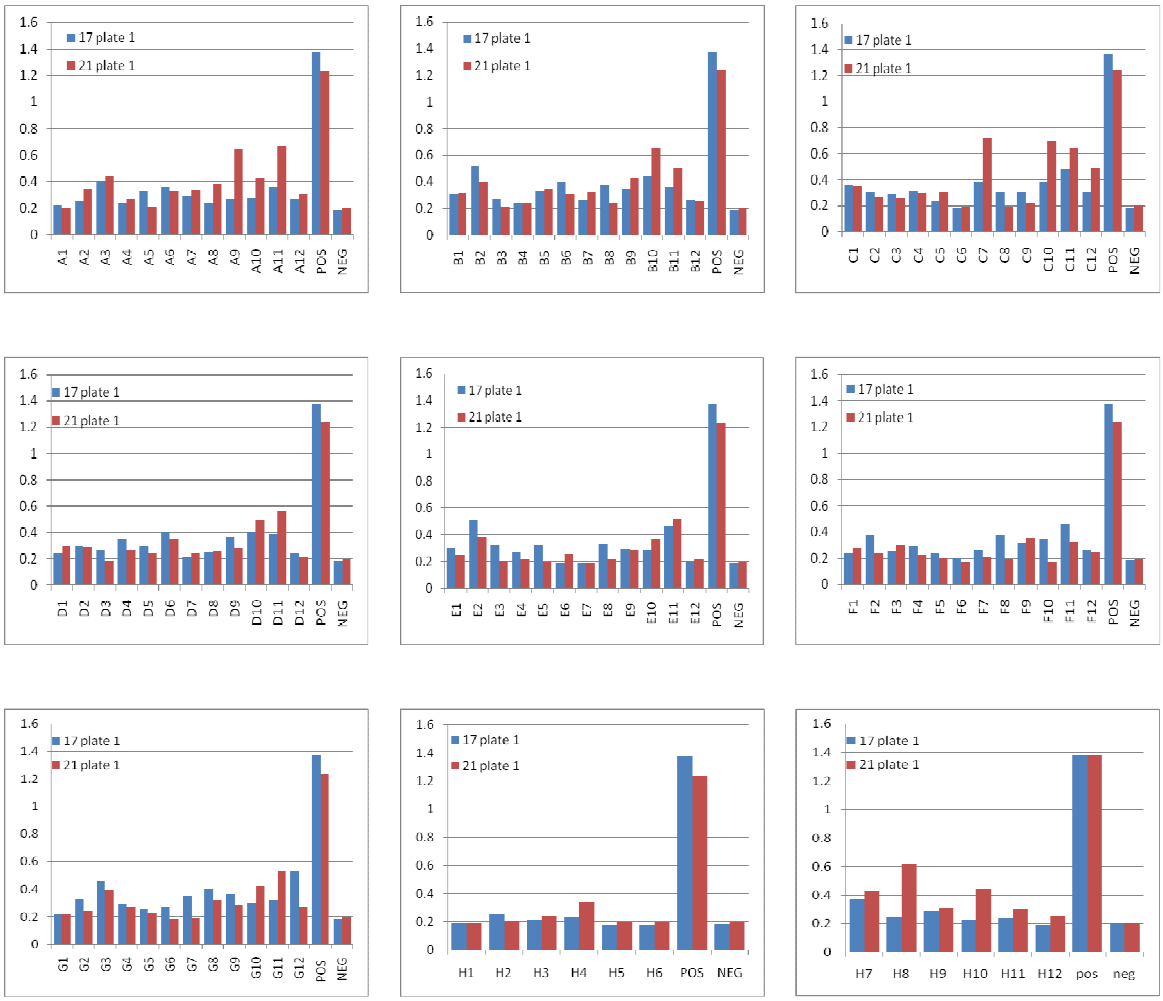

figure 56: ELISA results for plate 1 of fusions

figure 57: ELISA results for plate 2 of fusions

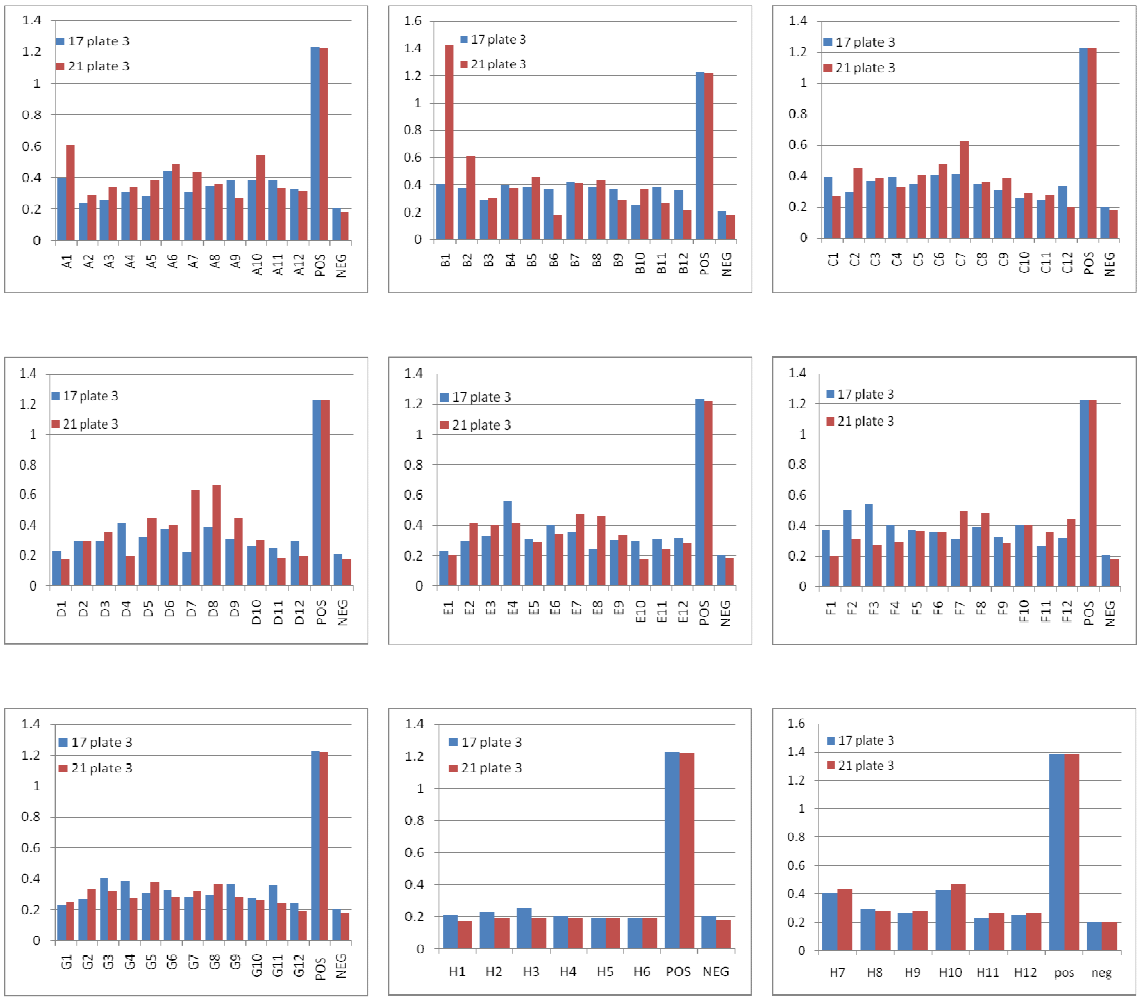

figure 58: ELISA results for plate 3 of fusions

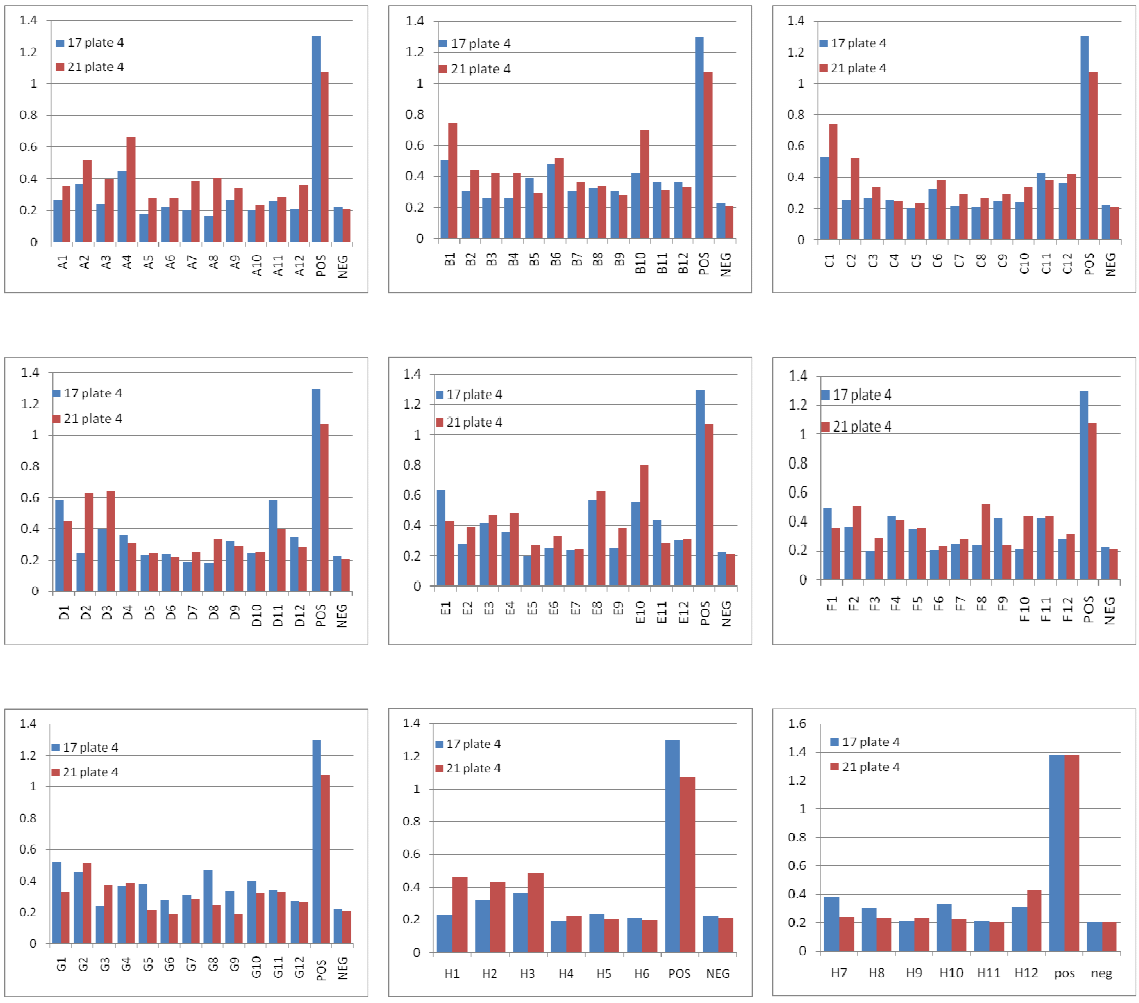

figure 59: ELISA results for plate 4 of fusions

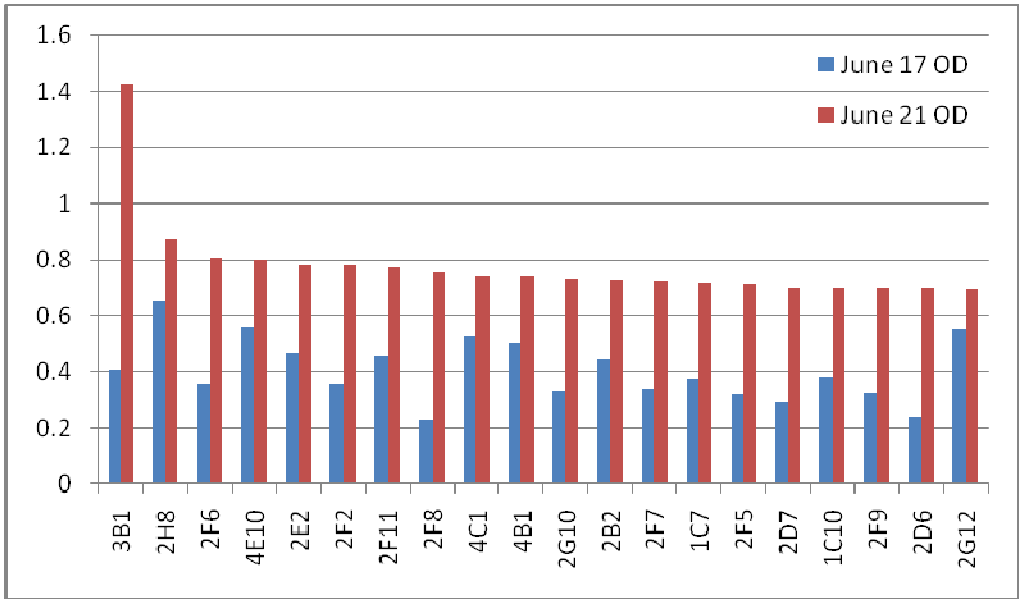

figure 60: OD450 readings for the highest 20 positive fusions chosen for subcloning, the label on the x-axis refers to the plate number, row value, and well number

cell line	well	OD 450	dilution (cells/well)	Subclone	Freeze	cell line	well	OD 450	dilution (cells/well)	Subclone	Freeze
2B2	G10	0.381	1	X		4A4	D2	0.585	1	X	
2B2	D9	0.365	1		X	4A4	C7	0.579	1		X
2B2	C2	0.35	1		X	4A4	C3	0.568	1		X
2D7	B2	0.14	10	X		4E10	B7	1.114	10	X	
2D7	B3	0.114	10		X	4E10	C6	0.688	100		X
2A11	E7	0.433	1	X		4E10	C7	0.686	100		X
2A11	E1	0.424	1		X	1A11	D11	0.198	1	X	
2A11	E2	0.358	1		X	1A11	A9	0.216	100		X
4B1	H7	1.044	1	X		1A11	A7	0.195	100		X
4B1	H11	1.02	1		X	2E2	E3	0.128	1	X	
4B1	H9	0.909	1		X	2E2	B2	0.128	10		X
2G10	C11	0.233	1	X		2E2	D2	0.323	10		X
2G10	A12	0.304	100		X	2F8	H3	1.371	1	X	
2G10	A9	0.301	100		X	2F8	H2	1.212	1		X
3B1	C12	0.896	1	X		2F8	H6	1.210	1		X
3B1	G12	0.857	1		X	2F11	E3	0.248	1	X	
3B1	D8	0.821	1		X	2F11	F4	0.237	1		X
3D8	C12	0.488	1	X		2F11	B7	0.191	10		X
3D8	C6	0.409	1		X	2F6	G5	0.370	1	X	
3D8	H11	0.385	1		X	2F6	G10	0.281	1		X
4C1	C12	0.474	1	X		2F6	G4	0.253	1		X
4C1	C3	0.449	1		X	1C7	D9	0.651	1	X	
4C1	H11	0.443	1		X	1C7	H3	0.398	1		X
4B1	C6	0.685	1	X		1C7	G10	0.380	1		X
4B1	C12	0.613	1		X						
4B1	H11	0.57	1		X						

table 5: ELISA Results for Subcloned Cell Lines

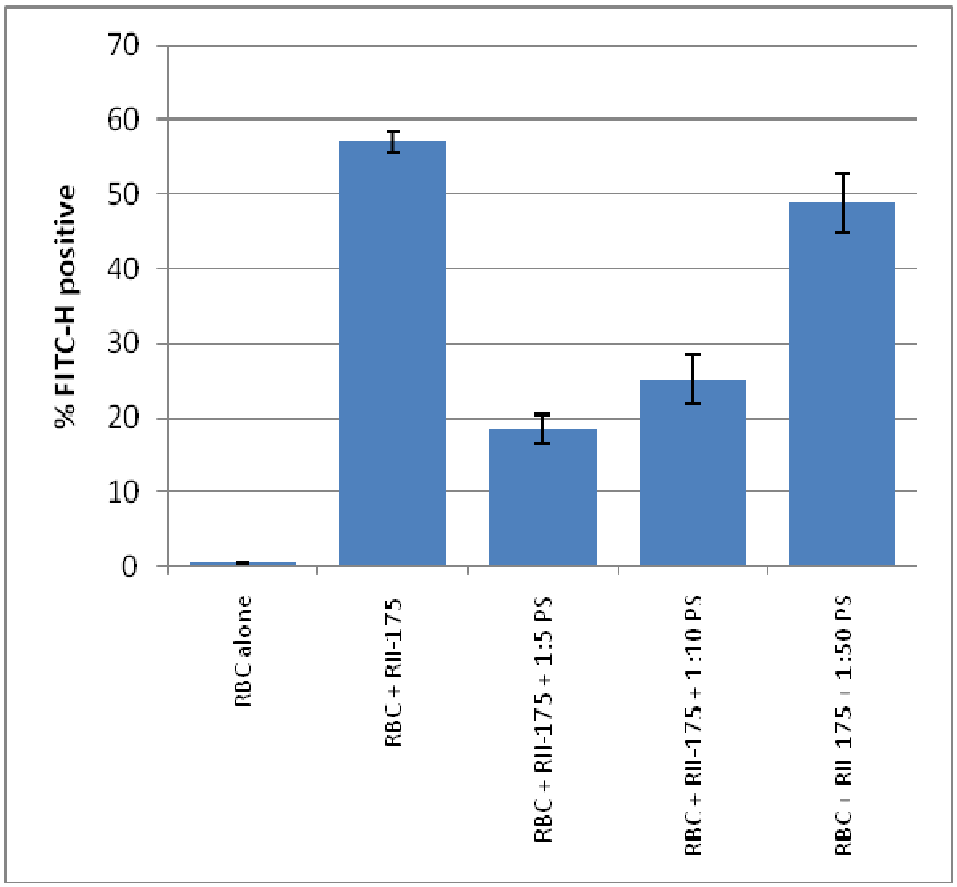

figure 61: Inhibition of RII-175 binding to RBCs by Mouse 588 polysera in FACS

Chapter 7: Summary of Results and Discussion of Future Directions

Approximately 2 million individuals a year die from malaria each year and an additional 200 million develop clinical illness characterized by the invasion and lysis of RBCs by *Plasmodium* parasites in the erythrocyte life stage [1, 2]. *Plasmodium falciparum* is the deadliest of the species of parasite that infect humans, and a large variety of proteins and cellular processes have been identified as potential targets for vaccines and drugs including EBA-175 [1, 2, 5].

EBA-175 is part of the EBL family and the sialic acid dependent pathway and is important for binding erythrocytes [1, 5]. The receptor for EBA-175 is GpA, a transmembrane glycoprotein on the surface of RBCs [6, 15, 16]. GpA contains 15 O-linked glycans and 1 N-linked glycan and the terminal α2-3 linked sialic acid from O-linked glycans is essential for EBA-175 binding [15, 16].

The structure of RII of EBA-175 reveals a dimer where each monomer is composed of one F1 and one F2 domain [5]. In the dimer, the F1 of one monomer interacts with the F2 of the other monomer in a handshake configuration creating two highly basic channels through the center of the dimer. Six glycan binding sites can also be found in the dimer with 4 sites inside the channels and the other 2 on the receptor facing surface. Mutations in the dimer interface and glycan binding sites showed a loss of RBC binding in rosetting assays indicating possible mechanisms of receptor/ligand interactions [5].

7.1: Components of the Receptor/Ligand System

The components of the receptor/ligand system consist of the RBC receptor GpA and the malaria ligand EBA-175. Previously both EBA-175 and GpA had been produced using *Pichia pastoris* and CHO cells respectively [5, 14]. The previous protocol developed for the production of EBA-175 was labor and time intensive and required the use of glycosylation mutants [5]. Also, the protocol for production of GpA only produced transmembrane anchored GpA in small quantities [14]. These protocols were not easily adaptable for producing the large quantities needed for biophysical experiments. As a result, a protocol to purify RII-175 and F2-175 from *E. coli* was developed and optimized for ease of production of large quantities of protein. The final yield for this protocol is approximately 1 to 5 mg/L refolding buffer. A protocol for the production of full length GpA and GpA truncations using HEK293 cells was also developed and optimized. The final yield for this protocol is approximately 13mg/L harvested media. The production of purified RII-175 and GpA allows for further investigation into the interactions between RII-175 with itself and its receptor.

7.2: Characterization of RII-175/GpA Interactions

To show that RII-175 and GpA (full length and truncations) are functional, a pulldown protocol was developed. In the pulldown, RII-175 binds both full length Gpa and truncation 4; and it is likely that this region of GpA, amino acids 30 to 50, is the minimal binding site for RII-175. RII-175 also binds truncation 2, which contains seven glycosylations and an additional three residues that could potentially be glycosylated, weakly and may be due to the large number of glycosylations. The importance of the

glycosylations on GpA is also seen in the pulldown with the anion exchange purified GpA. In this pulldown, RII-175 binds only the high molecular weight peaks which may correspond to a higher level of glycosylation.

A second functional assay was developed to test the influence of inhibitors on RII-175 binding RBCs and to characterize its interactions with GpA. In the FACS assay, RII-175 binds GpA on human RBCs and is detected through a fluorescently conjugated antibody against the 6X-his tag on the RII-175. FITC-RII-175 was also developed to decreases the amount of time required for the FACS assay and can be used to test inhibitors but not antibodies against RII-175 because the label could interfere with the ability of antibodies to bind their epitope. This assay was used to characterize the receptor specificity of the recombinant RII-175 and the inhibition of RII-175 binding by portions of the receptor.

The RII-175 bound GpA on the RBCs and this is supported by the RII-175 binding to chymotrypsin treated RBCs but not to trypsin treated cells. The receptor specificity is further supported by the reduction in binding upon RBC treatment with anti-GpA antibody, which blocks RII-175 binding by specifically targeting the receptor. The receptor is composed of both an amino-acid backbone and a large number of glycosylations that terminate in an α2-3 linked sialic acid. The ability of 3'-siallylactose and peptide backbone were tested for their ability to inhibit RII-175 binding. The IC50 for SL was in the low milimolar range and implies that SL, while important for binding, is not the only portion of the receptor responsible for interaction with RII-175. Peptide

backbone and peptide backbone with SL was not able to inhibit better than SL alone. Further studies would be to verify the minimal binding domain of GpA by FACS inhibition assays using GpA truncations and GpA glycosylation mutants.

7.3: Dimerization of RII-175

RII-175 is a weak dimer. Previously, mutation studies were used to support the dimer model[5]. This is now also supported by data from pulldowns and AUC experiments but not by MALS. RII-175-his is able to bind RII-175 in the pulldown indicating that the recombinant protein can interact with itself likely as a dimer. Dimerization is also supported by the AUC data. In the 1-component ideal model, the average molecular weight is around 100kDa, which is between that of the monomer and dimer, 70kDa and 140kDa respectively. The monomer/dimer equilibrium model also supports the dimer with the K_d ranging from 7-13uM for the salt gradient sedimentation experiment and 1-14uM for the SL, Pep, and SLP experiments. This experiment has yet to be done in the presence of GpA. In the presence of GpA, the RII-175 should transition to being mostly dimeric in the sample based on the proposed dimer model of binding. The MALS in contrast did not show any dimer in solution. This result may also be explained by the weak K_d and on-column dissociation.

7.4: Production of mAb against RII-175

Previous studies have shown that antibodies against RII-175 are present in patient sera[12, 13]. To better understand how antibodies against RII-175 interact with RII-175, monoclonal antibodies against RII-175 are being produced. To date, three mice have

been immunized with RII-175 and the titers of the mice tested. All three mice had positive titers to 1:10,000 and mouse 588 was chosen to be sacrificed for formation of hybridomas. The hybridomas were created and 20 chosen to be subcloned based on ELISA results. Of the subcloned cell lines, 3 failed to produce positive subclones in the first round while the other 17 produced positive subclones. The subclones still need to undergo a second round of subcloning before the antibodies can be deemed monoclonal. While the polysera inhibited RII-175 binding to RBCs, the antibodies produced by the hybridomas have yet to be characterized individually for binding of RII-175, neutralization of binding in FACS assys, and epitope.

7.5: Future Directions

While dimerization has been shown to occur with RII-175 samples in the absence of receptor, the significance of dimerization in receptor binding has yet to be determined. This could be determined through sedimentation equilibrium experiments with RII-175 in the presence of receptor, co-crystallization of RII-175 with GpA, and the mechanism of inhibition of RII-175 binding by antibodies. These experiments can also be used to verify the minimal binding domain of GpA. Characterization of how RII-175 interacts with GpA can ultimately be used to develop vaccines against malaria.

References:

1. **Alan F. Cowman, a.B.S.C., *Invasion of Red Blood Cells by Malaria Parasites.* Cell, 2006. 124.**
2. **World-Health-Organization, *World Malria Report 2008*. 2008.**
3. **Centers-for-Disease-Control-and-Prevention. *Malaria Biology*. 2010 Feb 8, 2010 [cited; Available from: http://www.cdc.gov/malaria/about/biology/index.html.**
4. **Alexander G. Maier, J.B., Brian Smith, David J. Conway, Alan F. Cowman, *Polymorphisms in Erythrocyte Binding Antigens 140 and 181 Affect Function and Binding but not Receptor Specificity in Plasmodium falciparum.* Infection and Immunity, 2009. 77(4).**
5. **Niraj H. Tolia, E.J.E., B. Kim Lee Sim, and Leemor Joshua-Tor, *Structural Basis for the EBA-175 Erythrocyte Invasion Pathway of the Malaria Parasite Plasmodium falciparum.* Cell, 2005. 122.**
6. **B.K.L. Sim, C.E.C., K. Wasniowska, T.J. Hadley, L.H. Miller, *Receptor and Ligand Domains for Invasion of Erythrocytes by Plasmodium falciparum.* Science, 1994. 264.**
7. **Christian F. Ockenhouse, A.B., Douglas P. Blackall, Cheryl I. Murphy, Oscar Kashala, Sheetij Dutta, David E. Lanar, Jon R. Daugherty, *Sialic acid-dependent binding of baculovirus-expressed recombinant antigens from Plasmodium falciparum EBA-175 to Glycophorin A.* Molecular and Biochemical Parasitology, 2001. 113.**
8. **D.C. Ghislaine Mayer, J.C., Lubin Jiang, Daniel L. Hart, Erin Tracy, Juraj Kabat, Laurence H. Mendoza, and Louis H. Miller, *Glycophorin B is the erythrocyte receptor of Plasmodium falciparum erythrocyte-binding ligand, EBL-1.* PNAS, 2009. Early Edition.**
9. **Manoj T. Duraisingh, A.G.M., Tony Triglia, Alan F. Cowman, *Erythrocyte-binding antigen 175 mediates invasion in Plasmodium falciparum utilizing sialic acid-dependent and -independent pathways.* PNAS, 2003. 100(8).**
10. **Palmer A. Orlandi, F.W.K., and J. David Haynes, *A Malaria Invasion Receptor, the 175-Kilodalton Erythrocyte Binding Antigen of Plasmodium falciparum Recognizes the Terminal Neu5Ac(a2-3)Gal- Sequences of GlycophorinA.* The Journal of Cell Biology, 1992. 116(4).**
11. **Hadley, D.C.a.T.J., *A Plasmodium falciparum Antigen that Binds to Host Erythrocytes and Merozoites.* Science, 1985. 230(4725).**
12. **Daniel M. N. Okenu, E.M.R., Quentin D. Bickle, Philip U. Agomo, Arnoldo Barbosa, Jon R. Daugherty, David E. Lanar, and David J Conway, *Analysis of Human Antibodies to Erythrocyte Binding Antigen 175 of Plasmodium falciparum.* Infection and Immunity, 2000. 68(10): p. 5559-5566.**

13. **Faith H. A. Osier, G.F., Spencer D. Polley, Linda Murungi, Federica Verra, Kevin K. A. Tetteh, Brett Lowe, Tabitha Mwangi, Peter C. Bull, Alan W. Thomas, David R. Cavanagh, Jana S. McBride, David E. Lanar, Margaret J. Mackinnon, David Conway, Kevin Marsh,** ***Breadth and Magnitude of Antibody Responses to Multiple Plasmodium falciparum Merozoite Antigens are Associated with Protection from Clinical Malaria.*** **Infection and Immunity, 2008. 76(5): p. 2240-2248.**
14. **Alan T. Remaley, M.U., Nancy Wu, Leslie Litzky, Scott R. Burger, Jonni S. Moore, Minoru Fukuda, and Steven L. Spitalnik,** ***Expression of Human Glycophorin A in Wild Thype and Glycosylation deficient Chinese Hamster Ovary Cells.*** **The Journal of Biological Chemistry, 1991. 266(35).**
15. **O.-O. Blumenfeld, C.-H.H.,** ***Molecular Genetics of Glycophorin MNS Variants.*** **Transfus Clin Biol, 1997. 4.**
16. **Poole, J.,** ***Red Cell Antigens on Band 3 and Glycophorin A.*** **Transfusion medicine, 2000. 14.**
17. **A. Radu Aricescu, W.L., and E. Yvonne Jones,** ***A time- and cost-efficient system for high-level protein production in mammalian cells.*** **Biological Crystallography, 2006. D62.**
18. **Givan, A.L.,** ***Flow Cytometry,*** **in** ***Methods in Molecular Biology: Flow Cytometry Protocols,*** **T.S.H.a.R.G. Hawley, Editor, Humana Press Inc.: Totowa, NJ. p. 1-31.**
19. **Ritica Bharara, S.S., Priyabrata Pattnik, Chetan E. Chitnis, Amit Sharma,** ***Structural analogs of sialic acid interfere with the binding of erythrocyte binding antigen-175 to glycophorinA, an interaction crucial for erythrocyte invasion by Plasmodium falciparum.*** **Molecular and Biochemical Parasitology, 2004. 138.**
20. **Ralston, G.,** ***Introduction to analytical Ultracentrifugation*****: Beckman Instuments Inc. 87.**
21. **Voelker, D.K.M.a.P.J.,** ***Self-Associating Systems in the Analytical Ultracentrifuge*****: Beckman Instruments, Inc. 49.**
22. **Jie Wen, T.A., John S. Philo,** ***Size-Exclusion Chromatography with On-Line Light-Scattering, Absorbance, and Refractive Index Detectors for Studying Proteins and Their Interactions.*** **Analytical Biochemistry, 1996. 240: p. 155-166.**
23. **Mogridge, J.,** ***Using Light Scattering to Determine the Stoichiometry of Protein Complexes,*** **in** ***Methods in Molecular Biology: Protein-Protein Interactions Methods and Protocols,*** **H. Fu, Editor, Humana Press Inc.: Totowa, NJ. p. 113-118.**
24. **Sheehan, K.C.F.,** ***Production of Monoclonal Antibodies,*** **in** ***Making and Using Antibodies: A Practical Handbook,*** **M.R.K. Gary C. Howard, Editor. 2006, CRC Press. p. 73-94.**